

31
32
33
34
35
36
37
38
39
40
41
42
43
44
45
46
47
48
49
50
51
52
53
54

Abstract

Arctic amplification (AA) is a coupled atmosphere-sea ice-ocean process. This understanding has evolved from the early concept of AA, as a consequence of snow-ice line progressions, through more than a century of research that has clarified the relevant processes and driving mechanisms of AA. The predictions made by early modeling studies, namely the fall/winter maximum, bottom-heavy structure, the prominence of surface albedo feedback, and the importance of stable stratification have withstood the scrutiny of multi-decadal observations and more complex models. Yet, the uncertainty in Arctic climate projections is larger than in any other region of the planet, making assessment of high-impact, near-term regional changes difficult or impossible. Reducing this large spread in Arctic climate projections requires a quantitative process understanding. This manuscript aims to build such understanding by synthesizing current knowledge of AA and to produce a set of recommendations to guide future research. It briefly reviews the history of AA science, summarizes observed Arctic changes, discusses modeling approaches and feedback diagnostics, and assesses the current understanding of the most relevant feedbacks to AA. These sections culminate in a conceptual model of the fundamental physical mechanisms causing AA and a collection of recommendations to accelerate progress towards reduced uncertainty in Arctic climate projections. Our conceptual model highlights the need to account for local feedback and remote process interactions, specifically the water vapor triple effect, within the context of the annual cycle to constrain projected AA. We recommend raising the priority of Arctic climate sensitivity research, improving the accuracy of Arctic surface energy budget observations, rethinking climate feedback definitions, coordinating new model experiments and intercomparisons, and pursuing the role of episodic variability in AA as a research focus area.

55 **1. Introduction**

56 Anthropogenic carbon dioxide (CO₂) emissions and other greenhouse gases are changing
57 Earth’s climate. Global mean surface temperature has risen by $\geq 1.0^{\circ}\text{C}$ relative to the pre-industrial
58 period, making this the warmest period in the history of modern civilization (Wuebbles et al 2017).
59 As the impacts of warming cascade through the physical climate and natural systems, society
60 grapples with decisions on the countermeasures needed to offset the increased vulnerability in the
61 systems that underpin modern society: food, energy, water, health, security, and economy. Global
62 temperature targets (e.g., Paris Climate Accord) serve as the basis to gauge the required
63 aggressiveness of countermeasures. Global targets, however, fail to consider the uncertainty and
64 high impact of dramatic regional changes, such as in the Arctic where consequential ice sheet melt
65 and untenable global sea level rise cannot be ruled out at 1.5°C of global warming (IPCC 2018;
66 Meredith et al. 2019; IPCC 2021). Global temperature targets leave substantial climate risks
67 unconsidered; using regional indicators as policy targets helps account for the uneven spatial
68 distribution of climate change impacts and risks.

69 Climate change is spread unevenly across the globe. The Arctic surface has warmed more than
70 twice as fast as the global average surface temperature (Fig. 1; Lenssen et al. 2019), a phenomenon
71 known as Arctic Amplification (AA). AA is part of the broader polar amplification phenomenon
72 that also applies to the Antarctic. However, amplified Antarctic warming is expected to be weaker
73 and delayed due to the effects of the Antarctic continent surface height, smaller albedo and lapse
74 rate feedbacks, and Southern Ocean upwelling (Salzmann 2017, Hahn et al. 2020). Rapid Arctic
75 surface warming is driving changes in a number of physical climate characteristics (e.g., sea ice
76 and snow cover) and impacting ecosystems and vegetation distribution (Taylor et al. 2017). The
77 use of climate change indicators from regions with the largest expected changes (e.g. Arctic surface

Non-peer reviewed EarthArXiv preprint submitted to Frontiers in Earth Science to the “Arctic Amplification: Feedback Process Interactions and Contributions” Research Topic.

78 temperature change and sea ice extent and thickness) ensures that high-impact regional climate
79 change outcomes are considered in climate risk assessment.

80 Accurate long-term observations and trustworthy climate projections are needed to effectively
81 inform regional targets; however, the harsh and complex Arctic environment makes the necessary
82 observations and climate projections challenging to obtain, resulting in substantial uncertainty. A
83 meaningful adoption of Arctic climate indicators as policy targets requires an improved process
84 understanding to reduce uncertainty in AA projections—the topic of this review.

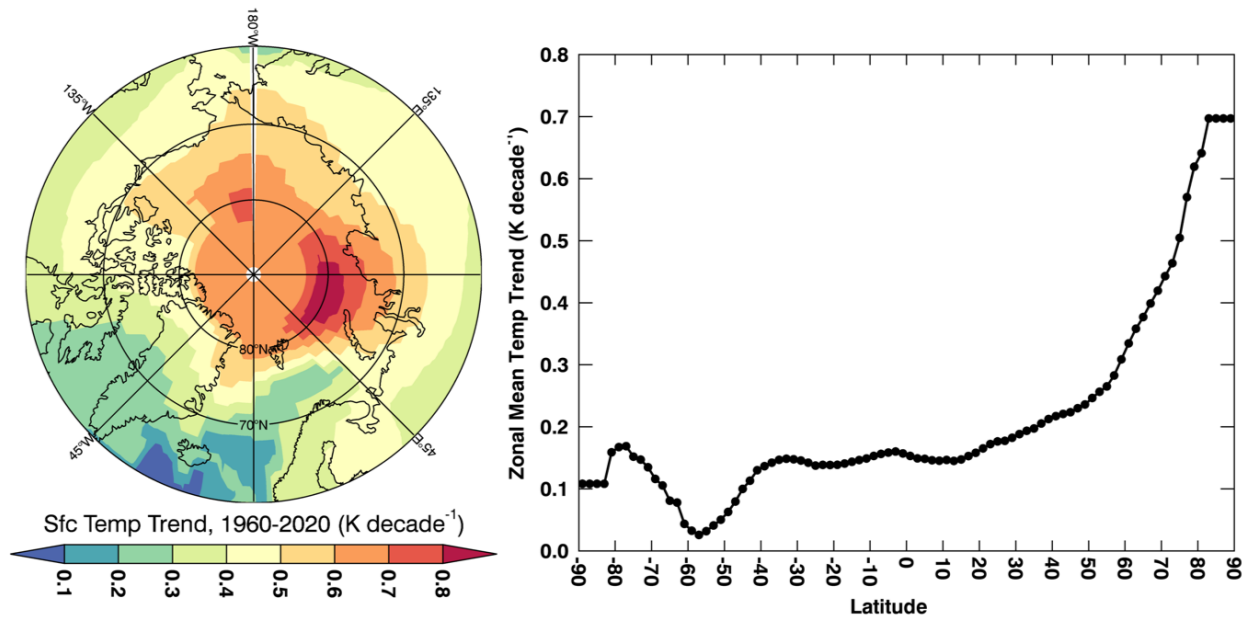


Figure 1: Arctic and zonal mean linear surface temperature trends since 1960. (a) The spatial pattern of the surface temperature trend at 2°x2° resolution and (b) the zonal mean surface temperature trend (K decade⁻¹) assessed by applying a ordinary least squares fit linear regression to the GISTEMP time series (Lenssen et al. 2019; GISTEMP Team 2021).

85 Research over the last 50 years has identified the fundamental characteristics of AA and
86 advanced our understanding. It is widely accepted that AA manifests as a surface-based warming
87 profile (Wetherald and Manabe 1975; hereafter WM75); it is strongest in fall and winter and absent
88 in summer (Manabe and Stouffer 1980; hereafter MS80); it is strongest in regions of sea ice retreat
89 (Washington and Meehl 1984) and that the seasonal energy transfer from summer to fall via ocean
90 heat storage plays a critical role in its seasonality and magnitude (MS80; Washington and Meehl

91 1986). Moreover, the melting of sea ice and snow represents a fundamental feedback mechanism
92 (e.g., Arrhenius 1896; Budyko 1966).

93 As our knowledge has deepened, additional considerations have been identified that make it
94 harder to reduce Arctic climate projection uncertainty. Natural variability complicates our ability
95 to quantify the forced Arctic climate change signal and distinguish the processes driving observed
96 AA. Natural variability also represents an irreducible uncertainty in decadal and multi-decadal
97 predictions (Kay et al. 2015; Swart et al. 2015; Swart 2017). In addition, the quantitative
98 assessment of specific process contributions is affected by the metric used to define AA and the
99 feedback diagnostic approach applied (Hind et al. 2016).

100 Important advances in AA science have occurred in the last decade. The aim of this manuscript
101 is to synthesize this knowledge and guide future research. Section 2 provides a brief history of AA
102 science, highlighting the most pertinent results and contributing factors. Section 3 provides an
103 overall context of the observed Arctic changes over the last several decades. Section 4 provides a
104 discussion of the modeling approaches and feedback diagnostic techniques. Section 5 describes
105 our current understanding of the processes driving AA. Section 6 provides a conceptual model of
106 the key physical mechanisms. Lastly, Section 7 proposes a collection of recommendations to
107 accelerate progress in AA science and reduce uncertainty in Arctic climate projections.

108 **2. Historical perspective**

109 The expectation that the polar regions are more sensitive to climate forcing has been around
110 since Arrhenius (1896) wrote on the ebb and flow of glacial periods in a seminal paper on the
111 impact of CO₂ concentrations on temperature. However, the phrase “amplified polar warming” or
112 “polar amplification” did not appear until nearly a century later (Broecker 1975; Schneider 1975).

113 The explanation for polar amplification has evolved from the earliest idea as a consequence of the
114 progression of the snow-ice line (e.g., Arrhenius 1896) to modern ideas of a coupled atmosphere-
115 sea ice-ocean process (e.g., MS80). While impossible to definitively say, it seems likely that the
116 origin of polar amplification within the context of ice ages favored hypotheses pertaining to ice
117 and snow. Computational expediency could have played a role, as the surface albedo feedback is
118 easily manipulated within energy balance models (EBMs). Be it by intuition or luck, early
119 scientists correctly identified the leading role of the surface albedo feedback. Despite this early
120 success, large gaps remain in our understanding of the Arctic climate system that preclude more
121 accurate predictions. In constructing a roadmap for improving Arctic climate projections, we
122 consider the historical evolution of polar amplification science.

123 Early studies employed EBMs—models representing the relationship between Earth’s surface
124 temperature and the top-of-atmosphere (TOA) energy budget—containing many shortcomings and
125 yet captured the essence of polar amplification. Budyko (1966) and Rapikova (1966) demonstrated
126 the fundamental role of surface albedo and the latitudinal position of the snow-ice line in
127 determining polar surface temperature sensitivity to climate forcing. An impressive
128 accomplishment considering that EBMs were informed by little snow and sea ice data and
129 contained invalid assumptions. The most consequential assumption was the exclusion of vertical
130 and horizontal heat transports.

131 The influence of vertical and horizontal heat transports on polar climate was considered in
132 EBMs later in the 1960s. Manabe and Wetherald (1967) found that the damping of vertical heat
133 transport by strong stability at high-latitudes caused a surface albedo perturbation to have a larger
134 effect on near-surface atmospheric temperature than at higher altitudes. Budyko (1969) and Sellers
135 (1969) represented horizontal poleward heat transport zonally-averaged EBMs as horizontal

136 diffusion proportional to the meridional temperature gradient. Sellers (1969) concluded that the
137 specific representation of poleward heat transport had the potential to offset polar amplification.
138 This research illustrated the substantial sensitivity of the polar climate to poleward heat transport
139 and the need to fully resolve the large-scale atmospheric circulation.

140 With this knowledge in hand, WM75 employed a GCM to resolve atmospheric eddies and
141 cemented polar amplification as a prominent feature of the global climate response to increased
142 CO₂. MW75 established the surface-based vertical structure of polar warming, confirmed in
143 modern studies (e.g., Graversen et al. 2008; Serreze et al. 2009), the role of strong atmospheric
144 stability in confining warming near the surface (e.g., Bintanja et al. 2011), and the compensation
145 between increased latent heat (LH) and decreased poleward sensible heat (SH) transport (e.g.,
146 Hwang et al. 2011). While including many simplifications (e.g., idealized geography, fixed clouds,
147 temperature-dependent sea ice and snow albedo, and annual mean insolation), much of our current
148 understanding of polar amplification can be traced to MW75.

149 MS80 extended MW75 by incorporating a mixed-layer ocean and the annual cycle of
150 insolation revealing that polar amplification is strongest in fall and winter and non-existent in
151 summer. The seasonality of polar amplification is partly attributed to the seasonal energy transfer
152 from summer to fall by the ocean (MS80); an explanation also supported by later studies
153 (Washington and Meehl 1984; Wilson and Mitchell 1987). While adding important ocean physics
154 to resolve the annual cycle, MW75 and MS80 did not consider oceanic poleward heat transport.

155 The eventual inclusion of poleward heat transport by ocean currents revealed a relationship
156 between high latitude control climate and global climate sensitivity. Spelman and Manabe (1984)
157 presented fully-coupled atmosphere-ocean simulations capturing the observed climate state with
158 some realism. The inclusion of poleward ocean heat transport yielded warmer high latitude surface

159 temperatures, a poleward shift of the snow and sea ice margin, a weakened albedo feedback, and
160 a reduced climate sensitivity. The influence of control climate surface temperature and sea ice
161 extent on high latitude climate sensitivity was recognized in other studies in relation to the surface
162 albedo parameterization (Budyko 1969; Washington and Meehl 1986) and recently shown to
163 influence CMIP5 inter-model spread (Hu et al. 2017). Rind et al. (1995) illustrated a dependence
164 of simulated sea ice decline on sea ice thickness. Control climate-climate sensitivity relationships
165 are attractive because of the potential ability to constrain model predictions; however, as noted by
166 Washington and Meehl (1986), control climate-climate sensitivity relationships may only be valid
167 when considering the same model.

168 Adding more climate models to the fold revealed the importance of interactions between the
169 ocean and sea ice to the polar climate response. Washington and Meehl (1984; 1986; 1989)
170 performed model simulations with increasingly complex representations of the ocean (swamp,
171 slab, and a coupled ocean circulation model) finding a smaller climate sensitivity and less polar
172 amplification than MW75 and MS80. These differences were attributed to different sea ice albedo-
173 temperature relationships (Washington and Meehl 1984). Additionally, MW75 allowed melt pond
174 formation to change sea ice albedo whereas Washington and Meehl (1984) did not. Washington
175 and Meehl (1989) showed that the regional sea ice distribution was sensitive to the representation
176 of the ocean circulation due to changes in poleward ocean heat transport and deep ocean
177 convection. Further, the manner in which ocean heat is applied to sea ice (e.g., to the bottom or to
178 the bottom and laterally) also strongly influences sea ice melt (Hansen et al. 1984). These early
179 model intercomparisons demonstrated their value for identifying key uncertainties.

180 Extracting maximum value from model comparisons requires diagnostic techniques that
181 consistently quantify the causes of model differences (Coakley 1977; Ramanathan 1977; Hansen

182 et al. 1984; Washington and Meehl 1986; Dickinson et al. 1987; Wetherald and Manabe 1988;
183 Section 4). Many of these studies focus on the surface albedo feedback, diagnosing it using slightly
184 different methods, and finding large inter-model differences. However, the inter-model differences
185 in the surface albedo feedback were mainly due to the different methods (Ingram et al. 1989).
186 Methods were also developed to diagnose all TOA radiative feedbacks (Hansen et al. 1984;
187 Wetherald and Manabe 1988). Moreover, Cess and Potter (1988) developed a methodology
188 designed to assess cloud feedback. Feedback diagnostic methods paved the way for broader model
189 intercomparisons and enabled a consistent understanding of why projections differ (see Section 4).

190 Early multi-model intercomparisons identified snow and sea ice albedo feedbacks and their
191 interactions with cloud feedback as a key polar climate uncertainty. The first large-scale,
192 coordinated climate model intercomparison occurred in the late 1980s finding a three-fold
193 difference in global climate sensitivity mainly due to cloud feedback differences (Cess et al. 1989;
194 1990). Using a similar set of models, Cess et al. (1991) reported substantial snow-albedo feedback
195 differences; interestingly, these differences stemmed not only from the snow-albedo treatment but
196 also from interactions with clouds. Given the demonstrated value of using the large-scale model
197 intercomparisons to indicate uncertainty, model intercomparison projects (MIPs) emerged as a
198 major research theme and continue to be a valuable resource for hypothesis testing, identifying
199 sources of projection uncertainty, and for informing climate observation system requirements (e.g.,
200 Wielicki et al. 2013).

201 In the 1990s, aided by improved computational capabilities, transient climate change
202 simulations became widespread alongside MIPs and advanced our understanding of the
203 interactions between ocean and atmosphere circulation and polar climate. A decade earlier, Bryan
204 et al. (1982) made the first attempt to simulate the transient climate response using a 1% per year

Non-peer reviewed EarthArXiv preprint submitted to Frontiers in Earth Science to the “Arctic Amplification: Feedback Process Interactions and Contributions” Research Topic.

205 CO₂ increase experiment finding different high- and low-latitude transient responses. Subsequent
206 transient experiments show a profound influence of the ocean circulation on the spatial distribution
207 of Arctic warming with slower warming over the ocean and in regions of deep water formation
208 (e.g., northern North Atlantic) and faster warming over land (Washington and Meehl 1989;
209 Manabe et al. 1991; Washington and Meehl 1996; Meehl et al. 2000). Manabe et al. (1992) argued
210 that the land-ocean warming contrast affects the land precipitation and soil moisture response by
211 delaying latent heat transport from ocean to land. Washington and Meehl (1989) found a time-
212 dependence of the high-latitude atmospheric circulation response suggesting that there may not be
213 a single atmospheric circulation pattern that amplifies monotonically with increased forcing. While
214 advancing our knowledge of the transient Arctic climate response, these studies did not change the
215 underlying understanding of the physical drivers of polar amplification.

216 In the 2000s, the mounting observed changes in the Arctic spurred a newfound urgency and
217 polar amplification began appearing as a unique research topic, as opposed to an aspect of CO₂-
218 induced climate change. Studies using multi-decadal records of Arctic temperature, snow cover,
219 and sea ice became prominent and enabled the verification of many early predictions of AA
220 including its fall/winter maximum, bottom-heavy structure, and the prominence of surface albedo
221 feedback (e.g., Serreze et al. 2009; Graversen et al. 2008; Pistone et al. 2014). This application of
222 observations is in sharp contrast to the 1980s when the quality and quantity of observations limited
223 their use to control climate tuning. Multi-decadal observations further enabled studies of emergent
224 constraints—relationships between an uncertain aspect of climate projections and an observable
225 quantity (e.g., Hall and Qu 2006; Caldwell et al. 2014; Hall et al. 2019). MIP activities revealed
226 that sea ice extent and thickness, ocean heat transport, and clouds were key sources of inter-model
227 differences (Holland and Bitz 2003) and potential emergent constraints.

228 Several studies in the early 2000s altered the trajectory of polar amplification research by
229 showing that polar amplification was possible without the surface albedo feedback. First,
230 aquaplanet experiments by Alexeev (2003) illustrated polar amplification in the absence of sea ice.
231 Second, coupled GCM experiments with a suppressed surface albedo feedback showed polar
232 amplification, albeit weaker (Hall 2004). These results appear at odds with earlier studies also
233 suppressing the surface albedo feedback that concluded the sea ice albedo feedback was necessary
234 for polar amplification (e.g., Ingram et al. 1989; Rind et al. 1995). The Ingram et al. (1989)
235 modeling setup prohibited ocean energy transfer across seasons, which may explain the different
236 conclusion; the reason for the difference with Rind et al. (1995) is unclear. Studies argue that
237 poleward heat transport produces polar amplification due to an increased efficiency, as poleward
238 traveling air is warmer and moister than before (Alexeev et al. 2005; Cai 2005). Differences in
239 insolation and clouds are also possible explanations and can control the existence of polar
240 amplification (Kim et al. 2018). This debate continues (Section 5e) and these studies mark an
241 inflection point in our thinking on the role of atmospheric poleward heat transport in polar
242 amplification.

243 Since 2010, studies have focused on using observations and coupled models synergistically to
244 understand polar amplification, including a reemergence of idealized model set-ups (e.g., Chung
245 and Räisänen, 2011; Feldl et al., 2017; Yoshimori et al., 2017; Park et al., 2018; Shaw and Tan,
246 2018; Stuecker et al., 2018; Semmler et al., 2020). New satellite data sets (Loeb et al. 2018; Kato
247 et al. 2018; Boisvert et al. 2013; Winker et al. 2010; Duncan et al. 2020) and more sophisticated
248 meteorological reanalysis are enabling factors (Screen and Simmonds 2010; Boisvert and Stroeve
249 2015). Key outcomes of recent work include confirming the role of ocean heat storage, seasonal
250 energy transfer, and the surface turbulent flux response on AA and inter-model spread (Screen and

Non-peer reviewed EarthArXiv preprint submitted to Frontiers in Earth Science to the “Arctic Amplification: Feedback Process Interactions and Contributions” Research Topic.

251 Simmonds 2010; Boeke and Taylor 2018; Kim and Kim 2019; Dai et al. 2019). Studies continue
252 to focus on understanding atmosphere, sea ice, and ocean processes with a keen focus on coupling.
253 Idealized model simulations have been combined with observations to understand shorter time
254 scale atmosphere-ocean-sea ice interactions, including links between air-mass transformation and
255 Arctic climate (e.g., atmospheric rivers and cold air outbreaks; Pithan et al. 2018). Additionally,
256 large single-model initial condition ensembles (e.g., Kay et al. 2015) hold incredible value for
257 understanding the impact of internal variability on observed and projected trends. Studies continue
258 to leverage the trove of information available from MIP activities including the first Polar
259 Amplification MIP (PAMIP; Smith et al. 2019). While our understanding of polar amplification
260 has advanced since Arrhenius, substantial uncertainty remains in polar climate projections
261 warranting continued research.

262 **3. Observational perspectives**

263 Sustained polar observations (satellite, ground-based, and airborne) have enabled the
264 identification of many fundamental characteristics of AA and the verification of early modeling
265 results. Technological advances in polar observation have led to higher quality data records and a
266 broader set of observed variables. Developments in meteorological, oceanic, and sea ice reanalysis
267 have made these a primary source of Arctic climate information and are invaluable to AA science.
268 In addition to multi-decadal records, observational capabilities now provide near-real time

269 monitoring of the Arctic, elevating the episodic nature and interconnectedness of the region to the
270 forefront of Arctic science. Detailed process-oriented observations reveal how sea ice, ocean and

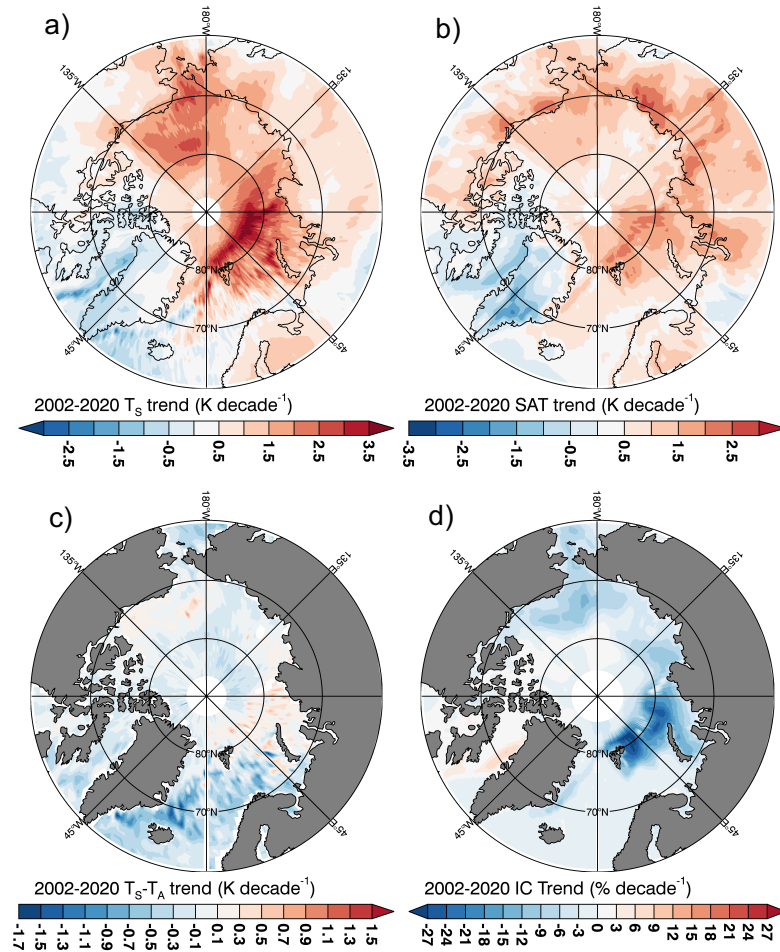


Figure 2: Recent changes in the Arctic surface climate.

Linear, annual mean trends from 2002-2020 for (a) skin temperature ($K\ decade^{-1}$), (b) surface air temperature ($K\ decade^{-1}$), (c) skin and surface air temperature difference ($K\ decade^{-1}$), and (d) sea ice concentration ($\%\ decade^{-1}$) from the Atmospheric Infrared Sounder (AIRS; Susskind et al. 2014) and passive microwave sea ice concentration data (Cavalieri et al. 1996).

atmosphere interact and which processes shape the surface energy budget (SEB; e.g., Uttal et al. 2002, Shupe et al. 2020).

Since 1960, the Arctic has warmed faster than any other region of the planet (Fig. 1). The zonal average surface temperature trends poleward of $60^{\circ}N$ range from ~ 0.3 to $0.7\ K\ decade^{-1}$ and are strongest near the pole. Spatially, Arctic surface temperature trends range from ~ 0.1 to $0.8\ K\ decade^{-1}$ with the largest warming

coinciding with substantial sea ice concentration declines (Fig. 2). The seasonal contrast in Arctic surface warming is also evident (Fig. 3) with

289 maximum warming in December-January-February (DJF), minimum warming in June-July-
290 August (JJA), and substantial warming in September-October-November (SON) and March-April-
291 May (MAM). Figure 3 indicates a spatial variation of the seasonal surface warming pattern that

292 coincides with the seasonality of sea ice loss modulated by atmospheric circulation variability
293 (Ding et al. 2017; Dai et al. 2019). The characteristic surface-based warming profile is evident in
294 the 1979-2020 ERA5 annual, zonal mean atmospheric temperature trends with surface trends
295 exceeding $0.8 \text{ K decade}^{-1}$ decreasing to $\sim 0.4 \text{ K decade}^{-1}$ at 300 hPa (Fig. 4).

296 Arctic sea ice cover and thickness have declined dramatically since 1979, further evidence that
297 sea ice is a key aspect of observed AA (Screen and Simmonds 2010; Dai et al. 2019). September
298 sea ice extent has declined more rapidly than during any other month, $\sim 13\% \text{ decade}^{-1}$ (e.g.,
299 Comiso and Hall 2014; Parkinson and Di Girolamo 2016). September sea ice volume has declined
300 by $>70\%$ since the early 1980s (Schweiger et al. 2011; Kwok 2018). The Arctic sea ice melt season
301 has also lengthened by $5\text{-}10 \text{ days decade}^{-1}$ over the last four decades (earlier melt onset and later
302 freeze-up) with larger regional changes (Parkinson 2014; Markus et al. 2009; Stroeve et al., 2014;

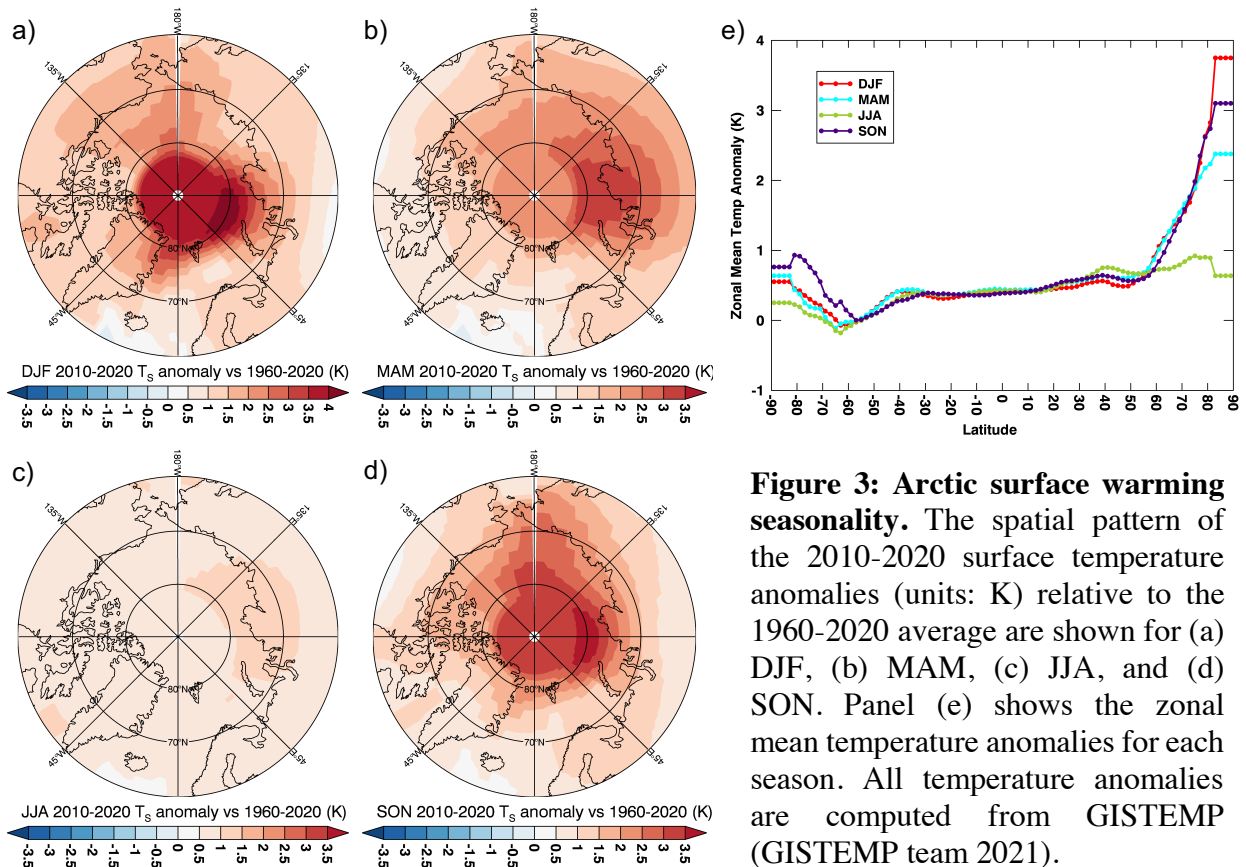
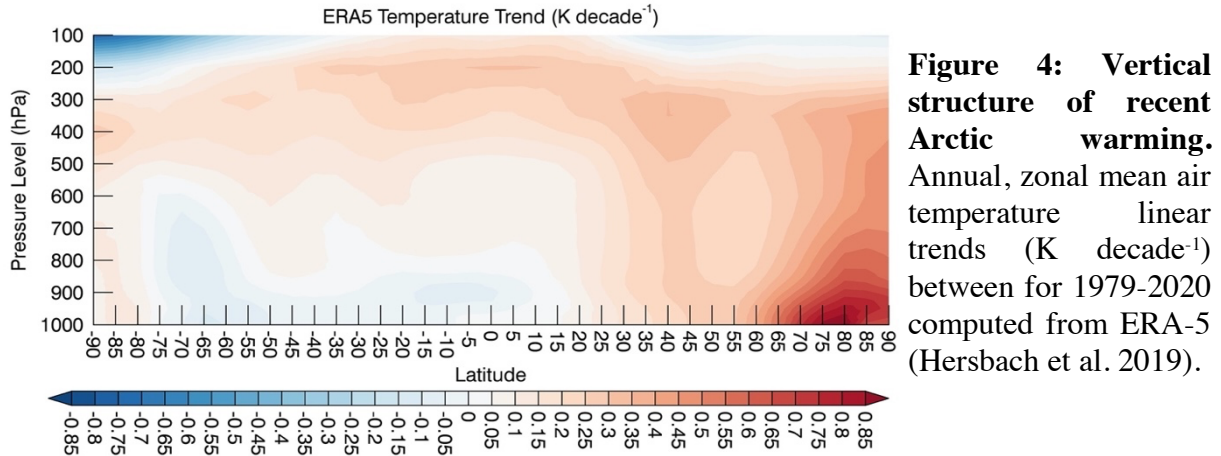


Figure 3: Arctic surface warming seasonality. The spatial pattern of the 2010-2020 surface temperature anomalies (units: K) relative to the 1960-2020 average are shown for (a) DJF, (b) MAM, (c) JJA, and (d) SON. Panel (e) shows the zonal mean temperature anomalies for each season. All temperature anomalies are computed from GISTEMP (GISTEMP team 2021).

303 Bliss and Anderson 2018). The thinner and less expansive sea ice cover is more susceptible to
304 thermodynamic and dynamic forcing (Hibler 1979; Maslanik et al., 1996; Hegyi and Deng 2017;
305 Zhao et al., 2018; Huang et al. 2019a) promoting earlier and more rapid spring melting (Maslanik
306 et al., 2007; Markus et al., 2009; Stroeve et al., 2014; Bliss and Anderson, 2018), contributing to
307 the observed AA.



308 The Arctic SEB has responded to the sea ice and temperature trends. Clouds and Earth’s
309 Radiant Energy System (CERES) data show strong trends in TOA and surface energy fluxes in
310 the Arctic (Loeb et al. 2018; Kato et al. 2018). Surface albedo has declined by $\sim 0.03\text{-}0.04$ decade⁻¹
311 over the central Arctic (Duncan et al. 2020) suggesting an additional ~ 1.2 Wm⁻² decade⁻¹ of
312 shortwave (SW) energy deposited in the Arctic Ocean since 2000 (Fig. 5). Strong SH and LH flux
313 increases (Fig. 5) have also occurred, coinciding with sea ice loss (Screen and Simmonds 2010;
314 Boisvert et al. 2013; 2015; Taylor et al. 2018). Importantly, polar radiative (SW and longwave
315 (LW)) and turbulent (SH and LH) energy flux observations contain substantial uncertainties—5-
316 20 Wm⁻² and 20%, respectively—that stymie studies of climate-relevant processes (Kato et al.
317 2018; Boisvert et al. 2015; Taylor et al. 2018).

318 Several key insights are gleaned from the observed Arctic changes. First, the spatially
319 coincident changes in the Arctic surface temperature, sea ice, and SEB demonstrates the

320 importance of atmosphere, sea ice,
321 and ocean coupling to observed
322 Arctic changes. Second,
323 observations verify the existence of
324 AA and key characteristics
325 including its seasonal, vertical, and
326 spatial structure. Lastly, the
327 expected SEB changes (e.g.,
328 reduced surface albedo and
329 increased SH and LH fluxes) are
330 observed, although observational
331 uncertainty limits progress.

332 4. Modeling perspectives

333 A hierarchy of models have
334 been used to advance AA science.
335 This evolution in modeling studies
336 coincided with advances in
337 computational capabilities and
338 trends towards increased
339 complexity beginning with EBMs
340 (Budyko 1966;1969; Sellers 1969),
341 simplified/idealized atmospheric

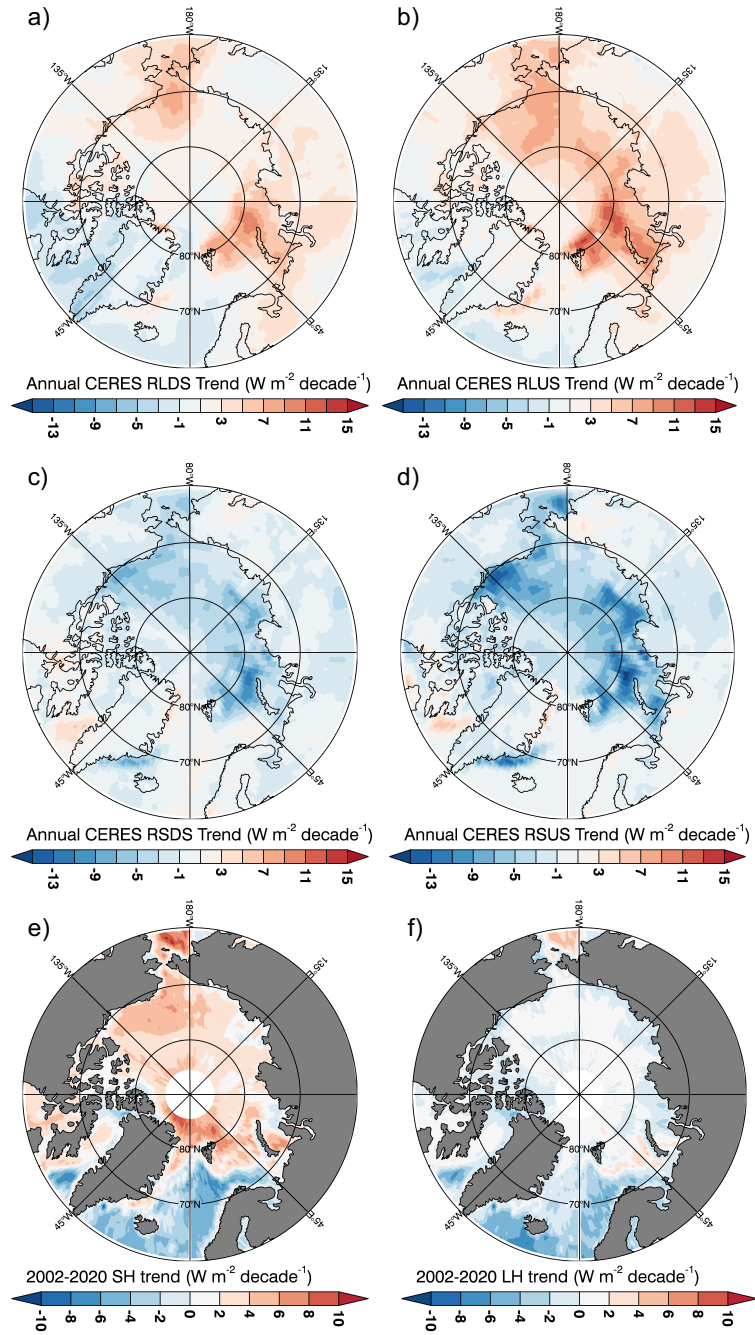


Figure 5: Recent changes in the Arctic surface energy budget. Linear, annual mean trends from 2002-2020 for surface (a) downwelling LW radiation, (b) upwelling LW radiation, (c) downwelling SW radiation, and (d) upwelling SW radiation, (e) sensible heat, and (d) latent heat flux trends ($W m^{-2} decade^{-1}$). Radiation data is taken from CERES (Kato et al. 2018) and SH and LH fluxes is derived from AIRS (Boisvert et al. 2013).

342 GCMs (MW75; MS80; Alexeev et al 2005), atmospheric GCMs (Washington and Meehl 1984),
343 coupled atmospheric-ocean GCMs (Bryan et al. 1982; Spelman and Manabe 1984; Washington
344 and Meehl 1989), and now Earth System Models. The march from idealized to complex progressed
345 piecewise, one new component at a time, providing insight into the influence of various climate
346 system components on Arctic climate.

347 The less complex, computationally-constrained models of the 1980s identified fundamental
348 features of AA that have withstood observational evidence and the scrutiny of more complex
349 models. These features include the magnitude of AA (~2-3 times global mean warming),

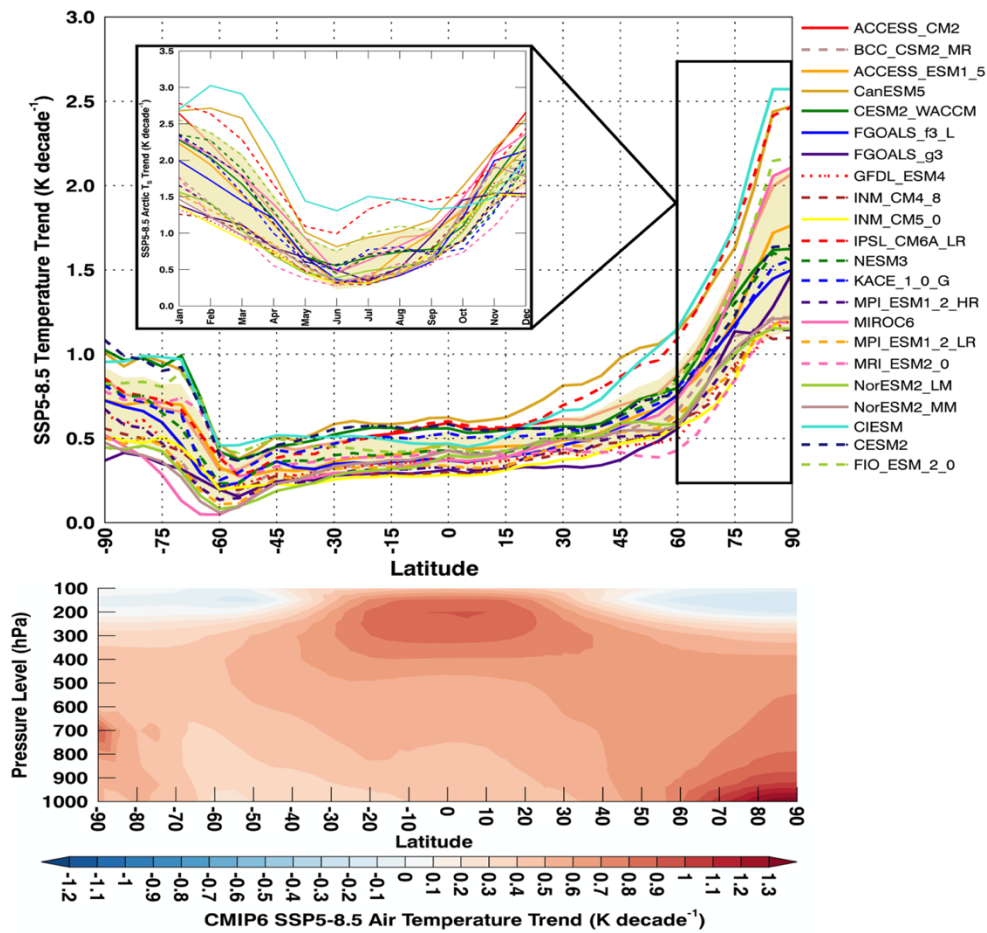


Figure 6: Arctic Amplification in CMIP6. (a) Zonal mean temperature trends (K decade⁻¹) for 22 CMIP6 models from the SSP5-8.5 simulation. Yellow shading represents the ensemble mean ± 1 inter-model standard deviation. The inset depicts the seasonal cycle of temperature trends for the Arctic domain (poleward of 60°N). (b) The vertical profile of zonal mean temperature trends (K decade⁻¹) for CMIP6 ensemble mean is shown.

350 seasonality and spatial variation of Arctic warming, bottom-heavy/surface-based profile, increased
351 poleward LH transport, and the acceleration of the hydrologic cycle. Reduced-complexity models
352 also captured the fundamental processes influencing the Arctic response to increased CO₂
353 including the sea ice and snow surface albedo, poleward atmospheric and oceanic heat transports,
354 seasonal energy transfer, atmosphere-sea ice-ocean coupling, and cloud radiative effects. While
355 increasingly complex and more realistic contemporary models provide similar insights into AA
356 (Fig. 6), they also provide refined quantitative estimates of process contributions and enable more
357 reliable projections of future climate. While no one argues for a return to reduced-complexity
358 representations of sea ice, clouds, and the ocean to produce climate projections, reduced-
359 complexity models enable an intuitive understanding of climate processes that is hard to glean
360 from comprehensive models (Held 2005, Jeevanjee et al. 2017, Maher et al. 2019).

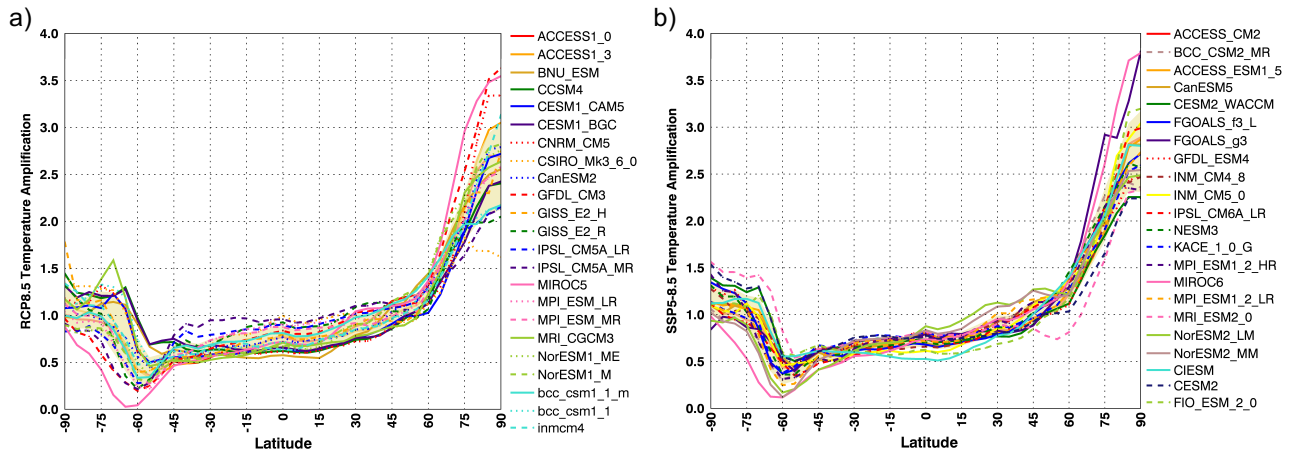


Figure 7: Arctic Amplification and Contemporary Climate Models. Zonal mean Arctic Amplification factor (ratio of zonal average to global mean surface temperature change) for (a) CMIP5 RCP8.5 and (b) CMIP6 SSP5-8.5. The surface temperature change is computed as the difference between the 2080-2100 and the 2015-2025 periods.

361 Climate community organization around MIP activities play a key role in AA science by
362 providing inputs for climate projections and uncertainty assessments. Model intercomparison
363 activities have grown from 14 models (Cess et al. 1989) to >40 models in Coupled MIP 5 and 6
364 (CMIP5 and 6) allowing for a robust assessment of inter-model spread. Considering the two most

Non-peer reviewed EarthArXiv preprint submitted to Frontiers in Earth Science to the “Arctic Amplification: Feedback Process Interactions and Contributions” Research Topic.

365 recent CMIPs, the overall spread in the AA factor (defined as the ratio of Arctic-to-global mean
366 warming) at the end of the 21st Century for the CMIP5 RCP8.5 (Taylor et al. 2012) and CMIP6
367 SSP8.5 scenarios (Eyring et al. 2016) has not narrowed significantly (Fig. 7). However, no CMIP6
368 model with the available output simulates an AA factor <2 . MIPs have also expanded to dedicated
369 projects organized around scientific themes, including the first Polar Amplification MIP (PAMIP;
370 Smith et al. 2019). Details on advances from model intercomparison studies can be found in
371 Sections 2 and 5.

372 Innovative modeling approaches and experimental designs are being developed to test AA
373 hypotheses, including a revitalization of idealized experiments. Specific results are covered in the
374 feedback diagnostics section and Section 5. The complementary use of complex and idealized
375 model experiments is a critical component of advancing AA science.

376 *Arctic feedback diagnosis frameworks*

377 Frameworks quantifying how forcings and feedbacks contribute to AA can be classified into
378 the following: energy budget-based diagnostics, mechanism denial experiments, latitudinally-
379 constrained or otherwise idealized forcing, and sea ice forcing experiments.

380 Energy budget decompositions have been widely used to diagnose climate feedback
381 contributions to surface warming. Individual feedback contributions are evaluated as climate
382 feedback parameters that quantify the global mean TOA energy flux perturbation per unit of
383 surface warming (e.g, Wetherald and Manabe 1988; Soden and Held 2006; Shell et al. 2008; Huang
384 et al. 2017, Pendergrass et al. 2018). Although this method assumes that feedbacks are linear and
385 additive, neural networks can account for nonlinearity (Zhu et al. 2019). The energy budget
386 decomposition method can also quantify the influence of regional feedbacks on the warming
387 pattern alongside the radiative forcing, atmospheric energy transport, and ocean heat uptake

388 (Colman 2002; Crook et al. 2011; Taylor et al. 2011a; Taylor et al. 2011b; Feldl and Roe 2013;
389 Armour et al. 2013; Pithan and Mauritsen 2014).

390 A complementary approach uses the SEB, which is important in the Arctic where the physical
391 validity of the TOA framework is questioned (Pithan and Mauritsen 2014; Payne et al. 2015;
392 Goosse et al. 2018; Henry et al. 2021). Similar to the TOA, the contributions of individual SEB
393 terms to surface temperature change can be diagnosed (Lu and Cai 2009a; Pithan and Mauritsen
394 2014; Sejas et al. 2014; Laine et al, 2016; Sejas and Cai 2016; Boeke and Taylor 2018). A SEB
395 decomposition includes additional non-radiative terms (surface turbulent fluxes and ocean heat
396 storage) that are especially important when considering the surface temperature response
397 seasonality.

398 An expansion of the SEB approach is the coupled atmosphere surface climate feedback
399 response analysis method (CFRAM)—a vertically-resolved version of the energy budget
400 decomposition method (Lu and Cai 2009b; Cai and Lu 2009; Taylor et al. 2013). CFRAM provides
401 a three-dimensional analysis of feedback contributions to the surface and atmospheric temperature
402 response from radiative processes and non-radiative processes (convection, condensational
403 heating, surface turbulent fluxes, and horizontal heat transport) (Song et al. 2014; Yoshimori et al.
404 2014). CFRAM does not include a lapse rate feedback and provides a clearer diagnosis of the
405 process contributions to the vertical warming structure. However, the CFRAM is computationally
406 expensive and computes heat transports as a residual; explicitly calculated heat transport terms are
407 straightforward to include in CFRAM however these terms are not routine model outputs. A
408 disadvantage of all energy budget decompositions is that they do not provide clear insights into
409 how different feedbacks are coupled. For example, the radiative sensitivity to albedo changes

410 varies by a factor of two across climate models in the Arctic and Southern Ocean due to inter-
411 model differences in mean-state cloudiness (Donohoe et al., 2020).

412 Mechanism denial experiments—model simulations where a physical process is “turned off”
413 or locked—also provide insights into the role of various feedbacks (e.g., Wetherald and Manabe
414 1988; Ingram et al. 1989; Rind et al. 1995; Hall 2004; Vavrus 2004; Graversen and Wang 2009).
415 These studies analyze differences between climate model simulations with a specific process
416 “turned off” and experiments with the process “turned on,” such as sea ice albedo locking (e.g.,
417 Graversen et al. 2014), cloud locking (Vavrus 2004; Middlemas et al. 2020), and atmospheric heat
418 transport divergence locking experiments (Graversen and Langen 2019). This approach highlights
419 the coupling between processes that energy budget decomposition approaches cannot (Merlis
420 2014). The disadvantages of mechanism denial experiments are that they can modify the reference
421 climate, introduce compensating effects, are challenging to apply to comprehensive climate
422 models, and the results are difficult to compare with observations.

423 Lastly, different modelling protocols have been designed to understand the local and remote
424 mechanisms to AA. Regionally applied greenhouse gas forcing experiments (Section 5e) are one
425 such protocol designed to separate these contributions to Arctic warming (Alexeev et al. 2005;
426 Chung and Räisänen 2011; Yoshimori et al. 2017; Stuecker et al. 2018; Shaw and Tan 2018).
427 Another protocol isolates local and remote mechanisms by prescribing local and remote changes
428 in sea surface temperature and sea ice concentration. Using this approach, Screen et al. (2012)
429 attribute near-surface Arctic warming to local feedbacks and upper tropospheric warming to
430 remote processes. Recent years have seen a proliferation of modeling experiments in which the
431 sea ice component of a coupled ocean-atmosphere model is perturbed, including albedo reduction
432 (e.g., Blackport and Kushner 2016; Liu and Fedorov, 2019), LW emissivity manipulation (e.g.,

Non-peer reviewed EarthArXiv preprint submitted to Frontiers in Earth Science to the “Arctic Amplification: Feedback Process Interactions and Contributions” Research Topic.

433 Liu et al. 2019); sea-ice ghost forcing (e.g., Deser et al. 2015), ocean heat flux adjustment (Oudar
 434 et al. 2017), and sea ice nudging (McCusker et al. 2017, Smith et al. 2017). Although they all
 435 produce a consistent atmospheric circulation response (Screen et al. 2018), the various protocols
 436 make different and confounding assumptions regarding conservation of energy and melt water.

437 Each diagnostic method has strengths and weaknesses (Table 1) associated with technical
 438 aspects and underlying assumptions. These differences confound the ability to clearly assess the
 439 process contributions to AA. The community needs to address this issue to advance AA science.

440 **Table 1: Summary of feedback diagnostic frameworks. The selected example reference in**
 441 **the right column represents a single study that demonstrates each framework.**

Diagnosis framework	Pros	Cons	Example reference
Global/Regional TOA (or surface) energy budget decomposition	<ul style="list-style-type: none"> • Easy to apply to comprehensive model output and model intercomparisons • Compares all the feedbacks 	<ul style="list-style-type: none"> • Assumes linearity and does not provide insights into how different feedbacks are coupled • Lapse rate feedback conceptually unclear at high latitudes in TOA frameworks 	Pithan and Mauritsen 2014
Coupled Feedback Response Analysis Method (CFRAM)	<ul style="list-style-type: none"> • 3D analysis of feedback contributions • Resolves process contributions to vertical warming profile 	<ul style="list-style-type: none"> • Does not provide insights into how different feedbacks are coupled • Computationally expensive 	Taylor et al. 2013
Mechanism denial	<ul style="list-style-type: none"> • Tests how a given process interacts with different feedbacks 	<ul style="list-style-type: none"> • Hard to implement in comprehensive models • Modifies the reference climate state 	Graversen and Wang 2009

Idealized forcing		Stuecker et al. 2018
	<ul style="list-style-type: none">• Compares roles of local and remote forcings and feedbacks	<ul style="list-style-type: none">• Separation between local and remote is sometimes unclear
Sea ice forcing		Screen et al. 2018
	<ul style="list-style-type: none">• Tests the importance of sea ice for Arctic warming.	<ul style="list-style-type: none">• Differing assumptions regarding conservation of energy and melt water.
Neural network		Zhu et al. 2019
	<ul style="list-style-type: none">• Captures nonlinear feedbacks either due to large perturbation or coupling effects, e.g. cloud-masking of the albedo and water vapor feedbacks	<ul style="list-style-type: none">• The valid value range and accuracy of predicted feedbacks depends on the training dataset

442

443 **5. Arctic Amplification Factors and Processes**

444 **a. Sea ice feedbacks**

445 Sea ice and snow cover changes via the positive surface albedo feedback are a principal driver
446 of AA (Arrhenius 1896; Budyko 1969; MW75; Hall 2004). The surface albedo feedback operates
447 when (high albedo) sea ice and snow cover melts and reduces surface albedo by uncovering the
448 (low albedo) ocean and land surfaces underneath. Reducing surface albedo causes greater
449 absorption of solar radiation that warms the surface and drives additional sea ice and snow melt.
450 Studies estimate that the sea ice-snow albedo feedback is responsible for 30 to 60% of the total
451 CO₂-induced Arctic warming (Dickinson and Meehl 1987; Hall 2004; Taylor et al. 2013; Boeke
452 and Taylor 2018; Duan et al. 2019) and is the largest local Arctic feedback (Taylor et al. 2013,
453 Yoshimori et al. 2014; Goosse et al. 2018). Multi-centennial climate simulations show that Arctic

454 warming slows after most of the sea ice melts, further highlighting the importance of sea ice
455 changes (Bintanja and van der Linden 2013; Dai et al. 2019).

456 The surface albedo feedback has substantially contributed to the observed Arctic warming.
457 Observations of a reduced snowpack (Warren et al., 1999; Brown and Robinson 2011; Webster et
458 al., 2014) and significant declines in sea ice extent, thickness, and age since 1979 indicate a
459 reduced Arctic surface albedo (Parkinson and DiGirolamo, 2016; Nghiem et al. 2007, Maslanik et
460 al., 2011; Kwok, 2018). Additionally, the albedo of multi-year sea ice has decreased (Riihelä et al.
461 2013). Perovich et al. (2007) computed that reduced surface albedo has increased the solar energy
462 deposited into the Arctic Ocean by 89% from 1979-2005. CERES data indicate a -0.025 ± 0.004
463 decade^{-1} Arctic average albedo decline and a $+1.2\text{-}1.3 \text{ Wm}^{-2} \text{ decade}^{-1}$ increase in absorbed TOA
464 solar radiation between 2000 and 2018 (Duncan et al. 2020).

465 The surface albedo feedback has contributed substantially to the inter-model spread in Arctic
466 warming across multiple generations of intercomparisons (Cess et al. 1991; Holland and Bitz,
467 2003; Hu et al. 2020). This uncertainty results from the complexities of modeling the continuously
468 evolving sea ice and snow coverage, thickness, and optical properties (Zhang et al., 2000; Laxon
469 et al., 2003)—processes for which available data is insufficient. Furthermore, the rapidly evolving
470 factors that govern surface albedo (e.g., snow and sea ice thickness distribution, topography, drift,
471 melt pond and floe size distribution) occur at small scales making parameterization challenging
472 (Schweiger et al., 2011; Stroeve et al., 2014; Holland et al., 2010; 2012; Jahn et al., 2012).

473 Sea ice and snow also modulate surface turbulent energy fluxes giving rise to the sea ice
474 insulation feedback. This feedback operates when changes in sea ice concentration and snow and
475 ice thickness alter the non-radiative surface fluxes (sea ice conductance and surface turbulent
476 fluxes; Burt et al. 2016). Sea ice loss exposes a larger area of the Arctic Ocean to the atmosphere

477 and allows for a freer exchange of water vapor, aerosol particles, energy, and momentum with the
478 atmosphere. The sea ice insulation feedback is strongest where there are large surface and near
479 surface air temperature differences collocated with reduced sea ice cover (Serreze et al., 2009;
480 Screen and Simmonds 2010a;b; Boisvert and Stroeve, 2016; Boisvert et al., 2015; Boeke and
481 Taylor 2018; Taylor et al., 2018). In addition, thinner and less snow-covered sea ice promotes
482 greater heat conduction through sea ice (MS80; Rind et al. 1995; Persson et al. 2016). Through
483 these mechanisms, the ice insulation feedback warms and moistens the lower Arctic atmosphere
484 promoting additional warming via an enhanced greenhouse effect (Kim et al. 2016; Boeke and
485 Taylor 2018; Kim et al. 2019; Feldl et al. 2020; Chung et al. 2020).

486 Sea ice cover influences the Arctic SEB differently during polar day and night and in both
487 cases strongly impacts surface temperature (Fig. 8). Less sea ice cover during polar day decreases
488 the surface albedo and increases SW absorption. Less sea ice cover also promotes larger ocean
489 waves due to longer fetches that have the potential to mechanically break-up sea ice (Rogers et al.
490 2016). The greater effective heat capacity of the ocean relative to sea ice suppresses warming
491 caused by the surface energy gain during polar day, leading to ocean heat storage and a delayed
492 sea ice freeze up (Dwyer et al. 2012). During polar night, less sea ice cover corresponds to a
493 warmer surface temperature, weaker static stability, and larger upwards surface turbulent fluxes.
494 Moreover, the temperature over ocean is constrained to the freezing point whereas the sea ice
495 surface temperature can vary. Atmospheric temperature tends to be warmer in regions with less
496 sea ice in part due to the warming and moistening of the lower atmosphere by increased surface
497 turbulent fluxes, increasing downwelling LW (DLW) radiation. The greater ocean effective heat

498 capacity also changes the relationship between DLW and upwelling LW (ULW); over sea ice
 499 surface DLW anomalies do not lead to strong net LW flux imbalances because sea ice temperature
 500 quickly warms in response (Persson et al. 2016; Hegyi and Taylor 2018). These differences in the

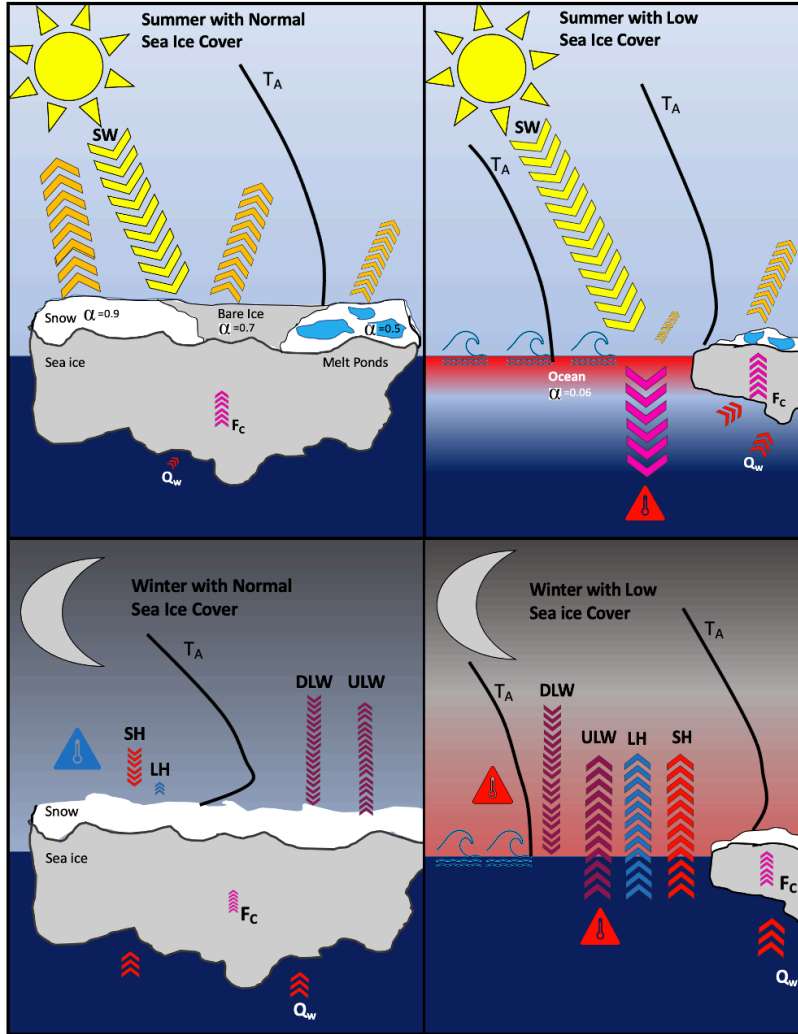


Figure 8: Modulation of surface energy fluxes by sea ice. A schematic illustration of the sea ice albedo and ice insulation feedbacks and associated surface energy budget changes from sea ice loss: shortwave (SW), downwelling longwave (DLW), upwelling LW (ULW), sensible heat (SH), latent heat (LH), conductive heat flux through sea ice (F_c) and oceanic heat flux to sea ice (Q_w). The black line represents the characteristic atmospheric temperature profiles (T_A) over ocean and sea ice during polar day and night.

519 uniform warming (the lapse rate feedback).

SEB response to a sea ice change during polar day and night are key components of our conceptual model (Section 6).

b. Temperature feedbacks

Temperature feedbacks are major contributors to AA and contribute substantially to the inter-model differences in CMIP5 (Pithan and Mauritsen 2014). Temperature feedbacks are related to the efficiency of radiative cooling to space and are decomposed into contributions from a vertically-uniform temperature change (the Planck feedback) and the effect of the deviation from a vertically-

520 The Planck feedback contribution to AA originates from the nonlinearity of blackbody
521 radiation with temperature, such that at colder temperatures, a larger increase in temperature is
522 required to increase outgoing LW radiation (OLR) by 1 W m^{-2} . The Planck feedback is negative at
523 all latitudes and contributes to AA because it is more negative at warmer low latitudes. However,
524 this nonlinearity effect may be small. Henry and Merlis (2019) replace the nonlinear temperature
525 dependence of blackbody radiation with a linearized version in an idealized moist GCM and find
526 that it does not modify the surface temperature change pattern, as energy transport and lapse rate
527 changes compensate.

528 The lapse rate feedback contribution to AA originates from the meridional gradient of the
529 feedback sign, negative at low latitudes and positive at high latitudes. In the tropics, convection
530 pins the atmospheric temperature profile to the moist adiabat leading to a larger warming in the
531 upper troposphere than at the surface. This “top-heavy” vertical warming structure leads to a larger
532 increase in OLR per unit increase in surface temperature—a negative lapse rate feedback. By
533 contrast, the Arctic lapse rate feedback is positive because stable stratification promotes bottom-
534 heavy warming. At high-latitudes, the atmosphere is close to radiative-advective equilibrium
535 causing the lapse rate feedback to depend on the type of perturbation: a change in greenhouse
536 forcing, for example, has a more bottom-heavy temperature response than a change in atmospheric
537 heat transport (Payne et al. 2015, Cronin and Jansen, 2016).

538 This dependence on perturbation type presents a challenge in determining the relative
539 importance of radiative, surface-based, and advective controls on the lapse rate feedback. In the
540 absence of a surface albedo feedback, Henry et al. (2020) find that the increase in CO_2 and water
541 vapor alone cause a surface-enhanced warming, consistent with analytic column model results
542 (Cronin and Jansen 2016). Song et al. (2014) argue that the water vapor and albedo feedbacks

543 cause the positive Arctic lapse rate feedback. Mechanism denial experiments reveal that the
544 surface albedo feedback enhances the high-latitude lapse rate feedback (Graversen et al. 2014,
545 Feldl et al. 2017a), or equivalently surface-amplified warming is found in targeted sea ice loss
546 experiments (e.g., Screen et al. 2018). Further, the Arctic lapse rate feedback is strongly correlated
547 across models with summer sea ice loss and cold-season increases in surface turbulent heat fluxes
548 (Feldl et al. 2020; Boeke et al. 2021). Atmospheric energy transport changes tend to reduce the
549 Arctic lapse rate feedback (Feldl et al. 2020) via increases in moist energy transport and decreases
550 in dry energy transport that warm the mid-troposphere and cool the near-surface atmosphere
551 (Henry et al. 2020). Moreover, the decrease in dry transport is strongly controlled by the surface
552 albedo feedback strength (Feldl et al. 2017b, Henry et al. 2020). The high latitude lapse rate
553 feedback results from the sum of these different processes with strong evidence for the importance
554 of surface processes (Cai and Lu 2009; Boeke et al. 2021).

555 From the surface perspective, the temperature feedback manifests as increased DLW radiation
556 due to atmospheric warming, warming the surface and increasing ULW radiation. The coupling
557 between increased DLW and ULW via the greenhouse effect constitutes a positive feedback loop
558 amplifying surface and atmospheric warming (Sejas and Cai 2016, Vargas Zeppetello et al. 2019).
559 Previous studies argue that this feedback accounts for most of the Arctic surface warming (Pithan
560 and Mauritsen 2014; Sejas and Cai 2016; Laîné et al. 2016). Additional studies point to the
561 importance of increased clear-sky DLW on the fall/winter Arctic warming maximum (Lu and Cai
562 2009; Boeke and Taylor 2018). Though important to AA, the surface perspective of the
563 temperature feedback does not provide clear insight into the processes that trigger it.

564 **c. Cloud feedbacks**

565 Cloud processes modulate the radiative fluxes and thermodynamic structure of the Arctic
566 atmosphere (Vihma et al. 2014). The TOA Arctic cloud feedback in CMIP5 is generally negative
567 (Zelinka et al. 2012) and is positive from the surface perspective (Taylor et al. 2013; Boeke and
568 Taylor 2018). This indicates that the cloud feedback both increases TOA reflected SW and
569 increases surface DLW (Taylor et al. 2011b; Taylor et al. 2013; Pithan and Mauritsen 2014). The
570 magnitude and large inter-model spread of the Arctic cloud feedback comes from model
571 discrepancies in the projected changes in cloud fraction, particularly at low-levels, and optical
572 depth (Vavrus 2004, Vavrus et al. 2009, Vavrus et al. 2011; Liu et al. 2012; Morrison et al. 2019;
573 English et al. 2015, Vignesh et al. 2020). Multiple interacting processes contribute to inter-model
574 differences in the Arctic cloud feedback: surface-atmosphere coupling, cloud microphysics and
575 precipitation, and interactions with large-scale meteorology (e.g., Curry et al. 1996).

576 The Arctic optical depth feedback is shaped by changes in cloud thermodynamic phase. In
577 response to warming, cloud ice transitions to water increasing cloud albedo and causing a negative
578 feedback (Mitchell et al. 1989; Li and LeTreut 1992). This feedback is sensitive to cloud ice in the
579 control climate, by determining the amount of ice available to transition. The cloud phase feedback
580 magnitude is likely biased negative in most contemporary climate models due to excessive cloud
581 ice and too little supercooled liquid under present-day conditions, yielding unrealistically large
582 increases in mixed-phase cloud optical thickness with warming (Tsushima et al. 2006; Klein et al.
583 2009, Komurcu et al. 2014, McCoy et al. 2016; Tan et al. 2016). This cloud optical depth feedback
584 bias may have broader implications to AA by enhancing the Arctic lapse rate feedback (Tan and
585 Storelvmo 2019). Recent model experiments revealed that while global cloud feedbacks warm the
586 Arctic, the local feedback contributes negligibly to Arctic warming (Middlemas et al. 2020)

587 suggesting a potential remote influence (Section 5e). However, the model exhibits a low mixed-
588 phase supercooled liquid bias and likely an optical depth feedback that is too negative.

589 The stability of the lower troposphere affects cloud processes and constitutes a cloud feedback
590 mechanism. Arctic cloud fraction and optical thickness tend to increase with reduced lower
591 tropospheric stability (LTS; Barton et al. 2012; Solomon et al. 2014; Taylor et al. 2015; Yu et al.
592 2019). In response to increased CO₂, LTS is expected to decrease, promoting increased cloud
593 fraction and optical depth with a seasonally varying character (Boeke et al. 2021). CMIP5 models
594 show substantial cloud-induced warming in fall and winter coincident with large reductions in LTS
595 (Boeke and Taylor 2018). These reductions in LTS are in part due to the large reductions in sea
596 ice (Pavelsky et al. 2011). Thus, cloud changes induced by the LTS mechanism are influenced by
597 cloud-surface coupling (Kay and Gettleman 2009; Shupe et al. 2013; Solomon et al. 2014; Taylor
598 et al. 2015; Yu et al. 2019).

599 Cloud-surface coupling represents the primary mechanism through which sea ice influences
600 cloud feedback. Sea ice loss tends to increase cloud fraction and optical depth through increased
601 surface evaporation (Curry et al. 1996; Taylor 2015; Abe et al. 2016; Huang et al. 2017; Morrison
602 et al. 2019). However, the sensitivity of clouds to sea ice loss depends on the cloud-surface
603 coupling state and the air-surface temperature gradient. This condition-dependent behavior is
604 responsible for the seasonality of the cloud response to sea ice loss; observational studies find that
605 more liquid clouds result from reduced sea ice in all seasons except summer (Kay and Gettleman
606 2009; Boisvert et al., 2015; Taylor et al 2015; Morrison et al. 2018; Huang et al. 2019). Weak air-
607 surface temperature gradients and decoupled cloud layers are typical in Arctic summer conditions
608 (Shupe et al. 2013). Recent research suggests that LH and SH flux increases may elicit different
609 cloud responses, whereby enhanced SH fluxes from sea ice leads dissipate winter low-clouds (Li

610 et al. 2020). The evidence suggests that the cloud-sea ice feedback promotes surface warming in
611 non-summer months.

612 Cloud masking effects influence AA by modifying the strength of other feedbacks. Cloud
613 masking operates by damping the TOA radiative perturbation from a feedback relative to clear-
614 sky and is sensitive to present-day cloud properties. For example, cloud masking reduces the TOA
615 radiative perturbation from surface albedo changes. Several studies indicate that the cloud masking
616 effect reduced the TOA radiative impact of observed surface albedo decline by ~50% (Sledd and
617 L’Ecuyer 2019, He et al. 2019, Alkama et al. 2020, Stapf et al. 2020). While not a feedback, the
618 cloud masking effect highlights a mechanism through which present-day cloud properties
619 influence Arctic climate change.

620 Lastly, microphysical processes influence the evolution of cloud radiative properties and
621 modulate cloud feedback. Cloud microphysical processes represent sources and sinks of mixed-
622 phase cloud liquid and ice and modulate the water amount, phase partitioning, and the number and
623 size of hydrometeors (Curry et al. 1996; Beesley and Moritz 1999; Klein et al. 2009, Tan &
624 Storelvmo 2016, Barrett et al. 2017, Furtado & Field 2017, Wang et al. 2018). However, cloud
625 microphysical processes and their interactions with aerosols are poorly represented in climate
626 models. Ice nucleation mechanisms and ice-nucleating particle (INP) properties and sources are
627 either poorly constrained or not represented in models (Xie et al. 2013, English et al. 2014;
628 Schmale et al. 2021, Komurcu et al. 2014). Mixed-phase cloud INP recycling (Solomon et al. 2018,
629 Fan et al. 2015), secondary ice production (Lawson et al. 2001; Rangno and Hobbs 2001;
630 Sotiropoulou et al. 2020, Zhao et al. 2021)) and biological INP-sea ice interactions (Wilson et al.
631 2015; Irish et al. 2017; Quinn et al. 2017; Hartmann et al. 2019; Creamean et al. 2020) remain
632 unresolved or unrepresented. In addition, the efficiency of the Wegener-Bergeron-Findeisen

633 process (Tan and Storelvmo 2016) and the updraft velocity and ice crystal fall speeds (Tan and
634 Storelvmo 2019; Ervens et al. 2011) are also poorly constrained. These gaps in our understanding
635 of cloud microphysical processes preclude a more quantitative assessment of the Arctic cloud
636 feedback and its influence on AA. Observational constraints that statistically characterize the range
637 of Arctic cloud types are needed to improve parameterized processes and reduce cloud-related
638 uncertainty.

639 **d. Surface type dependence and seasonality of Arctic Amplification**

640 The diversity of Arctic surface types (e.g., sea ice, ocean, land) dictates features of the spatial
641 structure and seasonality of AA. Surface-type dependent characteristics and processes such as
642 albedo, surface turbulent fluxes, vertical and horizontal heat transport, and heat capacity control
643 the impact of each surface type. Understanding how specific surface types influence the spatial
644 distribution and seasonality of AA may help reduce the inter-model spread.

645 Explanations of regional variations in AA must consider the underlying surface. Observed
646 temperature changes indicate that regions with the largest sea ice loss are warming most rapidly
647 (Screen and Simmonds et al. 2010; Bekryaev et al. 2011; Fig. 2). Moreover, the regional
648 characteristics of warming within a climate model is driven by differences in surface properties
649 and feedbacks (Lainé et al 2016). Figure 9 illustrates CMIP6 model projections showing that the
650 magnitude and seasonality of warming is a function surface type: namely, sea ice-retreat, sea ice-
651 covered, ice-free ocean, and land (Fig. 9; definitions in caption).

652 Several processes conspire to cause the largest Arctic warming in sea ice-retreat and sea ice-
653 covered regions (Fig. 9). Surface albedo and sea ice insulation feedbacks strongly enhance surface
654 warming (MS80; Screen and Simmonds et al. 2010; Taylor et al. 2013; Pistone et al. 2014; Boeke
655 and Taylor 2018). Cloud feedbacks are also positive in these regions, especially in fall/winter

656 (Section 5c). Strong LTS, seasonal ocean energy transfer drive the release of stored ocean heat via
 657 SH and LH fluxes (Fig. 10), and changes in surface thermal inertia contribute to the maximum
 658 winter warming in these regions (Sejas et al. 2014; Sejas and Cai 2016; Laîné et al 2016; Boeke
 659 and Taylor 2018, Feldl et al. 2020).

660 The characteristics of the warming response in ice-free ocean regions differ from sea ice

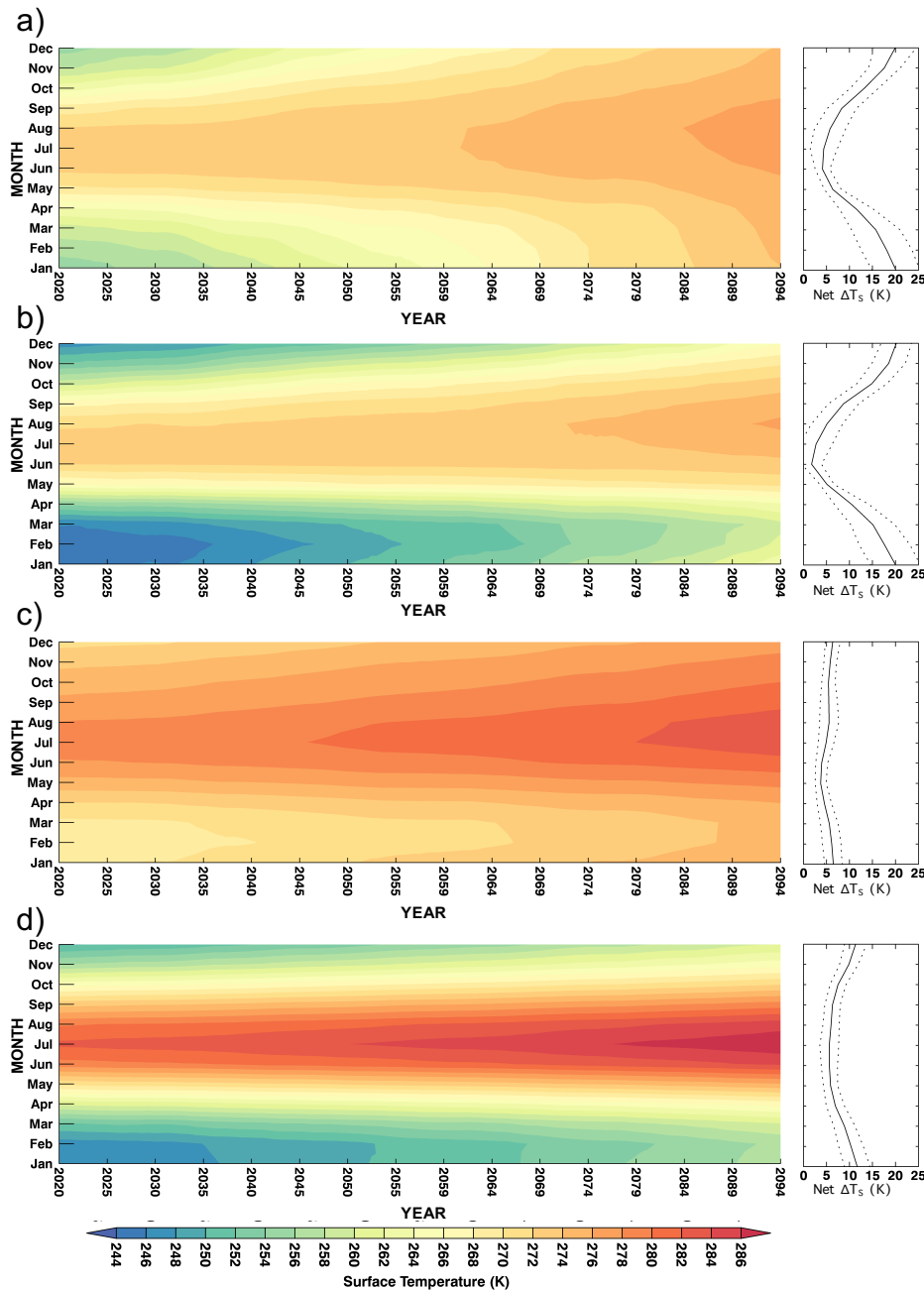


Figure 9: Hovmoller plot of the monthly time series of the CMIP6 ensemble average Arctic surface temperature changes in SSP5-8.5 for a) ice-retreat regions (present-day sea ice concentration >15% and future sea ice concentration <15%), b) ice-covered regions (sea ice concentration >15% in present and future), c) ice-free ocean (present-day sea ice concentration <15%), and d) land. The right panels show the total surface warming (K) by 2100 as the difference between the 2090-2100 and 2015-2025 periods for each surface type (solid black line) and the across-model standard deviation (dotted line).

661 regions. Ice-free regions have a weaker and almost seasonally uniform warming (Fig. 9) resulting

662 from the large ocean heat capacity (Dwyer et al. 2012) and weaker positive feedbacks (especially
663 the surface albedo feedback; Boeke and Taylor 2018). Thus, the SEB response is smaller than in
664 sea ice regions and shows an opposite net flux change during winter from differing SH flux
665 responses (Fig. 10). Additionally, changes in ocean heat transport also influence the warming
666 (Section 5f), however it is unclear if these changes affect these regions differently.

667 While warming in land regions has a similar seasonal structure as sea ice, different surface
668 characteristics indicate that a

669 different set of processes cause this
670 signal. Seasonal differences in the
671 surface albedo feedback occur due to
672 the earlier spring peak in land
673 snowmelt compared to sea ice melt
674 (Taylor et al. 2011b). Additionally,

675 the surface albedo feedback is
676 weaker (smaller increases in surface
677 absorbed SW; Fig. 10) over snow-
678 covered land than over sea ice
679 because of smaller albedo

680 differences with the underlying
681 surface, despite being at a lower-
682 latitude (Taylor et al. 2011a).

683 Surface turbulent flux changes cool the land during summer as opposed to during winter as in sea
684 ice regions (Fig. 10; L  n   et al 2016; Letterly et al. 2018); the summer warming minimum over

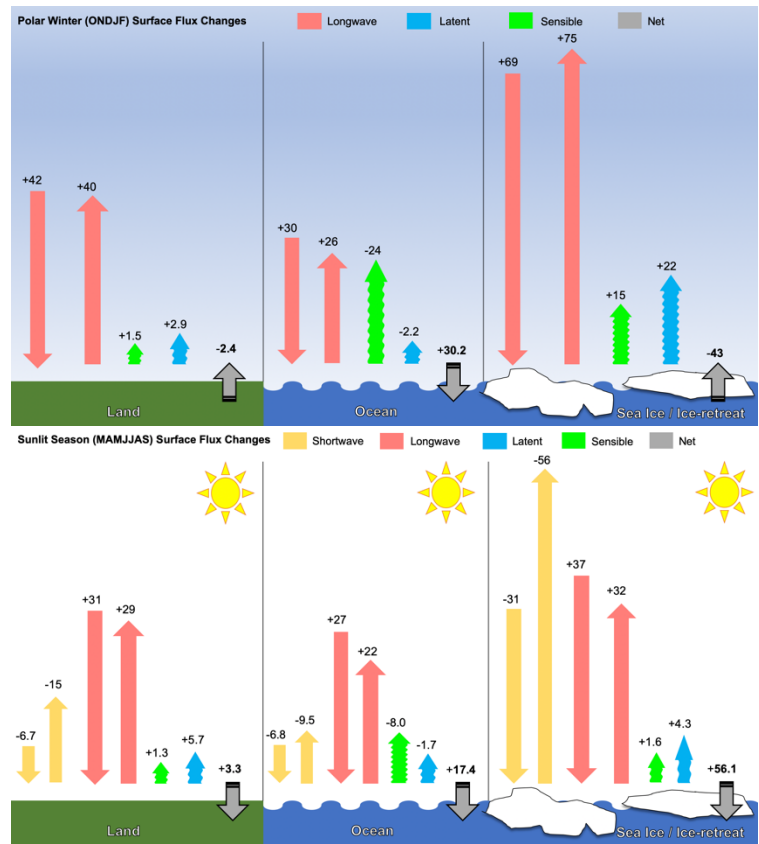


Figure 10: Surface energy budget response by surface type. CMIP6 SSP5-8.5 ensemble mean surface energy budget changes by surface type (as defined in Fig. 9) for (a) polar night and (b) polar day. Changes are computed as the difference between the 2080-2100 period and the first 20-years of the simulation (2015-2035).

Non-peer reviewed EarthArXiv preprint submitted to Frontiers in Earth Science to the “Arctic Amplification: Feedback Process Interactions and Contributions” Research Topic.

685 land results from increased cooling and earlier snowmelt rather than increased heat storage as in
686 sea ice regions (Boeke et al. 2021). The small heat capacity of land combined with the nonlinearity
687 of the temperature dependence of LW surface cooling (Henry and Vallis 2021) and increased local
688 atmospheric heat transport from sea ice loss to land regions (Deser et al. 2010; Burt et al. 2016;
689 Boeke and Taylor 2018) also contribute to the winter amplification over land.

690 **e. Atmospheric heat transport effects**

691 Despite considerable efforts particularly over the last decade, the role of remote influences on
692 AA is still debated. Here, we define remote impacts on Arctic warming as any warming that occurs
693 due to non-Arctic changes (equatorward of 60°N). Thereby, remote effects are not merely
694 associated with changes in meridional heat transports but include the local feedbacks they initiate
695 or mediate (e.g., water vapor and cloud feedbacks). Understanding the partitioning between local
696 and remotely-induced warming is crucial for reducing uncertainty in the impacts of non-well
697 mixed climate forcings (e.g., aerosols and the effects of emission reductions; Chung and Räisänen,
698 2011). Further, simulated Arctic warming and variability may depend on the models’
699 representation of tropical Pacific variability (e.g., Ding et al., 2019; Baxter et al. 2019) and
700 improving Arctic projections may require improved modeling of teleconnections.

701 Early EBM studies identified the strong impact of meridional heat transports on polar
702 temperatures (Budyko 1969, Sellers 1969, North 1975), and, in GCMs, the opposing responses of
703 dry static energy (DSE) and LH transports due to reductions in the meridional temperature gradient
704 and increases in the moisture gradient (MW80). Flannery (1984) extended the dry EBM approach
705 to include the separate effect of increased LH transport with warming; EBMs continue to be used
706 to study polar warming (Frierson et al. 2007, Hwang and Frierson 2010, Rose et al. 2014, Roe et
707 al. 2015, Merlis and Henry 2018, Bonan et al. 2018, Armour et al. 2019).

708 In spite of different meridional shapes of the forcing due to CO₂ and solar constant changes,
709 MW80 found that the meridional shape of the response was similar. Langen and Alexeev (2007)
710 identified a preferred polar amplified response mode whose shape is determined by the strength of
711 the TOA radiative restoring feedback and the DSE and LH transports (also see Merlis and Henry
712 (2018)). The concept of a preferred mode is strengthened by the linearity between Arctic and global
713 mean temperature change inferred from the paleoclimate record (Miller et al. 2010) and CMIP5
714 models (Yoshimori et al. 2017).

715 GCM experiments have been performed to gauge the remote impact on Arctic warming. Some
716 used a direct extra energy term added to the SEB (“ghost forcing”, Alexeev et al., 2005; Park et
717 al., 2018), some used latitudinally confined CO₂ increases (Chung and Räisänen, 2011; Shaw and
718 Tan, 2018; Stuecker et al., 2018; Semmler et al., 2020) while others specified SST increases at
719 lower latitudes (Yoshimori et al., 2017). Common to these approaches is that any Arctic warming
720 that occurs, does so due to the indirect effects of the remote warming. Chung and Räisänen (2011)
721 attribute 60-85% of Arctic warming to non-local drivers, Yoshimori et al. (2017) find 60-70%,
722 Park et al. (2018) about 50%, Shaw and Tan (2018) about 60%, and Stuecker et al. (2018) about
723 50%. These studies indicate that non-Arctic forcing increases non-Arctic temperatures, which in
724 turn increase Arctic temperatures. Local-Arctic feedbacks then amplify this remotely-induced
725 Arctic warming to produce a final warming that accounts for half or more of the full Arctic
726 warming.

727 AA therefore arises in part due to an asymmetry between low-to-high and high-to-low latitude
728 impacts: low-latitude warming is efficiently communicated poleward while high-latitude warming
729 is less efficiently communicated equatorward (Alexeev et al., 2005; Chung and Räisänen, 2011;
730 Shaw and Tan, 2018; Park et al., 2018; Stuecker et al., 2018, Semmler et al., 2020). Non-Arctic

731 warming tends to produce a rather uniform meridional warming pattern and thereby does not itself
732 cause AA (Park et al. 2018; Stuecker et al. 2018). Nevertheless, the fact that non-Arctic warming
733 does not stay localized, as opposed to local-Arctic induced warming, implies that remote effects
734 contribute significantly to Arctic warming. Similarly, moist EBMs and idealized GCMs produce
735 polar amplification in the absence of a surface albedo feedback due to the down-gradient transport
736 of moist static energy (Alexeev et al. 2005, Langen and Alexeev 2007, Roe et al. 2015, Armour et
737 al. 2019, Russotto and Biasutti 2020).

738 Tropical impacts on Arctic warming (e.g., Schneider et al., 1997; Rodgers et al., 2003) have
739 been elaborated in the “tropically excited Arctic warming mechanism” (TEAM, Lee et al. 2011a,
740 2011b, Lee 2012; 2014). Enhanced convection in the Pacific warm pool leads to strengthened or
741 more frequent excitement of poleward propagating Rossby waves. Through dynamic heating and
742 increased moisture transport into the Arctic, the wave dynamics increase the DLW radiation and
743 lead to warming. The role of tropical Pacific Rossby wave-driven teleconnections to the Arctic has
744 been highlighted for observed warming over northeastern Canada and Greenland (Ding et al.,
745 2014) and Arctic sea ice trends and variability (Ding et al. 2017; Ding et al. 2019; Baxter et al.
746 2019, Topal et al. 2020). Planetary waves dominate the transport of heat and moisture into the
747 Arctic and can drive temperature increases (Graversen and Burtu 2016; Baggett and Lee 2017).
748 Synoptic waves also transport heat and moisture to the Arctic, but in smaller amounts and only in
749 conjunction with a background of amplified planetary waves (Baggett and Lee 2017).

750 Several studies have concluded that atmospheric heat transport changes play a small or
751 negligible role in AA, finding a negative correlation between polar amplification and atmospheric
752 heat transport changes (Hwang et al. 2011; Kay et al. 2012; Boeke and Taylor 2018). Due to the
753 opposing effects of increased LH transport and decreasing DSE transport, models with high AA

754 tend to simulate only small or even negative net heat transport changes. Similar conclusions of a
755 subsidiary role for atmospheric heat transport were drawn by Pithan and Mauritsen (2014),
756 Stuecker et al. (2018) and Feldl et al. (2020) using a TOA kernel-based approach and Taylor et al.
757 (2013) using the CFRAM approach. The discrepancy between these studies and those showing the
758 importance of low-latitude impacts and LH transports is likely due to i) the effect of transport-
759 driven increases in LH is amplified by accompanying changes in specific humidity and clouds
760 (i.e., a “water vapor triple effect”; Cai and Lu 2007; Graversen and Burtu, 2016; Baggett and Lee,
761 2017; Lee et al., 2017; Yoshimori et al., 2017; Graversen and Langen, 2019), ii) differing
762 attribution of warming to local and remote processes, and iii) a focus on vertically-integrated
763 energy transport, which does not account for a disproportionate effect of lower versus upper
764 tropospheric transport on surface temperature (Feldl et al. 2020). Graversen and Burtu (2016)
765 found that for a given amount of dry static or latent energy transported into the Arctic, LH transport
766 eventually leads to Arctic warming that is an order of magnitude greater than DSE transport. When
767 looking just at net heat transport changes, this amplified effect is overlooked and the change in
768 total atmospheric heat transport is an unreliable measure of the full effect of atmospheric dynamics
769 (Yoshimori et al. 2017). In offline feedback diagnostic approaches, the water vapor triple effect is
770 attributed to local feedbacks (e.g., water vapor, cloud, lapse rate). Thus, many local feedbacks, as
771 conventionally defined, are not exclusively local in nature.

772 **f. Oceanic heat transport effects**

773 The transport of energy by the oceanic circulation modulates Arctic temperature and sea ice
774 and thus can influence AA. Observations show enhanced ocean heat transports into the Arctic
775 through the Fram Strait and the Barents Sea in recent years (Årthun et al. 2012; Dmitrenko et al.,
776 2008; Karcher et al. 2003; Schauer et al., 2004; Skagseth et al., 2008; Spielhagen et al. 2011).

Non-peer reviewed EarthArXiv preprint submitted to Frontiers in Earth Science to the “Arctic Amplification: Feedback Process Interactions and Contributions” Research Topic.

777 Climate models simulate enhanced high-latitude ocean heat transport under global warming (e.g.,
778 Bitz et al., 2006; Holland & Bitz, 2003; Hwang et al., 2011; van der Linden et al. 2019). Several
779 studies suggest that this increased ocean heat transport contributes to Arctic warming (Holland and
780 Bitz, 2003; Hwang et al., 2011; Mahlstein and Knutti, 2011; Singh et al. 2017); in contrast, other
781 studies argue that changes in ocean transport are not correlated with Arctic warming (e.g., Pithan
782 and Mauritsen, 2014; Laîné et al. 2016). This discrepancy mostly comes from the difference of the
783 latitudes where the ocean heat transport is focused (Nummelin et al. 2017). Ocean heat transport
784 increases poleward of 60°N are positively correlated with AA (Holland and Bitz 2003; Hwang et
785 al. 2011; Mahlstein and Knutti 2011).

786 Several mechanisms contribute to enhanced poleward ocean heat transport under
787 anthropogenic warming. Several studies indicate that increased ocean heat transport in the subpolar
788 North Atlantic is mainly due to warmer Atlantic water (Koenigk and Brodeau 2014; Jungclaus et
789 al. 2014; Nummelin et al. 2017), while other studies highlight ocean circulation changes (Bitz et
790 al. 2006; Rugenstein et al. 2013; Winton et al. 2013; Marshall et al. 2015; Oldenburg et al. 2018;
791 van der Linden et al. 2019). In the latter mechanism, changes in the North Atlantic subpolar gyre
792 or the Atlantic Meridional Overturning Circulation (AMOC) are argued to be important. For
793 example, a strengthened subpolar gyre causes increased oceanic heat transport into the Barents
794 Sea that decreases sea ice and increases oceanic heat release. An anomalous cyclonic circulation
795 is then induced over the Barents Sea that intensifies westerly winds and further promotes oceanic
796 heat transport and warming in the Barents Sea (Ådlandsvik and Loeng, 1991; Arzel et al., 2008;
797 Bengtsson et al., 2004; Goosse et al., 2003; Guemas and Salas-Melia, 2008; Semenov et al. 2009).

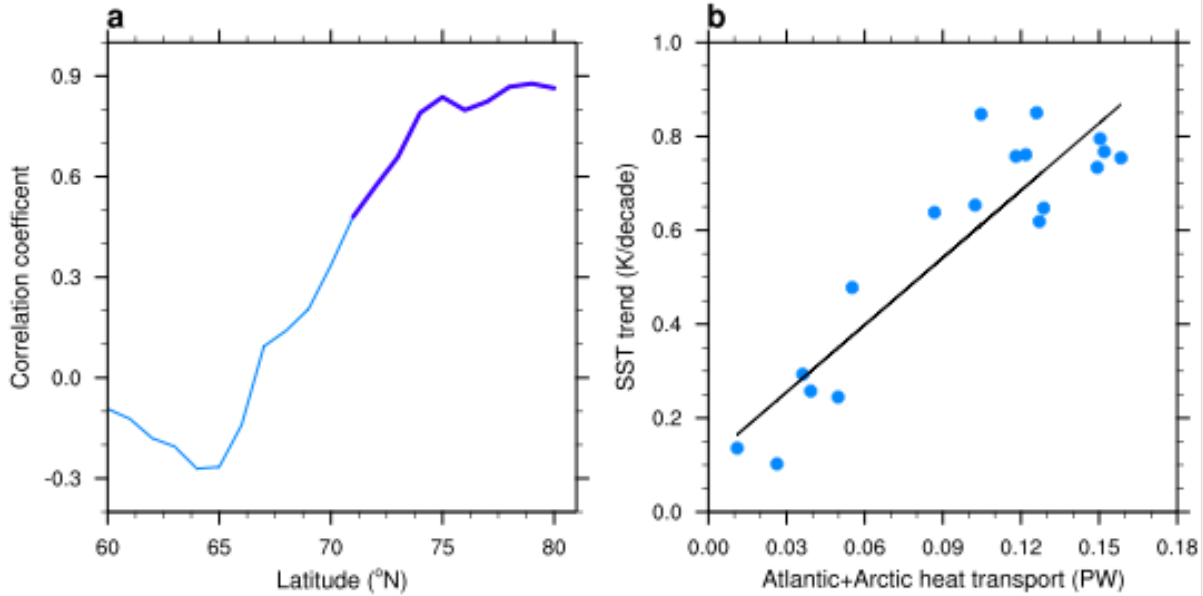


Figure 11: Ocean heat transport and Arctic Warming. (a) The correlation between the trend of average SST over 60-90°N during 2015-2100 and northward ocean heat transport averaged over 2015-2100 across different latitudes in the Atlantic basin among 18 CMIP6 climate models under the SSP5-8.5 scenario. For each model, only the first ensemble simulation is used to ensure an equal weight among models. Dark blue indicates the latitudes where the correlation is significant with 95% confidence by Pearson’s r test. (b) The scatter plot of SST trends during 2015-2100 and northward ocean heat transport averaged over 2015-2100 across 80°N in the Atlantic sector, with the regression line of the two variables (black).

798 Alternatively, the role of AMOC change in high-latitude ocean heat transport and AA is
799 debated. In GFDL models, a stronger AMOC weakening is linked with less high-latitude warming
800 (Rugenstein et al. 2013; Winton et al. 2013). van der Linden et al. (2019) show that changes in the
801 North Atlantic subpolar gyre play a prominent role in modulating ocean heat transport into the
802 Arctic, while AMOC change is a secondary factor in the EC-Earth model. Additionally, the
803 relationship between AMOC and high-latitude ocean heat transport could be different under
804 interval variability and anthropogenic warming (Oldenburg et al. 2018). AMOC is not a one-way
805 forcing on Arctic climate; Arctic sea ice melt under anthropogenic warming may also slow the
806 AMOC after multiple decades (Sévellec et al. 2017; Liu et al. 2019; Li et al. 2021).

807 Ocean heat transported into the Arctic from the Atlantic influences Arctic warming and relates
808 to the inter-model spread. Inter-model differences across 18 CMIP6 models (Fig. 11) illustrate the
809 relationship between Arctic warming and ocean heat transport across different latitudes. The
810 correlation is positive and becomes statistically significant near 70°N and strengthens moving
811 poleward (Fig. 11a), a result consistent with previous studies (Holland and Bitz 2003, Hwang et
812 al. 2011, Mahlstein and Knutti 2011). At 80°N where much of the Atlantic ocean heat enters the
813 Arctic via the Fram Strait, the correlation between Arctic warming and ocean heat transport
814 reaches 0.91. Thus, models with more (less) ocean heat imported into the Arctic via the Atlantic
815 sector simulate stronger (weaker) warming during 2015-2100 under SSP5-8.5 (Fig. 11b).

816 **g. Role of episodic variability: Air mass transformation and moisture intrusions**

817 Long-term climate change and mean energy budgets symbolize the accumulation of short
818 timescale, episodic events. The nature of episodic events has implications for our understanding
819 and projecting of AA. In the seasonal mean, the wintertime Arctic SEB and lower tropospheric
820 temperature profiles are dominated by radiative cooling and strong stable stratification (Serreze et
821 al. 1992). However, at any point in time and space, the Arctic winter boundary layer over sea ice
822 or land tends to be either in a radiatively clear state with no clouds or ice clouds or a cloudy state
823 with low-level liquid containing clouds (Stramler et al. 2011). In the radiatively clear state over
824 sea ice, surface radiative cooling ($\sim 40 \text{ W m}^{-2}$) drives surface-based temperature inversions with
825 strengths of $\sim 10\text{-}15 \text{ K}$. In the radiatively cloudy state, the surface is in approximate radiative
826 balance with the cloud layer and a weaker temperature inversion is elevated to or above cloud-top
827 (Sedlar et al. 2012, Pithan et al. 2014).

828 These two states occur at different stages of air-mass transformations (Pithan et al. 2018,
829 Nygård et al. 2019). Following the intrusion of warm, moist air masses from lower latitudes,
830 radiative cooling leads to cloud formation driving the boundary layer into the cloudy state. After
831 several days over Arctic sea ice or land, cooling and drying of the air-mass causes the mixed-phase
832 cloud to glaciate or decay, transitioning to the clear state. The moisture supply aloft and cloud-top
833 radiative cooling lead to cloud top moisture inversions (e.g., increases in specific humidity with
834 height). Given the differences in the thermodynamic profile and the SEB between these states,
835 changes in their frequency of occurrence can impact wintertime sea-ice growth, near-surface air
836 temperature and lapse-rate, water vapor and cloud feedbacks.

837 Episodic variability can influence AA through multiple mechanisms. Changes in the frequency
838 of radiatively clear and cloudy states due to a change in the magnitude or frequency of moist air
839 mass intrusions and atmospheric rivers could alter the SEB and cloud feedback. Observational
840 analyses suggest an increase in the number of moist intrusions has already contributed to
841 wintertime Arctic warming and reduced sea-ice growth (Woods and Caballero 2016, Graham et
842 al. 2017; Hegyi and Taylor 2018). The initial properties of incoming air-masses could also change,
843 influencing the longevity of mixed-phase clouds; warmer, more moist, and potentially more
844 aerosol laden air-masses are possible due to warming at lower latitudes. The potential impact of
845 AA and sea ice loss on the frequency of circulation states with strong meridional advection has
846 been intensely investigated over the past decade and continues to be debated (e.g., Cohen et al.
847 2020). Lastly, surface turbulent fluxes over the ice-free ocean represent another mechanism by
848 which episodic variability can influence AA as the magnitude of SH and LH fluxes can change by
849 $\sim 100 \text{ Wm}^{-2}$ depending upon whether the prevailing winds are from sea ice to ice-free ocean or vice
850 versa (Taylor et al. 2018). A quantitative understanding of the Arctic system response to episodic

851 heat and moisture transport events, air-mass transformation, and cloud formation is needed to
852 reduce uncertainty in Arctic projections.

853 **6. Conceptual picture of Arctic Amplification**

854 AA results from a collection of interacting processes. Based upon the available evidence, we
855 deduce five fundamental concepts for AA (Fig. 12): (C1) local positive feedbacks amplify the
856 initial local forcing more strongly in the Arctic than elsewhere, (C2) the predominance of stable
857 atmospheric stratification (inversion denoted by the color bar in Fig. 12) restricts convective
858 mixing and focuses warming in a shallow near-surface layer, (C3) the seasonal transfer of energy
859 from summer to fall/winter by ocean heat storage in combination with sea ice loss exposing the
860 larger thermal inertia of the ocean and drives the maximum warming in winter, (C4) increased
861 poleward LH transport amplifies Arctic warming through a “water vapor triple effect”, and (C5)
862 activation of local feedbacks by remote atmospheric and oceanic processes drive additional
863 warming. Next, we employ these concepts to describe the AA process.

864 Initially, rising CO₂ levels increase DLW radiation warming the Arctic surface and overlying
865 air with a surface-based vertical structure. Arctic warming excites a suite of positive local
866 feedbacks (C1; cloud, water vapor, and surface albedo) that lead to further warming. The surface
867 albedo feedback represents the strongest positive local feedback and also favors a surface-based
868 warming profile that is further promoted by strong atmospheric stable stratification (C2).

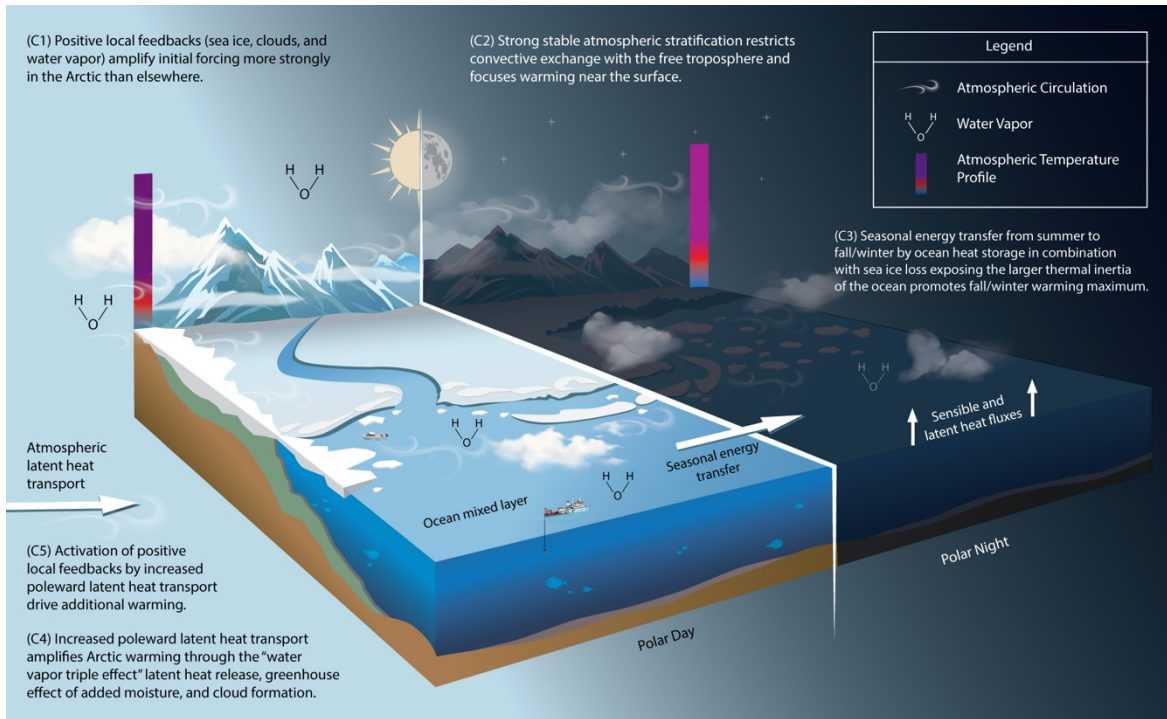


Figure 12: Illustration of the fundamental processes generating AA in the conceptual model.

869 Each local feedback has a unique seasonal signature that shapes its contributions to AA. Sea
870 ice decline is strongest in summer, increasing absorbed solar radiation into the Arctic Ocean;
871 however, summer warming is small due to the Arctic Ocean’s large heat capacity and the LH
872 associated with sea ice melt. These processes sequester the surplus energy and transfer it to
873 fall/winter (C3) producing larger warming during these months. The increased upper Arctic Ocean
874 heat content delays fall sea ice freeze onset, exposes the ocean to the atmosphere for a longer time,
875 and increases surface turbulent fluxes from ocean-to-atmosphere. The combination of delayed
876 freeze onset and warmer temperatures promotes less winter sea ice growth and thinner spring sea
877 ice that is more susceptible to earlier summer melt out. This provides more time to accumulate
878 solar radiation in summer, further delaying fall freeze-up.

879 Simultaneously with these local processes, the rest of the globe warms and moistens in
880 response to increased CO₂ causing the air transported into the Arctic to have a larger moist static

881 energy. The poleward moisture transport contributes not only to the LH release associated with
882 condensation but also to an increased greenhouse effect prior to condensation and subsequent
883 increased cloudiness. Through this water vapor triple effect, increased LH transport (C4)
884 overcomes the countering effect of reduced DSE transports due to a weakened equator-to-pole
885 temperature gradient. As a result, remote atmospheric and oceanic processes drive additional
886 surface warming that triggers interactions with local feedbacks (from C1) that cause further
887 warming (C5).

888 Our conceptual model describes five overall ideas fundamental to AA. We acknowledge that
889 an improved understanding of individual processes is critical for producing reliable Arctic
890 warming projections and resolving inter-model differences. However, our conceptual model
891 highlights the need to accurately account for local feedback and remote process interactions within
892 the context of the annual cycle to constrain the likelihood that future AA will be on the high-end
893 of model projections.

894 Our conceptual model describes five overall ideas fundamental to AA, but are not all-
895 encompassing. We acknowledge that the highly coupled nature of the atmosphere, hydrosphere,
896 cryosphere, land, and biosphere means other processes such as permafrost thawing, aerosol-cloud
897 interactions, glacier melt, land use change, among others can influence future AA. These
898 processes, however, are either not included or overly simplified in model simulations or are
899 considered of secondary importance. An improved understanding of individual processes is critical
900 for producing reliable Arctic climate projections and resolving inter-model differences. As model
901 fidelity advances and our knowledge expands, we envision that new knowledge will build upon
902 the fundamentals described in our conceptual model.

903 **7. Conclusion, next steps, and future work**

904 Arctic Amplification is a fundamental aspect of Earth’s climate as documented in a range of
905 contexts: paleoclimate, present-day observations, and models of varying complexities. Despite
906 these observations and available understanding, a complete theory of Arctic Amplification remains
907 elusive. Gaps in our understanding have thwarted reliable surface temperature and sea ice
908 projections due to anthropogenic forcing. After reviewing the current understanding of Arctic
909 Amplification and proposing a conceptual model, we have identified key knowledge gaps and
910 recommendations to accelerate progress.

911 **Recommendations:**

- 912 1. A sustained observing system that resolves key Arctic processes is vital. A pursuit is
913 underway (e.g., integrated Arctic Observing Network (AON)) and this work must continue. In
914 addition, we recommend routine Arctic field expeditions with a MOSAiC-like ([https://mosaic-](https://mosaic-expedition.org)
915 [expedition.org](https://mosaic-expedition.org)) scope to provide the missing data needed to advance understanding (Shupe et
916 al. 2020). Our vision is a permanent, manned floating Central Arctic observatory.
- 917 2. Arctic surface energy budget uncertainties inhibit robust conclusions of critical atmosphere-
918 sea ice-ocean processes with signals $<10\text{-}20\text{ W m}^{-2}$. We recommend a focus on advancing
919 satellite-based measurement approaches to obtain Arctic-wide surface energy budget
920 information (e.g., advanced IR sounder radiance assimilation; Smith et al. 2021).
- 921 3. A quantitative understanding of how individual physical parameterization schemes influence
922 feedback uncertainty is lacking. We recommend modeling experiments, intercomparison
923 studies, and sophisticated statistical analyses (e.g., data-driven causality discovery methods)
924 to quantify the sensitivity of Arctic feedbacks to physical parameterization schemes. An
925 experimental protocol enabling the community to characterize these links across models and
926 parameterization schemes is needed.

- 927 4. Surface turbulent flux schemes vary across climate models, producing fluxes that differ
928 markedly from observations. We recommend a coordinated intercomparison of high-latitude
929 surface turbulent flux parameterizations for “standard” cases (e.g., on-sea ice flow, off-sea ice
930 flow, ocean with and without sea ice, etc.) with adequate observational constraints to identify
931 the magnitude and source of model bias.
- 932 5. Reliable Arctic projections require an accurate accounting of local feedback and remote
933 process interactions within the context of the annual cycle. We recommend that research on
934 how local feedback and remote process interactions influence the sea ice annual cycle should
935 be a near-term research focus. An improved understanding of these energy exchanges and
936 interactions will accelerate our understanding of Arctic Amplification.
- 937 6. While energy balance models and feedback diagnostic frameworks are indispensable, these
938 frameworks obscure the episodic nature of time-averaged quantities and the links between
939 small-scale processes and long-term change. We recommend the influence of episodic
940 variability on Arctic Amplification as a key research focus area, complementary to
941 recommendation 5. Specifically, research into how the Arctic system dissipates energy from
942 heat and moisture transport events, air mass transformation, and cloud formation is needed.
- 943 7. Regional climate change indicators for policy targets should be adopted to account for the
944 uneven spatial distribution of climate change impacts and risks. The adoption of regional
945 climate change targets would help to raise the priority of Arctic science.
- 946 8. Feedback diagnostic frameworks contain ambiguities and inconsistencies that make physical
947 interpretation unclear. For instance, the lapse rate feedback is defensible in the tropics where
948 moist convection couples the surface and upper troposphere, however its interpretation at high

949 latitudes is less clear. We recommend a working group tasked to rethink feedback definitions
950 and diagnostic frameworks, making them more process-oriented.

951 Polar amplification has been studied in depth for at least 50 years. While the leading
952 explanation for amplified polar warming remains the surface albedo feedback and strong
953 stratification at high latitudes, new details highlight the important role of atmosphere, ocean, and
954 sea ice coupling processes. The highly coupled nature of the polar regions is a source of substantial
955 uncertainty in regional climate projections. Our understanding of polar amplification has been
956 wedded to computational and technological advances that have enabled more complex climate
957 simulations with more detailed physical parameterizations. The role of observations has also
958 evolved from a tool for model tuning to now being used for direct analysis.

959 While these advances have contributed to our understanding of polar amplification and must
960 continue, an important step remains; to raise Arctic climate sensitivity on the climate modeling
961 priority list, giving it equal priority to global climate sensitivity. Currently, state-of-the-art
962 knowledge of Arctic processes (e.g., surface turbulent flux bulk formula) have not yet been widely
963 implemented in climate models (Bourassa et al. 2013). Given the rapidly changing Arctic sea ice
964 conditions, older parameterizations developed under thicker, multi-year sea ice conditions are
965 likely to be less applicable in the ‘new’ Arctic with a predominantly seasonal sea ice cover. Giving
966 Arctic climate sensitivity a high priority ensures the rapid integration of knowledge into climate
967 models and will accelerate the reduction in Arctic climate projection uncertainty.

968

969 **8. References**

- 970 Abe, M., Nozawa, T., Ogura, T., & Takata, K. (2015). Effect of retreating sea ice on Arctic cloud
971 cover in simulated recent global warming. *Atmospheric Chemistry and Physics Discussions*,
972 *15*(12), 17527–17552. <https://doi.org/10.5194/acpd-15-17527-2015>
- 973 Ådlandsvik, B., & Loeng, H. (1991). A study of the climatic system in the Barents Sea. *Polar*
974 *Research*, *10*(1), 45–50. <https://doi.org/10.3402/polar.v10i1.6726>
- 975 Alexeev, V. A. (2003). Sensitivity to CO₂ doubling of an atmospheric GCM coupled to an oceanic
976 mixed layer: a linear analysis. *Climate Dynamics*, *20*(7), 775–787. <https://doi.org/10.1007/s00382-003-0312-x>
- 978 Alexeev, V. A., Langen, P. L., & Bates, J. R. (2005). Polar amplification of surface warming on an
979 aquaplanet in “ghost forcing” experiments without sea ice feedbacks. *Climate Dynamics*, *24*(7–8),
980 655–666. <https://doi.org/10.1007/s00382-005-0018-3>
- 981 Alkama, R., Taylor, P. C., Garcia-San Martin, L., Douville, H., Duveiller, G., Forzieri, G.,
982 Swingedouw, D., & Cescatti, A. (2020). Clouds damp the radiative impacts of polar sea ice loss.
983 *The Cryosphere*, *14*(8), 2673–2686. <https://doi.org/10.5194/tc-14-2673-2020>
- 984 Armour, K. C., Bitz, C. M., & Roe, G. H. (2013). Time-Varying Climate Sensitivity from Regional
985 Feedbacks. *Journal of Climate*, *26*(13), 4518–4534. <https://doi.org/10.1175/JCLI-D-12-00544.1>
- 986 Armour, K. C., Siler, N., Donohoe, A., & Roe, G. H. (2019). Meridional Atmospheric Heat Transport
987 Constrained by Energetics and Mediated by Large-Scale Diffusion, *Journal of Climate*, *32*(12),
988 3655–3680. Retrieved Aug 12, 2021,
989 from <https://journals.ametsoc.org/view/journals/clim/32/12/jcli-d-18-0563.1.xml>
- 990 Arrhenius, P. S. (1896). XXXI. On the influence of carbonic acid in the air upon the temperature of
991 the ground. *The London, Edinburgh, and Dublin Philosophical Magazine and Journal of Science*,
992 *41*(251), 237–276. <https://doi.org/10.1080/14786449608620846>
- 993 Årthun, M., Eldevik, T., Smedsrud, L. H., Skagseth, Ø., & Ingvaldsen, R. B. (2012). Quantifying the
994 Influence of Atlantic Heat on Barents Sea Ice Variability and Retreat. *Journal of Climate*, *25*(13),
995 4736–4743. <https://doi.org/10.1175/JCLI-D-11-00466.1>
- 996 Arzel, O., Fichefet, T., Goosse, H., & Dufresne, J.-L. (2008). Causes and impacts of changes in the
997 Arctic freshwater budget during the twentieth and twenty-first centuries in an AOGCM. *Climate*
998 *Dynamics*, *30*(1), 37–58. <https://doi.org/10.1007/s00382-007-0258-5>
- 999 Barrett, A. I., Hogan, R. J., & Forbes, R. M. (2017). Why are mixed-phase altocumulus clouds poorly
1000 predicted by large-scale models? Part 1. Physical processes. *Journal of Geophysical Research:*
1001 *Atmospheres*, *122*(18), 9903–9926. <https://doi.org/10.1002/2016JD026321>
- 1002 Barton, N. P., Klein, S. A., Boyle, J. S., & Zhang, Y. Y. (2012). Arctic synoptic regimes: Comparing
1003 domain-wide Arctic cloud observations with CAM4 and CAM5 during similar dynamics. *Journal*
1004 *of Geophysical Research: Atmospheres*, *117*(D15). <https://doi.org/10.1029/2012JD017589>

- 1005 Beesley, J. A., & Moritz, R. E. (1999). Toward an Explanation of the Annual Cycle of Cloudiness
1006 over the Arctic Ocean. *Journal of Climate*, *12*(2), 395–415. <https://doi.org/10.1175/1520->
1007 0442(1999)012<0395:TAEOTA>2.0.CO;2
- 1008 Bekryaev, R. V., Polyakov, I. V., & Alexeev, V. A. (2010). Role of Polar Amplification in Long-
1009 Term Surface Air Temperature Variations and Modern Arctic Warming. *Journal of Climate*,
1010 *23*(14), 3888–3906. <https://doi.org/10.1175/2010JCLI3297.1>
- 1011 Bengtsson, L., Semenov, V. A., & Johannessen, O. M. (2004). The Early Twentieth-Century
1012 Warming in the Arctic—A Possible Mechanism. *Journal of Climate*, *17*(20), 4045–4057.
1013 [https://doi.org/10.1175/1520-0442\(2004\)017<4045:TETWIT>2.0.CO;2](https://doi.org/10.1175/1520-0442(2004)017<4045:TETWIT>2.0.CO;2)
- 1014 Bintanja, R., Graverson, R. G., & Hazeleger, W. (2011). Arctic winter warming amplified by the
1015 thermal inversion and consequent low infrared cooling to space. *Nature Geoscience*, *4*(11), 758–
1016 761. <https://doi.org/10.1038/ngeo1285>
- 1017 Bintanja, R., & van der Linden, E. C. (2013). The changing seasonal climate in the Arctic. *Scientific*
1018 *Reports*, *3*(1), 1556. <https://doi.org/10.1038/srep01556>
- 1019 Bitz, C. M., Gent, P. R., Woodgate, R. A., Holland, M. M., & Lindsay, R. (2006). The Influence of
1020 Sea Ice on Ocean Heat Uptake in Response to Increasing CO₂. *Journal of Climate*, *19*(11), 2437–
1021 2450. <https://doi.org/10.1175/JCLI3756.1>
- 1022 Blackport, R., & Kushner, P. J. (2016). The Transient and Equilibrium Climate Response to Rapid
1023 Summertime Sea Ice Loss in CCSM4. *Journal of Climate*, *29*(2), 401–417.
1024 <https://doi.org/10.1175/JCLI-D-15-0284.1>
- 1025 Blanchard-Wrigglesworth, E., & Ding, Q. (2019). Tropical and Midlatitude Impact on Seasonal Polar
1026 Predictability in the Community Earth System Model. *Journal of Climate*, *32*(18), 5997–6014.
1027 <https://doi.org/10.1175/JCLI-D-19-0088.1>
- 1028 Bliss, A. C., & Anderson, M. R. (2018). Arctic sea ice melt onset timing from passive microwave-
1029 based and surface air temperature-based methods. *Journal of Geophysical Research: Atmospheres*,
1030 *123*(17), 9063–9080.
- 1031 Boeke, R. C., & Taylor, P. C. (2018). Seasonal energy exchange in sea ice retreat regions contributes
1032 to differences in projected Arctic warming. *Nature Communications*, *9*(1), 5017.
1033 <https://doi.org/10.1038/s41467-018-07061-9>
- 1034 Boeke, R. C., Taylor, P. C., & Sejas, S. A. (2021). On the Nature of the Arctic’s Positive Lapse-Rate
1035 Feedback. *Geophysical Research Letters*, *48*(1), e2020GL091109.
1036 <https://doi.org/10.1029/2020GL091109>
- 1037 Boisvert, L. N., & Stroeve, J. C. (2015). The Arctic is becoming warmer and wetter as revealed by
1038 the Atmospheric Infrared Sounder. *Geophysical Research Letters*, *42*(11), 4439–4446.
1039 <https://doi.org/10.1002/2015GL063775>
- 1040 Boisvert, L. N., Wu, D. L., & Shie, C.-L. (2015). Increasing evaporation amounts seen in the Arctic
1041 between 2003 and 2013 from AIRS data. *Journal of Geophysical Research: Atmospheres*, *120*(14),
1042 6865–6881. <https://doi.org/10.1002/2015JD023258>

- 1043 Boisvert, Linette N., Markus, T., & Vihma, T. (2013). Moisture flux changes and trends for the entire
1044 Arctic in 2003–2011 derived from EOS Aqua data. *Journal of Geophysical Research: Oceans*,
1045 *118*(10), 5829–5843. <https://doi.org/10.1002/jgrc.20414>
- 1046 Broecker, W. S. (1975). Climatic Change: Are We on the Brink of a Pronounced Global Warming?
1047 *Science*, *189*(4201), 460–463. <https://doi.org/10.1126/science.189.4201.460>
- 1048 Brown, R. D., & Robinson, D. A. (2011). Northern Hemisphere spring snow cover variability and
1049 change over 1922–2010 including an assessment of uncertainty. *The Cryosphere*, *5*(1), 219–229.
1050 <https://doi.org/10.5194/tc-5-219-2011>
- 1051 Bryan, K., Komro, F. G., Manabe, S., & Spelman M. J. (1982) Transient climate response to
1052 increasing atmospheric carbon dioxide. *Science*, *215*, 56–58, DOI: 10.1126/science.215.4528.56.
- 1053 Budyko, M. I. (1966). Polar ice and climate. Proceedings of the Symposium on the Arctic heat budget
1054 and atmospheric circulation.
- 1055 Budyko, M. I. (1969). The effect of solar radiation variations on the climate of the Earth. *Tellus*,
1056 *21*(5), 611–619. <https://doi.org/10.3402/tellusa.v21i5.10109>
- 1057 Burt, M. A., Randall, D. A., & Branson, M. D. (2016). Dark Warming, *Journal of Climate*, *29*(2),
1058 705–719. Retrieved Jul 30, 2021, from [https://journals.ametsoc.org/view/journals/clim/29/2/jcli-d-](https://journals.ametsoc.org/view/journals/clim/29/2/jcli-d-15-0147.1.xml)
1059 [15-0147.1.xml](https://journals.ametsoc.org/view/journals/clim/29/2/jcli-d-15-0147.1.xml)
- 1060 Cai, M. (2005). Dynamical amplification of polar warming. *Geophysical Research Letters*, *32*(22).
1061 <https://doi.org/10.1029/2005GL024481>
- 1062 Cai, M. (2006). Dynamical greenhouse-plus feedback and polar warming amplification. Part I: A dry
1063 radiative-transportive climate model. *Climate Dynamics*, *26*(7–8), 661–675.
1064 <https://doi.org/10.1007/s00382-005-0104-6>
- 1065 Cai, M., & Lu, J. (2009). A new framework for isolating individual feedback processes in coupled
1066 general circulation climate models. Part II: Method demonstrations and comparisons. *Climate*
1067 *Dynamics*, *32*(6), 887–900. <https://doi.org/10.1007/s00382-008-0424-4>
- 1068 Caldwell, P. M., Bretherton, C. S., Zelinka, M. D., Klein, S. A., Santer, B. D., & Sanderson, B. M.
1069 (2014). Statistical significance of climate sensitivity predictors obtained by data mining.
1070 *Geophysical Research Letters*, *41*(5), 1803–1808. <https://doi.org/10.1002/2014GL059205>
- 1071 Cavalieri, D. J., C. L. Parkinson, P. Gloersen, and H. Zwally (1996). Sea Ice Concentrations From
1072 Nimbus-7 SMMR and DMSP SSM/I-SSMIS Passive Microwave Data. [2003–2016], NASA
1073 DAAC at the Natl. Snow and Ice Data Cent., Boulder, Colo. [Updated yearly].
- 1074 Cess, R. D., Potter, G. L., Blanchet, J. P., Boer, G. J., Genio, A. D. D., Déqué, M., Dymnikov, V.,
1075 Galin, V., Gates, W. L., Ghan, S. J., Kiehl, J. T., Lacis, A. A., Treut, H. L., Li, Z.-X., Liang, X.-
1076 Z., McAvaney, B. J., Meleshko, V. P., Mitchell, J. F. B., Morcrette, J.-J., ... Zhang, M.-H. (1990).
1077 Intercomparison and interpretation of climate feedback processes in 19 atmospheric general
1078 circulation models. *Journal of Geophysical Research: Atmospheres*, *95*(D10), 16601–16615.
1079 <https://doi.org/10.1029/JD095iD10p16601>

- 1080 Cess, R. D., Potter, G. L., Blanchet, J. P., Boer, G. J., Ghan, S. J., Kiehl, J. T., Treut, H. L., Li, Z.-
1081 X., Liang, X.-Z., Mitchell, J. F. B., Morcrette, J.-J., Randall, D. A., Riches, M. R., Roeckner, E.,
1082 Schlese, U., Slingo, A., Taylor, K. E., Washington, W. M., Wetherald, R. T., & Yagai, I. (1989).
1083 Interpretation of Cloud-Climate Feedback as Produced by 14 Atmospheric General Circulation
1084 Models. *Science*, 245(4917), 513–516. <https://doi.org/10.1126/science.245.4917.513>
- 1085 Cess, R. D., Potter, G. L., Zhang, M.-H., Blanchet, J.-P., Chalita, S., Colman, R., Dazlich, D. A.,
1086 Genio, A. D. D., Dymnikov, V., Galin, V., Jerrett, D., Keup, E., Lacis, A. A., Treut, H. L., Liang,
1087 X.-Z., Mahfouf, J.-F., Mcavaney, B. J., Meleshko, V. P., Mitchell, J. F. B., ... Yagai, I. (1991).
1088 Interpretation of Snow-Climate Feedback as Produced by 17 General Circulation Models. *Science*,
1089 253(5022), 888–892. <https://doi.org/10.1126/science.253.5022.888>
- 1090 Cess, Robert D., & Potter, G. L. (1988). A methodology for understanding and intercomparing
1091 atmospheric climate feedback processes in general circulation models. *Journal of Geophysical*
1092 *Research: Atmospheres*, 93(D7), 8305–8314. <https://doi.org/10.1029/JD093iD07p08305>
- 1093 Chung, C. E., & Räisänen, P. (2011). Origin of the Arctic warming in climate models. *Geophysical*
1094 *Research Letters*, 38(21). <https://doi.org/10.1029/2011GL049816>
- 1095 Chung, E.-S., Ha, K.-J., Timmermann, A., Stuecker, M. F., Bodai, T., & Lee, S.-K. (2021). Cold-
1096 Season Arctic Amplification Driven by Arctic Ocean-Mediated Seasonal Energy Transfer. *Earth's*
1097 *Future*, 9(2), e2020EF001898. <https://doi.org/10.1029/2020EF001898>
- 1098 Coakley, J. A. (1977). Feedbacks in vertical-column energy balance models. *J. Atmos. Res.* 34, 465-
1099 470, [https://doi.org/10.1175/1520-0469\(1977\)034<0465:FIVCEB>2.0.CO;2](https://doi.org/10.1175/1520-0469(1977)034<0465:FIVCEB>2.0.CO;2).
- 1100 Cohen, J., Zhang, X., Francis, J., Jung, T., Kwok, R., Overland, J., Ballinger, T. J., Bhatt, U. S.,
1101 Chen, H. W., Coumou, D., Feldstein, S., Gu, H., Handorf, D., Henderson, G., Ionita, M.,
1102 Kretschmer, M., Laliberte, F., Lee, S., Linderholm, H. W., ... Yoon, J. (2020). Divergent
1103 consensus on Arctic amplification influence on midlatitude severe winter weather. *Nature*
1104 *Climate Change*, 10(1), 20–29. <https://doi.org/10.1038/s41558-019-0662-y>
- 1105 Creamean, J. M., Hill, T. C. J., DeMott, P. J., Uetake, J., Kreidenweis, S., & Douglas, T. A. (2020).
1106 Thawing permafrost: an overlooked source of seeds for Arctic cloud formation. *Environmental*
1107 *Research Letters*, 15(8), 084022. <https://doi.org/10.1088/1748-9326/ab87d3>
- 1108 Cronin, T. W., & Jansen, M. F. (2016). Analytic radiative-advective equilibrium as a model for high-
1109 latitude climate. *Geophysical Research Letters*, 43(1), 449–457.
1110 <https://doi.org/10.1002/2015GL067172>
- 1111 Crook, J. A., Forster, P. M., & Stuber, N. (2011). Spatial Patterns of Modeled Climate Feedback and
1112 Contributions to Temperature Response and Polar Amplification. *Journal of Climate*, 24(14),
1113 3575–3592. <https://doi.org/10.1175/2011JCLI3863.1>
- 1114 Curry, J. A., Schramm, J. L., Rossow, W. B., & Randall, D. (n.d.). *Overview of Arctic cloud and*
1115 *radiation characteristics*. 9(8), 1731–1764.
- 1116 Curry, Judith A., Schramm, J. L., Rossow, W. B., & Randall, D. (1996). Overview of Arctic Cloud
1117 and Radiation Characteristics. *Journal of Climate*, 9(8), 1731–1764. [https://doi.org/10.1175/1520-0442\(1996\)009<1731:OOACAR>2.0.CO;2](https://doi.org/10.1175/1520-0442(1996)009<1731:OOACAR>2.0.CO;2)

- 1119 Dai, A., Luo, D., Song, M., & Liu, J. (2019). Arctic amplification is caused by sea-ice loss under
1120 increasing CO₂. *Nature Communications*, *10*(1), 121. [https://doi.org/10.1038/s41467-018-07954-](https://doi.org/10.1038/s41467-018-07954-9)
1121 [9](https://doi.org/10.1038/s41467-018-07954-9).
- 1122 Deser, C., Tomas, R., Alexander, M., & Lawrence, D. (2010). The Seasonal Atmospheric Response
1123 to Projected Arctic Sea Ice Loss in the Late Twenty-First Century, *Journal of Climate*, *23*(2), 333-
1124 351. Retrieved Jul 30, 2021,
1125 from <https://journals.ametsoc.org/view/journals/clim/23/2/2009jcli3053.1.xml>
- 1126
- 1127 Deser, C., Tomas, R. A., & Sun, L. (2015). The Role of Ocean–Atmosphere Coupling in the Zonal-
1128 Mean Atmospheric Response to Arctic Sea Ice Loss. *Journal of Climate*, *28*(6), 2168–2186.
1129 <https://doi.org/10.1175/JCLI-D-14-00325.1>
- 1130 Dickinson, R. E., Meehl, G. A., & Washington, W. M. (1987). Ice-albedo feedback in a CO₂-
1131 doubling simulation. *Climatic Change*, *10*(3), 241–248. <https://doi.org/10.1007/BF00143904>
- 1132 Dmitrenko, I. A., Polyakov, I. V., Kirillov, S. A., Timokhov, L. A., Frolov, I. E., Sokolov, V. T.,
1133 Simmons, H. L., Ivanov, V. V., & Walsh, D. (2008). Toward a warmer Arctic Ocean: Spreading
1134 of the early 21st century Atlantic Water warm anomaly along the Eurasian Basin margins. *Journal*
1135 *of Geophysical Research: Oceans*, *113*(C5). <https://doi.org/10.1029/2007JC004158>
- 1136 Donohoe, A., Blanchard-Wrigglesworth, E., Schweiger, A., & Rasch, P. J. (2020). The Effect of
1137 Atmospheric Transmissivity on Model and Observational Estimates of the Sea Ice Albedo
1138 Feedback. *Journal of Climate*, *33*(13), 5743–5765. <https://doi.org/10.1175/JCLI-D-19-0674.1>
- 1139 Duan, L., Cao, L., & Caldeira, K. (2019). Estimating Contributions of Sea Ice and Land Snow to
1140 Climate Feedback. *Journal of Geophysical Research: Atmospheres*, *124*(1), 199–208.
1141 <https://doi.org/10.1029/2018JD029093>
- 1142 Duncan, B. N., Ott, L. E., Abshire, J. B., Brucker, L., Carroll, M. L., Carton, J., Comiso, J. C., Dinnat,
1143 E. P., Forbes, B. C., Gonsamo, A., Gregg, W. W., Hall, D. K., Ialongo, I., Jandt, R., Kahn, R. A.,
1144 Karpechko, A., Kawa, S. R., Kato, S., Kumpula, T., ... Wu, D. L. (2020). Space-Based
1145 Observations for Understanding Changes in the Arctic-Boreal Zone. *Reviews of Geophysics*, *58*(1),
1146 e2019RG000652. <https://doi.org/10.1029/2019RG000652>
- 1147 Dwyer, J. G., Biasutti, M., & Sobel, A. H. (2012). Projected Changes in the Seasonal Cycle of
1148 Surface Temperature. *Journal of Climate*, *25*(18), 6359–6374. [https://doi.org/10.1175/JCLI-D-11-](https://doi.org/10.1175/JCLI-D-11-00741.1)
1149 [00741.1](https://doi.org/10.1175/JCLI-D-11-00741.1)
- 1150 English, J. M., Kay, J. E., Gettelman, A., Liu, X., Wang, Y., Zhang, Y., & Chepfer, H. (2014).
1151 Contributions of Clouds, Surface Albedos, and Mixed-Phase Ice Nucleation Schemes to Arctic
1152 Radiation Biases in CAM5. *Journal of Climate*, *27*(13), 5174–5197. [https://doi.org/10.1175/JCLI-](https://doi.org/10.1175/JCLI-D-13-00608.1)
1153 [D-13-00608.1](https://doi.org/10.1175/JCLI-D-13-00608.1)
- 1154 Ervens, B., Feingold, G., Sulia, K., & Harrington, J. (2011). The impact of microphysical parameters,
1155 ice nucleation mode, and habit growth on the ice/liquid partitioning in mixed-phase Arctic clouds.
1156 *Journal of Geophysical Research: Atmospheres*, *116*(D17).
1157 <https://doi.org/10.1029/2011JD015729>

- 1158 Eyring, V.; Bony, S.; Meehl, G.A.; Senior, C.A.; Stevens, B.; Stouffer, R.J.; Taylor, K.E. (2016).
1159 Overview of the Coupled Model Intercomparison Project Phase 6 (CMIP6) experimental design
1160 and organization. *Geoscientific Model Development*, 9, 1937–1958, doi:10.5194/gmd-9-1937-
1161 2016.
- 1162
1163 Feldl, N., & Bordoni, S. (2016). Characterizing the Hadley Circulation Response through Regional
1164 Climate Feedbacks. *Journal of Climate*, 29(2), 613–622. <https://doi.org/10.1175/JCLI-D-15-0424.1>
- 1166 Feldl, N., & Roe, G. H. (2013). Four perspectives on climate feedbacks. *Geophysical Research
1167 Letters*, 40(15), 4007–4011. <https://doi.org/10.1002/grl.50711>
- 1168 Feldl, Nicole, Anderson, B. T., & Bordoni, S. (2017b). Atmospheric Eddies Mediate Lapse Rate
1169 Feedback and Arctic Amplification. *Journal of Climate*, 30(22), 9213–9224.
1170 <https://doi.org/10.1175/JCLI-D-16-0706.1>
- 1171 Feldl, Nicole, Bordoni, S., & Merlis, T. M. (2017a). Coupled High-Latitude Climate Feedbacks and
1172 Their Impact on Atmospheric Heat Transport. *Journal of Climate*, 30(1), 189–201.
1173 <https://doi.org/10.1175/JCLI-D-16-0324.1>
- 1174 Feldl, Nicole, Po-Chedley, S., Singh, H. K. A., Hay, S., & Kushner, P. J. (2020). Sea ice and
1175 atmospheric circulation shape the high-latitude lapse rate feedback. *Npj Climate and Atmospheric
1176 Science*, 3(1), 1–9. <https://doi.org/10.1038/s41612-020-00146-7>
- 1177 Furtado, K., & Field, P. (2017). The Role of Ice Microphysics Parametrizations in Determining the
1178 Prevalence of Supercooled Liquid Water in High-Resolution Simulations of a Southern Ocean
1179 Midlatitude Cyclone. *Journal of the Atmospheric Sciences*, 74(6), 2001–2021.
1180 <https://doi.org/10.1175/JAS-D-16-0165.1>
- 1181 GISTEMP Team, 2021: GISS Surface Temperature Analysis (GISTEMP), version 4. NASA
1182 Goddard Institute for Space Studies. Dataset accessed 2021-01-20 at data.giss.nasa.gov/gistemp/.
- 1183 Goosse, H., Selten, F., Haarsma, R., & Opsteegh, J. (2003). Large sea-ice volume anomalies
1184 simulated in a coupled climate model. *Climate Dynamics*, 20(5), 523–536.
1185 <https://doi.org/10.1007/s00382-002-0290-4>
- 1186 Goosse, Hugues, Kay, J. E., Armour, K. C., Bodas-Salcedo, A., Chepfer, H., Docquier, D., Jonko,
1187 A., Kushner, P. J., Lecomte, O., Massonnet, F., Park, H.-S., Pithan, F., Svensson, G., &
1188 Vancoppenolle, M. (2018). Quantifying climate feedbacks in polar regions. *Nature
1189 Communications*, 9(1), 1919. <https://doi.org/10.1038/s41467-018-04173-0>
- 1190 Graham, R. M., Cohen, L., Petty, A. A., Boisvert, L. N., Rinke, A., Hudson, S. R., Nicolaus, M., &
1191 Granskog, M. A. (2017a). Increasing frequency and duration of Arctic winter warming events.
1192 *Geophysical Research Letters*, 44(13), 6974–6983. <https://doi.org/10.1002/2017GL073395>
- 1193 Graham, R. M., Cohen, L., Petty, A. A., Boisvert, L. N., Rinke, A., Hudson, S. R., Nicolaus, M., &
1194 Granskog, M. A. (2017b). Increasing frequency and duration of Arctic winter warming events.
1195 *Geophysical Research Letters*, 44(13), 6974–6983. <https://doi.org/10.1002/2017GL073395>

- 1196 Graversen, Rune G., & Burtu, M. (2016). Arctic amplification enhanced by latent energy transport
1197 of atmospheric planetary waves. *Quarterly Journal of the Royal Meteorological Society*, 142(698),
1198 2046–2054. <https://doi.org/10.1002/qj.2802>
- 1199 Graversen, Rune G., Langen, P. L., & Mauritsen, T. (2014). Polar Amplification in CCSM4:
1200 Contributions from the Lapse Rate and Surface Albedo Feedbacks. *Journal of Climate*, 27(12),
1201 4433–4450. <https://doi.org/10.1175/JCLI-D-13-00551.1>
- 1202 Graversen, Rune G., Mauritsen, T., Tjernström, M., Källén, E., & Svensson, G. (2008). Vertical
1203 structure of recent Arctic warming. *Nature*, 451(7174), 53–56.
1204 <https://doi.org/10.1038/nature06502>
- 1205 Graversen, Rune Grand, & Wang, M. (2009). Polar amplification in a coupled climate model with
1206 locked albedo. *Climate Dynamics*, 33(5), 629–643. <https://doi.org/10.1007/s00382-009-0535-6>
- 1207 Guemas, V., & Salas-Méla, D. (2008). Simulation of the Atlantic meridional overturning circulation
1208 in an atmosphere-ocean global coupled model. Part II: weakening in a climate change experiment:
1209 a feedback mechanism. *Climate Dynamics*, 30(7), 831–844. <https://doi.org/10.1007/s00382-007->
1210 0328-8
- 1211 Hall, A. (2004). The role of surface albedo feedback in climate. *Journal of Climate*, 17(7), 1550–
1212 1568.
- 1213 Hall, A., Cox, P., Huntingford, C., & Klein, S. (2019). Progressing emergent constraints on future
1214 climate change. *Nature Climate Change*, 9(4), 269–278. <https://doi.org/10.1038/s41558-019->
1215 0436-6
- 1216 Hall, A., & Qu, X. (2006). Using the current seasonal cycle to constrain snow albedo feedback in
1217 future climate change. *Geophysical Research Letters*, 33(3).
1218 <https://doi.org/10.1029/2005GL025127>
- 1219 Hansen, J., Lacis, A., Rind, D., Russell, G., Stone, P., Fung, I., Ruedy, R., & Lerner, J. (1984).
1220 Climate sensitivity: Analysis of feedback mechanisms. *Feedback*, 1, 1–3.
- 1221 Hartmann, M., Blunier, T., Brügger, S. O., Schmale, J., Schwikowski, M., Vogel, A., Wex, H., &
1222 Stratmann, F. (2019). Variation of Ice Nucleating Particles in the European Arctic Over the Last
1223 Centuries. *Geophysical Research Letters*, 46(7), 4007–4016.
1224 <https://doi.org/10.1029/2019GL082311>
- 1225 He, M., Hu, Y., Chen, N., Wang, D., Huang, J., & Stamnes, K. (2019). High cloud coverage over
1226 melted areas dominates the impact of clouds on the albedo feedback in the Arctic. *Scientific*
1227 *Reports*, 9(1), 9529. <https://doi.org/10.1038/s41598-019-44155-w>
- 1228 Hegyi, B. M., & Deng, Y. (2017). Dynamical and Thermodynamical Impacts of High- and Low-
1229 Frequency Atmospheric Eddies on the Initial Melt of Arctic Sea Ice. *Journal of Climate*, 30(3),
1230 865–883. <https://doi.org/10.1175/JCLI-D-15-0366.1>
- 1231 Hegyi, B. M., & Taylor, P. C. (2018). The Unprecedented 2016–2017 Arctic Sea Ice Growth Season:
1232 The Crucial Role of Atmospheric Rivers and Longwave Fluxes. *Geophysical Research Letters*,
1233 45(10), 5204–5212. <https://doi.org/10.1029/2017GL076717>

- 1234 Held, I. M. (2005). The Gap between Simulation and Understanding in Climate Modeling. *Bulletin*
1235 *of the American Meteorological Society*, 86(11), 1609–1614. <https://doi.org/10.1175/BAMS-86->
1236 11-1609
- 1237 Henry, M., & Merlis, T. M. (2019). The Role of the Nonlinearity of the Stefan–Boltzmann Law on
1238 the Structure of Radiatively Forced Temperature Change. *Journal of Climate*, 32(2), 335–348.
1239 <https://doi.org/10.1175/JCLI-D-17-0603.1>
- 1240 Henry, M., Merlis, T. M., Lutsko, N. J., & Rose, B. E. J. (2021). Decomposing the Drivers of Polar
1241 Amplification with a Single-Column Model. *Journal of Climate*, 34(6), 2355–2365.
1242 <https://doi.org/10.1175/JCLI-D-20-0178.1>
- 1243 Henry, M., & Vallis, G. K. (2021). Reduced High-Latitude Land Seasonality in Climates with Very
1244 High Carbon Dioxide. *Journal of Climate*, 1(aop), 1–38. <https://doi.org/10.1175/JCLI-D-21->
1245 [0131.1](https://doi.org/10.1175/JCLI-D-21-0131.1)
- 1246 Hersbach, H., Bell, B., Berrisford, P., Biavati, G., Horányi, A., Muñoz Sabater, J., Nicolas, J.,
1247 Peubey, C., Radu, R., Rozum, I., Schepers, D., Simmons, A., Soci, C., Dee, D., Thépaut, J-N.
1248 (2019): ERA5 monthly averaged data on pressure levels from 1979 to present. Copernicus Climate
1249 Change Service (C3S) Climate Data Store (CDS). (Accessed on March 3, 2021).
- 1250 Hind, A., Zhang, Q., & Brattström, G. (2016). Problems encountered when defining Arctic
1251 amplification as a ratio. *Scientific Reports*, 6(1), 30469. <https://doi.org/10.1038/srep30469>
- 1252 Holland, M., & Bitz, C. (2003). Polar amplification of climate change in coupled models. *Climate*
1253 *Dynamics*, 21, 221–232. <https://doi.org/10.1007/s00382-003-0332-6>
- 1254 Holland, M. M., Bailey, D. A., Briegleb, B. P., Light, B., & Hunke, E. (2012). Improved Sea Ice
1255 Shortwave Radiation Physics in CCSM4: The Impact of Melt Ponds and Aerosols on Arctic Sea
1256 Ice. *Journal of Climate*, 25(5), 1413–1430. <https://doi.org/10.1175/JCLI-D-11-00078.1>
- 1257 Holland, M. M., Serreze, M. C., & Stroeve, J. (2010). The sea ice mass budget of the Arctic and its
1258 future change as simulated by coupled climate models. *Climate Dynamics*, 34(2–3), 185–200.
1259 <https://doi.org/10.1007/s00382-008-0493-4>
- 1260 Hu, X., Fan, H., Cai, M., Sejas, S. A., Taylor, P., & Yang, S. (2020). A less cloudy picture of the
1261 inter-model spread in future global warming projections. *Nature Communications*, 11(1), 4472.
1262 <https://doi.org/10.1038/s41467-020-18227-9>
- 1263 Hu, X., Taylor, P. C., Cai, M., Yang, S., Deng, Y., & Sejas, S. (2017). Inter-Model Warming
1264 Projection Spread: Inherited Traits from Control Climate Diversity. *Scientific Reports*, 7(1), 4300.
1265 <https://doi.org/10.1038/s41598-017-04623-7>
- 1266 Huang, Yi, Xia, Y., & Tan, X. (2017). On the pattern of CO₂ radiative forcing and poleward energy
1267 transport. *Journal of Geophysical Research: Atmospheres*, 122(20), 10,578–10,593.
1268 <https://doi.org/10.1002/2017JD027221>
- 1269 Huang, Yiyi, Ding, Q., Dong, X., Xi, B., & Baxter, I. (2021). Summertime low clouds mediate the
1270 impact of the large-scale circulation on Arctic sea ice. *Communications Earth & Environment*,
1271 2(1), 1–10. <https://doi.org/10.1038/s43247-021-00114-w>

- 1272 Huang, Yiyi, Dong, X., Bailey, D. A., Holland, M. M., Xi, B., DuVivier, A. K., Kay, J. E., Landrum,
1273 L. L., & Deng, Y. (2019). Thicker Clouds and Accelerated Arctic Sea Ice Decline: The
1274 Atmosphere-Sea Ice Interactions in Spring. *Geophysical Research Letters*, 46(12), 6980–6989.
1275 <https://doi.org/10.1029/2019GL082791>
- 1276 Huang, Yiyi, Dong, X., Xi, B., & Deng, Y. (2019). A survey of the atmospheric physical processes
1277 key to the onset of Arctic sea ice melt in spring. *Climate Dynamics*, 52(7), 4907–4922.
1278 <https://doi.org/10.1007/s00382-018-4422-x>
- 1279 Huang, Yiyi, Dong, X., Xi, B., Dolinar, E. K., & Stanfield, R. E. (2017). The footprints of 16 year
1280 trends of Arctic springtime cloud and radiation properties on September sea ice retreat. *Journal of*
1281 *Geophysical Research: Atmospheres*, 122(4), 2179–2193. <https://doi.org/10.1002/2016JD026020>
- 1282 Hwang, Y.-T., Frierson, D. M. W., & Kay, J. E. (2011). Coupling between Arctic feedbacks and
1283 changes in poleward energy transport. *Geophysical Research Letters*, 38(17).
1284 <https://doi.org/10.1029/2011GL048546>
- 1285 Ingram, W. J., Wilson, C. A., & Mitchell, J. F. B. (1989). Modeling climate change: An assessment
1286 of sea ice and surface albedo feedbacks. *Journal of Geophysical Research: Atmospheres*, 94(D6),
1287 8609–8622. <https://doi.org/10.1029/JD094iD06p08609>
- 1288 IPCC, 2018: Summary for Policymakers. In: *Global Warming of 1.5°C. An IPCC Special Report on*
1289 *the impacts of global warming of 1.5°C above pre-industrial levels and related global greenhouse*
1290 *gas emission pathways, in the context of strengthening the global response to the threat of climate*
1291 *change, sustainable development, and efforts to eradicate poverty* [Masson-Delmotte, V., P. Zhai,
1292 H.-O. Pörtner, D. Roberts, J. Skea, P.R. Shukla, A. Pirani, W. Moufouma-Okia, C. Péan, R.
1293 Pidcock, S. Connors, J.B.R. Matthews, Y. Chen, X. Zhou, M.I. Gomis, E. Lonnoy, T. Maycock,
1294 M. Tignor, and T. Waterfield (eds.)]. *World Meteorological Organization, Geneva, Switzerland,*
1295 *32 pp.*
- 1296 IPCC, 2021: *Climate Change 2021: The Physical Science Basis. Contribution of Working Group I*
1297 *to the Sixth Assessment Report of the Intergovernmental Panel on Climate Change* [Masson-
1298 Delmotte, V., P. Zhai, A. Pirani, S. L. Connors, C. Péan, S. Berger, N. Caud, Y. Chen, L. Goldfarb,
1299 M. I. Gomis, M. Huang, K. Leitzell, E. Lonnoy, J. B. R. Matthews, T. K. Maycock, T. Waterfield,
1300 O. Yelekçi, R. Yu and B. Zhou (eds.)]. Cambridge University Press. In Press.
- 1301 Irish, V. E., Elizondo, P., Chen, J., Chou, C., Charette, J., Lizotte, M., Ladino, L. A., Wilson, T. W.,
1302 Gosselin, M., Murray, B. J., Polishchuk, E., Abbatt, J. P. D., Miller, L. A., & Bertram, A. K.
1303 (2017). Ice-nucleating particles in Canadian Arctic sea-surface microlayer and bulk seawater.
1304 *Atmospheric Chemistry and Physics*, 17(17), 10583–10595. [https://doi.org/10.5194/acp-17-](https://doi.org/10.5194/acp-17-10583-2017)
1305 [10583-2017](https://doi.org/10.5194/acp-17-10583-2017)
- 1306 Jahn, A., Sterling, K., Holland, M. M., Kay, J. E., Maslanik, J. A., Bitz, C. M., Bailey, D. A., Stroeve,
1307 J., Hunke, E. C., Lipscomb, W. H., & Pollak, D. A. (2012). Late-Twentieth-Century Simulation
1308 of Arctic Sea Ice and Ocean Properties in the CCSM4. *Journal of Climate*, 25(5), 1431–1452.
1309 <https://doi.org/10.1175/JCLI-D-11-00201.1>

- 1310 Jeevanjee, N., Hassanzadeh, P., Hill, S., & Sheshadri, A. (2017). A perspective on climate model
1311 hierarchies. *Journal of Advances in Modeling Earth Systems*, 9(4), 1760–1771.
1312 <https://doi.org/10.1002/2017MS001038>
- 1313 Jungclaus, J. H., Lohmann, K., & Zanchettin, D. (2014). Enhanced 20th-century heat transfer to the
1314 Arctic simulated in the context of climate variations over the last millennium. *Climate of the Past*,
1315 10(6), 2201–2213. <https://doi.org/10.5194/cp-10-2201-2014>
- 1316 Karcher, M. J., Gerdes, R., Kauker, F., & Köberle, C. (2003). Arctic warming: Evolution and
1317 spreading of the 1990s warm event in the Nordic seas and the Arctic Ocean. *Journal of*
1318 *Geophysical Research: Oceans*, 108(C2). <https://doi.org/10.1029/2001JC001265>
- 1319 Kay, J. E., & Gettelman, A. (2009). Cloud influence on and response to seasonal Arctic sea ice loss.
1320 *Journal of Geophysical Research: Atmospheres*, 114(D18).
1321 <https://doi.org/10.1029/2009JD011773>
- 1322 Kay, J. E., Holland, M. M., & Jahn, A. (2011). Inter-annual to multi-decadal Arctic sea ice extent
1323 trends in a warming world. *Geophysical Research Letters*, 38(15).
1324 <https://doi.org/10.1029/2011GL048008>
- 1325 Kay, J. E., Deser, C., Phillips, A., Mai, A., Hannay, C., Strand, G., Arblaster, J. M., Bates, S. C.,
1326 Danabasoglu, G., Edwards, J., Holland, M., Kushner, P., Lamarque, J.-F., Lawrence, D., Lindsay,
1327 K., Middleton, A., Munoz, E., Neale, R., Oleson, K., ... Vertenstein, M. (2015). The Community
1328 Earth System Model (CESM) Large Ensemble Project: A Community Resource for Studying
1329 Climate Change in the Presence of Internal Climate Variability. *Bulletin of the American*
1330 *Meteorological Society*, 96(8), 1333–1349. <https://doi.org/10.1175/BAMS-D-13-00255.1>
- 1331 Kato, S., Rose, F. G., Rutan, D. A., Thorsen, T. J., Loeb, N. G., Doelling, D. R., Huang, X., Smith,
1332 W. L., Su, W., & Ham, S. (2018). Surface Irradiances of Edition 4.0 Clouds and the Earth’s Radiant
1333 Energy System (CERES) Energy Balanced and Filled (EBAF) Data Product, *Journal of*
1334 *Climate*, 31(11), 4501–4527. Retrieved Jul 30, 2021,
1335 from <https://journals.ametsoc.org/view/journals/clim/31/11/jcli-d-17-0523.1.xml>
- 1336 Kim, D., Kang, S. M., Shin, Y., & Feldl, N. (2018). Sensitivity of Polar Amplification to Varying
1337 Insolation Conditions. *Journal of Climate*, 31(12), 4933–4947. <https://doi.org/10.1175/JCLI-D-17-0627.1>
- 1339 Kim, K.-Y., Hamlington, B. D., Na, H., & Kim, J. (2016). Mechanism of seasonal Arctic sea ice
1340 evolution and Arctic amplification. *The Cryosphere*, 10(5), 2191–2202. <https://doi.org/10.5194/tc-10-2191-2016>
- 1342 Kim, K.-Y., Kim, J.-Y., Kim, J., Yeo, S., Na, H., Hamlington, B. D., & Leben, R. R. (2019). Vertical
1343 Feedback Mechanism of Winter Arctic Amplification and Sea Ice Loss. *Scientific Reports*, 9(1),
1344 1184. <https://doi.org/10.1038/s41598-018-38109-x>
- 1345 Klein, S. A., McCoy, R. B., Morrison, H., Ackerman, A. S., Avramov, A., Boer, G. de, Chen, M.,
1346 Cole, J. N. S., Genio, A. D. D., Falk, M., Foster, M. J., Fridlind, A., Golaz, J.-C., Hashino, T.,
1347 Harrington, J. Y., Hoose, C., Khairoutdinov, M. F., Larson, V. E., Liu, X., ... Zhang, G. (2009).
1348 Intercomparison of model simulations of mixed-phase clouds observed during the ARM Mixed-

- 1349 Phase Arctic Cloud Experiment. I: single-layer cloud. *Quarterly Journal of the Royal*
1350 *Meteorological Society*, 135(641), 979–1002. <https://doi.org/10.1002/qj.416>
- 1351 Koenigk, T., & Brodeau, L. (2014). Ocean heat transport into the Arctic in the twentieth and twenty-
1352 first century in EC-Earth. *Climate Dynamics*, 42(11), 3101–3120. <https://doi.org/10.1007/s00382->
1353 013-1821-x
- 1354 Komurcu, M., Storelvmo, T., Tan, I., Lohmann, U., Yun, Y., Penner, J. E., Wang, Y., Liu, X., &
1355 Takemura, T. (2014). Intercomparison of the cloud water phase among global climate models.
1356 *Journal of Geophysical Research: Atmospheres*, 119(6), 3372–3400.
1357 <https://doi.org/10.1002/2013JD021119>
- 1358 Kwok, R. (2018). Arctic sea ice thickness, volume, and multiyear ice coverage: losses and coupled
1359 variability (1958–2018). *Environmental Research Letters*, 13(10), 105005.
1360 <https://doi.org/10.1088/1748-9326/aae3ec>
- 1361 Laine, A., Yoshimori, M., & Abe-Ouchi, A. (2016). Surface Arctic Amplification Factors in CMIP5
1362 Models: Land and Oceanic Surfaces and Seasonality. *Journal of Climate*, 29(9), 3297–3316.
1363 <https://doi.org/10.1175/JCLI-D-15-0497.1>
- 1364 Langen, P. & V. A. Alexeev (2007): Polar amplification as a preferred response in an idealized
1365 aquaplanet GCM. *Clim. Dyn.* 29, 305–317, <https://doi.org/10.1007/S00382-006-0221-X>.
- 1366 Lawson, P., Gurganus, C., Woods, S., & Brintjes, R. (2017). Aircraft Observations of Cumulus
1367 Microphysics Ranging from the Tropics to Midlatitudes: Implications for a “New” Secondary Ice
1368 Process. *Journal of the Atmospheric Sciences*, 74(9), 2899–2920. <https://doi.org/10.1175/JAS-D->
1369 17-0033.1
- 1370 Laxon, S., Peacock, N., & Smith, D. (2003). High interannual variability of sea ice thickness in the
1371 Arctic region. *Nature*, 425(6961), 947–950. <https://doi.org/10.1038/nature02050>
- 1372 Lenssen, N. J. L., Schmidt, G. A., Hansen, J. E., Menne, M. J., Persin, A., Ruedy, R., & Zyss, D.
1373 (2019). Improvements in the GISTEMP Uncertainty Model. *Journal of Geophysical Research:*
1374 *Atmospheres*, 124(12), 6307–6326. <https://doi.org/10.1029/2018JD029522>
- 1375 Letterly, A., Key, J., & Liu, Y. (2018). Arctic climate: changes in sea ice extent outweigh changes
1376 in snow cover, *The Cryosphere*, 12, 3373–3382, <https://doi.org/10.5194/tc-12-3373-2018>.
- 1377 Li, H., Fedorov, A., & Liu, W. (2021). AMOC Stability and Diverging Response to Arctic Sea Ice
1378 Decline in Two Climate Models. *Journal of Climate*, 34(13), 5443–5460.
1379 <https://doi.org/10.1175/JCLI-D-20-0572.1>
- 1380 Li, X., Krueger, S. K., Strong, C., Mace, G. G., & Benson, S. (2020). Midwinter Arctic leads form
1381 and dissipate low clouds. *Nature Communications*, 11(1), 206. <https://doi.org/10.1038/s41467->
1382 019-14074-5
- 1383 Li, Z.-X., & Le Treut, H. (1992). Cloud-radiation feedbacks in a general circulation model and their
1384 dependence on cloud modelling assumptions. *Climate Dynamics*, 7(3), 133–139.
1385 <https://doi.org/10.1007/BF00211155>

- 1386 Liu, W., Fedorov, A., & Sévellec, F. (2019). The Mechanisms of the Atlantic Meridional Overturning
1387 Circulation Slowdown Induced by Arctic Sea Ice Decline. *Journal of Climate*, 32(4), 977–996.
1388 <https://doi.org/10.1175/JCLI-D-18-0231.1>
- 1389 Liu, W., & Fedorov, A. V. (2019). Global Impacts of Arctic Sea Ice Loss Mediated by the Atlantic
1390 Meridional Overturning Circulation. *Geophysical Research Letters*, 46(2), 944–952.
1391 <https://doi.org/10.1029/2018GL080602>
- 1392 Liu, Y., Key, J. R., Liu, Z., Wang, X., & Vavrus, S. J. (2012). A cloudier Arctic expected with
1393 diminishing sea ice. *Geophysical Research Letters*, 39(5). <https://doi.org/10.1029/2012GL051251>
- 1394 Loeb, N. G., Doelling, D. R., Wang, H., Su, W., Nguyen, C., Corbett, J. G., Liang, L., Mitrescu, C.,
1395 Rose, F. G., & Kato, S. (2018). Clouds and the Earth’s Radiant Energy System (CERES) Energy
1396 Balanced and Filled (EBAF) Top-of-Atmosphere (TOA) Edition-4.0 Data Product, *Journal of*
1397 *Climate*, 31(2), 895–918. Retrieved Jul 30, 2021,
1398 from <https://journals.ametsoc.org/view/journals/clim/31/2/jcli-d-17-0208.1.xml>
- 1399 Lu, J., & Cai, M. (2009a). Seasonality of polar surface warming amplification in climate simulations.
1400 *Geophysical Research Letters*, 36(16). <https://doi.org/10.1029/2009GL040133>
- 1401 Lu, J., & Cai, M. (2009b). A new framework for isolating individual feedback processes in coupled
1402 general circulation climate models. Part I: formulation. *Climate Dynamics*, 32(6), 873–885.
1403 <https://doi.org/10.1007/s00382-008-0425-3>
- 1404 Maher, P., Gerber, E. P., Medeiros, B., Merlis, T. M., Sherwood, S., Sheshadri, A., Sobel, A. H.,
1405 Vallis, G. K., Voigt, A., & Zurita-Gotor, P. (2019). Model Hierarchies for Understanding
1406 Atmospheric Circulation. *Reviews of Geophysics*, 57(2), 250–280.
1407 <https://doi.org/10.1029/2018RG000607>
- 1408 Mahlstein, I., & Knutti, R. (2011). Ocean Heat Transport as a Cause for Model Uncertainty in
1409 Projected Arctic Warming. *Journal of Climate*, 24(5), 1451–1460.
1410 <https://doi.org/10.1175/2010JCLI3713.1>
- 1411 Manabe, S., Spelman, M. J., & Stouffer, R. J. (1992). Transient Responses of a Coupled Ocean-
1412 Atmosphere Model to Gradual Changes of Atmospheric CO₂. Part II: Seasonal Response. *Journal*
1413 *of Climate*, 5(2), 105–126. [https://doi.org/10.1175/1520-0442\(1992\)005<0105:TROACO>2.0.CO;2](https://doi.org/10.1175/1520-0442(1992)005<0105:TROACO>2.0.CO;2)
- 1415 Manabe, S., Stouffer, R. J., Spelman, M. J., & Bryan, K. (1991). Transient Responses of a Coupled
1416 Ocean–Atmosphere Model to Gradual Changes of Atmospheric CO₂. Part I. Annual Mean
1417 Response. *Journal of Climate*, 4(8), 785–818. [https://doi.org/10.1175/1520-0442\(1991\)004<0785:TROACO>2.0.CO;2](https://doi.org/10.1175/1520-0442(1991)004<0785:TROACO>2.0.CO;2)
- 1419 Manabe, Syukoro, & Wetherald, R. T. (1967). Thermal Equilibrium of the Atmosphere with a Given
1420 Distribution of Relative Humidity. *Journal of the Atmospheric Sciences*, 24(3), 241–258.
- 1421 Manabe, Syukuro, & Stouffer, R. J. (1980). Sensitivity of a global climate model to an increase of
1422 CO₂ concentration in the atmosphere. *Journal of Geophysical Research: Oceans*, 85(C10), 5529–
1423 5554. <https://doi.org/10.1029/JC085iC10p05529>

- 1424 Manabe, Syukuro, & Wetherald, R. T. (1975). The Effects of Doubling the CO₂ Concentration on
1425 the climate of a General Circulation Model. *Journal of the Atmospheric Sciences*, 32(1), 3–15.
1426 [https://doi.org/10.1175/1520-0469\(1975\)032<0003:TEODTC>2.0.CO;2](https://doi.org/10.1175/1520-0469(1975)032<0003:TEODTC>2.0.CO;2)
- 1427 Markus, T., Stroeve, J. C., & Miller, J. (2009). Recent changes in Arctic sea ice melt onset, freezeup,
1428 and melt season length. *Journal of Geophysical Research: Oceans*, 114(C12).
- 1429
- 1430 Marshall, J., Scott, J. R., Armour, K. C., Campin, J.-M., Kelley, M., & Romanou, A. (2015). The
1431 ocean’s role in the transient response of climate to abrupt greenhouse gas forcing. *Climate*
1432 *Dynamics*, 44(7), 2287–2299. <https://doi.org/10.1007/s00382-014-2308-0>
- 1433 Maslanik, J., Stroeve, J., Fowler, C., & Emery, W. (2011). Distribution and trends in Arctic sea ice
1434 age through spring 2011. *Geophysical Research Letters*, 38(13).
1435 <https://doi.org/10.1029/2011GL047735>
- 1436 McCoy, D. T., Tan, I., Hartmann, D. L., Zelinka, M. D., & Storelvmo, T. (2016). On the relationships
1437 among cloud cover, mixed-phase partitioning, and planetary albedo in GCMs. *Journal of Advances*
1438 *in Modeling Earth Systems*, 8(2), 650–668. <https://doi.org/10.1002/2015MS000589>
- 1439 McCusker, K. E., Kushner, P. J., Fyfe, J. C., Sigmond, M., Kharin, V. V., & Bitz, C. M. (2017).
1440 Remarkable separability of circulation response to Arctic sea ice loss and greenhouse gas forcing.
1441 *Geophysical Research Letters*, 44(15), 7955–7964. <https://doi.org/10.1002/2017GL074327>
- 1442 Meehl, G. A., Collins, W. D., Boville, B. A., Kiehl, J. T., Wigley, T. M. L., & Arblaster, J. M. (2000).
1443 Response of the NCAR Climate System Model to Increased CO₂ and the Role of Physical
1444 Processes, *Journal of Climate*, 13(11), 1879-1898. Retrieved Jul 30, 2021,
1445 from [https://journals.ametsoc.org/view/journals/clim/13/11/1520-](https://journals.ametsoc.org/view/journals/clim/13/11/1520-0442_2000_013_1879_rotncs_2.0.co_2.xml)
1446 [0442_2000_013_1879_rotncs_2.0.co_2.xml](https://journals.ametsoc.org/view/journals/clim/13/11/1520-0442_2000_013_1879_rotncs_2.0.co_2.xml)
- 1447
- 1448 Meredith, M., M. Sommerkorn, S. Cassotta, C. Derksen, A. Ekaykin, A. Hollowed, G. Kofinas, A.
1449 Mackintosh, J. Melbourne-Thomas, M.M.C. Muelbert, G. Ottersen, H. Pritchard, and E.A.G.
1450 Schuur, 2019: Polar Regions. In: IPCC Special Report on the Ocean and Cryosphere in a Changing
1451 Climate [H.-O. Pörtner, D.C. Roberts, V. Masson-Delmotte, P. Zhai, M. Tignor, E. Poloczanska,
1452 K. Mintenbeck, A. Alegría, M. Nicolai, A. Okem, J. Petzold, B. Rama, N.M. Weyer (eds.)]. In
1453 press.
- 1454 Merlis, T. M. (2014). Interacting components of the top-of-atmosphere energy balance affect changes
1455 in regional surface temperature. *Geophysical Research Letters*, 41(20), 7291–7297.
1456 <https://doi.org/10.1002/2014GL061700>
- 1457 Merlis, T. M., & Henry, M. (2018). Simple Estimates of Polar Amplification in Moist Diffusive
1458 Energy Balance Models. *Journal of Climate*, 31(15), 5811–5824. [https://doi.org/10.1175/JCLI-D-](https://doi.org/10.1175/JCLI-D-17-0578.1)
1459 [17-0578.1](https://doi.org/10.1175/JCLI-D-17-0578.1)
- 1460 Middlemas, E. A., Kay, J. E., Medeiros, B. M., & Maroon, E. A. (2020). Quantifying the Influence
1461 of Cloud Radiative Feedbacks on Arctic Surface Warming Using Cloud Locking in an Earth

- 1462 System Model. *Geophysical Research Letters*, 47(15), e2020GL089207.
1463 <https://doi.org/10.1029/2020GL089207>
- 1464 Mitchell, J. F. B., Senior, C. A., & Ingram, W. J. (1989). CO₂ and climate: a missing feedback?
1465 *Nature*, 341(6238), 132–134. <https://doi.org/10.1038/341132a0>
- 1466 Morrison, A. L., Kay, J. E., Chepfer, H., Guzman, R., & Yettella, V. (2018). Isolating the Liquid
1467 Cloud Response to Recent Arctic Sea Ice Variability Using Spaceborne Lidar Observations.
1468 *Journal of Geophysical Research: Atmospheres*, 123(1), 473–490.
1469 <https://doi.org/10.1002/2017JD027248>
- 1470 Morrison, A. L., Kay, J. E., Frey, W. R., Chepfer, H., & Guzman, R. (2019). Cloud Response to
1471 Arctic Sea Ice Loss and Implications for Future Feedback in the CESM1 Climate Model. *Journal*
1472 *of Geophysical Research: Atmospheres*, 124(2), 1003–1020.
1473 <https://doi.org/10.1029/2018JD029142>
- 1474 Nghiem, S. V., Rigor, I. G., Perovich, D. K., Clemente-Colón, P., Weatherly, J. W., & Neumann, G.
1475 (2007). Rapid reduction of Arctic perennial sea ice. *Geophysical Research Letters*, 34(19).
1476 <https://doi.org/10.1029/2007GL031138>
- 1477 Nummelin, A., Li, C., & Hezel, P. J. (2017). Connecting ocean heat transport changes from the
1478 midlatitudes to the Arctic Ocean. *Geophysical Research Letters*, 44(4), 1899–1908.
1479 <https://doi.org/10.1002/2016GL071333>
- 1480 Nygård, T., Graverson, R. G., Uotila, P., Naakka, T., & Vihma, T. (2019). Strong Dependence of
1481 Wintertime Arctic Moisture and Cloud Distributions on Atmospheric Large-Scale Circulation.
1482 *Journal of Climate*, 32(24), 8771–8790. <https://doi.org/10.1175/JCLI-D-19-0242.1>
- 1483 Oldenburg, D., Armour, K. C., Thompson, L., & Bitz, C. M. (2018). Distinct Mechanisms of Ocean
1484 Heat Transport Into the Arctic Under Internal Variability and Climate Change. *Geophysical*
1485 *Research Letters*, 45(15), 7692–7700. <https://doi.org/10.1029/2018GL078719>
- 1486 Oudar, T., Sanchez-Gomez, E., Chauvin, F., Cattiaux, J., Terray, L., & Cassou, C. (2017). Respective
1487 roles of direct GHG radiative forcing and induced Arctic sea ice loss on the Northern Hemisphere
1488 atmospheric circulation. *Climate Dynamics*, 49(11), 3693–3713. [https://doi.org/10.1007/s00382-](https://doi.org/10.1007/s00382-1489-017-3541-0)
1489 017-3541-0
- 1490 Park, H.-S., Kim, S.-J., Seo, K.-H., Stewart, A. L., Kim, S.-Y., & Son, S.-W. (2018). The impact of
1491 Arctic sea ice loss on mid-Holocene climate. *Nature Communications*, 9(1), 4571.
1492 <https://doi.org/10.1038/s41467-018-07068-2>
- 1493 Parkinson and DiGirolamo. (2016). New visualizations highlight new information on the contrasting
1494 Arctic and Antarctic sea-ice trends since the late 1970s. *Remote Sensing of Environment*, 183,
1495 198–204. <https://doi.org/10.1016/j.rse.2016.05.020>
- 1496 Pavelsky, T. M., Boé, J., Hall, A., & Fetzer, E. J. (2011). Atmospheric inversion strength over polar
1497 oceans in winter regulated by sea ice. *Climate Dynamics*, 36(5), 945–955.
1498 <https://doi.org/10.1007/s00382-010-0756-8>

- 1499 Payne, A. E., Jansen, M. F., & Cronin, T. W. (2015). Conceptual model analysis of the influence of
1500 temperature feedbacks on polar amplification. *Geophysical Research Letters*, *42*(21), 9561–9570.
1501 <https://doi.org/10.1002/2015GL065889>
- 1502 Pendergrass, A. G., Conley, A., & Vitt, F. M. (2018). Surface and top-of-atmosphere radiative
1503 feedback kernels for CESM-CAM5. *Earth System Science Data*, *10*(1), 317–324.
1504 <https://doi.org/10.5194/essd-10-317-2018>
- 1505 Perovich, D. K., Light, B., Eicken, H., Jones, K. F., Runciman, K., & Nghiem, S. V. (2007).
1506 Increasing solar heating of the Arctic Ocean and adjacent seas, 1979–2005: Attribution and role in
1507 the ice-albedo feedback. *Geophysical Research Letters*, *34*(19).
1508 <https://doi.org/10.1029/2007GL031480>
- 1509 Persson, P. O. G., Shupe, M. D., Perovich, D., & Solomon, A. (2017). Linking atmospheric synoptic
1510 transport, cloud phase, surface energy fluxes, and sea-ice growth: observations of midwinter
1511 SHEBA conditions. *Climate Dynamics*, *49*(4), 1341–1364. [https://doi.org/10.1007/s00382-016-](https://doi.org/10.1007/s00382-016-3383-1)
1512 [3383-1](https://doi.org/10.1007/s00382-016-3383-1)
- 1513 Pistone, K., Eisenman, I., & Ramanathan, V. (2014). Observational determination of albedo decrease
1514 caused by vanishing Arctic sea ice. *Proceedings of the National Academy of Sciences*, *111*(9),
1515 3322–3326.
- 1516 Pithan, F., & Mauritsen, T. (2014). Arctic amplification dominated by temperature feedbacks in
1517 contemporary climate models. *Nature Geoscience*, *7*(3), 181–184.
1518 <https://doi.org/10.1038/ngeo2071>
- 1519 Pithan, F., Medeiros, B., & Mauritsen, T. (2014). Mixed-phase clouds cause climate model biases in
1520 Arctic wintertime temperature inversions. *Climate Dynamics*, *43*(1), 289–303.
1521 <https://doi.org/10.1007/s00382-013-1964-9>
- 1522 Pithan, F., Svensson, G., Caballero, R., Chechin, D., Cronin, T. W., Ekman, A. M. L., Neggers, R.,
1523 Shupe, M. D., Solomon, A., Tjernström, M., & Wendisch, M. (2018). Role of air-mass
1524 transformations in exchange between the Arctic and mid-latitudes. *Nature Geoscience*, *11*(11),
1525 805–812. <https://doi.org/10.1038/s41561-018-0234-1>
- 1526 Previdi, M., Janoski, T. P., Chiodo, G., Smith, K. L., & Polvani, L. M. (2020). Arctic Amplification:
1527 A Rapid Response to Radiative Forcing. *Geophysical Research Letters*, *47*(17), e2020GL089933.
1528 <https://doi.org/https://doi.org/10.1029/2020GL089933>
- 1529 Ramanathan, V. (1977). Interactions between Ice-Albedo, Lapse-Rate and Cloud-Top Feedbacks:
1530 An Analysis of the Nonlinear Response of a GCM Climate Model. *Journal of the Atmospheric*
1531 *Sciences*, *34*(12), 1885–1897. [https://doi.org/10.1175/1520-](https://doi.org/10.1175/1520-0469(1977)034<1885:IBIALR>2.0.CO;2)
1532 [0469\(1977\)034<1885:IBIALR>2.0.CO;2](https://doi.org/10.1175/1520-0469(1977)034<1885:IBIALR>2.0.CO;2)
- 1533 Rangno, A. L., & Hobbs, P. V. (2001). Ice particles in stratiform clouds in the Arctic and possible
1534 mechanisms for the production of high ice concentrations. *Journal of Geophysical Research:*
1535 *Atmospheres*, *106*(D14), 15065–15075. <https://doi.org/10.1029/2000JD900286>
- 1536 Rakipova, L. R. (1966). The influence of the Arctic ice cover on the zonal distribution of atmospheric
1537 temperature. Proceedings of the Symposium on the Arctic heat budget and atmospheric circulation.

- 1538 Riihelä, A., Manninen, T., & Laine, V. (2013). Observed changes in the albedo of the Arctic sea-ice
1539 zone for the period 1982–2009. *Nature Climate Change*, 3(10), 895–898.
1540 <https://doi.org/10.1038/nclimate1963>
- 1541 Rind, D., Healy, R., Parkinson, C., & Martinson, D. (1995). The Role of Sea Ice in 2×CO₂ Climate
1542 Model Sensitivity. Part I: The Total Influence of Sea Ice Thickness and Extent. *Journal of Climate*,
1543 8(3), 449–463. [https://doi.org/10.1175/1520-0442\(1995\)008<0449:TROSII>2.0.CO;2](https://doi.org/10.1175/1520-0442(1995)008<0449:TROSII>2.0.CO;2)
- 1544 Robock, A. (1983). Ice and Snow Feedbacks and the Latitudinal and Seasonal Distribution of
1545 Climate Sensitivity. *Journal of the Atmospheric Sciences*, 40, 986–997.
1546 [https://doi.org/10.1175/1520-0469\(1983\)040<0986:IASFAT>2.0.CO;2](https://doi.org/10.1175/1520-0469(1983)040<0986:IASFAT>2.0.CO;2)
- 1547 Roe, G., and coauthors. (2015). The remote impacts of climate feedbacks on regional climate
1548 predictability. *Nature Geosci* 8, 135–139. <https://doi.org/10.1038/ngeo2346>
- 1549 Rogers, W. E., Thomson, J., Shen, H. H., Doble, M. J., Wadhams, P., & Cheng,
1550 S. (2016). Dissipation of wind waves by pancake and frazil ice in the autumn Beaufort
1551 Sea. *Journal of Geophysical Research: Oceans*, 121(11), 7991–8007. <https://doi.org/10.1002/2016JC012251>
- 1553 Rugenstein, M. A. A., Winton, M., Stouffer, R. J., Griffies, S. M., & Hallberg, R. (2013). Northern
1554 High-Latitude Heat Budget Decomposition and Transient Warming. *Journal of Climate*, 26(2),
1555 609–621. <https://doi.org/10.1175/JCLI-D-11-00695.1>
- 1556 Russotto, R. D., & Biasutti, M. (2020). Polar Amplification as an Inherent Response of a Circulating
1557 Atmosphere: Results From the TRACMIP Aquaplanets. *Geophysical Research Letters*.
1558 <https://agupubs.onlinelibrary.wiley.com/doi/abs/10.1029/2019GL086771>
- 1559 Salzmann, M. (2017). The polar amplification asymmetry: role of Antarctic surface height. *Earth*
1560 *System Dynamics*, 8(2), 323–336. <https://doi.org/10.5194/esd-8-323-2017>
- 1561 Schauer, U., Fahrbach, E., Osterhus, S., & Rohardt, G. (2004). Arctic warming through the Fram
1562 Strait: Oceanic heat transport from 3 years of measurements. *Journal of Geophysical Research:*
1563 *Oceans*, 109(C6). <https://doi.org/10.1029/2003JC001823>
- 1564 Schmale, J., Zieger, P., & Ekman, A. M. L. (2021). Aerosols in current and future Arctic climate.
1565 *Nature Climate Change*, 11(2), 95–105. <https://doi.org/10.1038/s41558-020-00969-5>
- 1566 Schneider, S. H. (1975). On the Carbon Dioxide–Climate Confusion. *Journal of the Atmospheric*
1567 *Sciences*, 32(11), 2060–2066. [https://doi.org/10.1175/1520-0469\(1975\)032<2060:OTCDC>2.0.CO;2](https://doi.org/10.1175/1520-0469(1975)032<2060:OTCDC>2.0.CO;2)
- 1569 Schweiger, A., Lindsay, R., Zhang, J., Steele, M., Stern, H., & Kwok, R. (2011). Uncertainty in
1570 modeled Arctic sea ice volume. *Journal of Geophysical Research: Oceans*, 116(C8).
1571 <https://doi.org/10.1029/2011JC007084>
- 1572 Screen, J. A., Deser, C., & Simmonds, I. (2012). Local and remote controls on observed Arctic
1573 warming. *Geophysical Research Letters*, 39(10). <https://doi.org/10.1029/2012GL051598>

- 1574 Screen, J., & Francis, J. (2016). Contribution of sea-ice loss to Arctic amplification is regulated by
1575 Pacific Ocean decadal variability. *Nature Climate Change*, 6.
1576 <https://doi.org/10.1038/nclimate3011>
- 1577 Screen, James A., Deser, C., Smith, D. M., Zhang, X., Blackport, R., Kushner, P. J., Oudar, T.,
1578 McCusker, K. E., & Sun, L. (2018). Consistency and discrepancy in the atmospheric response to
1579 Arctic sea-ice loss across climate models. *Nature Geoscience*, 11(3), 155–163.
1580 <https://doi.org/10.1038/s41561-018-0059-y>
- 1581 Screen, James A., & Simmonds, I. (2010a). Increasing fall-winter energy loss from the Arctic Ocean
1582 and its role in Arctic temperature amplification. *Geophysical Research Letters*, 37(16).
1583 <https://doi.org/10.1029/2010GL044136>
- 1584 Screen, James A., & Simmonds, I. (2010b). The central role of diminishing sea ice in recent Arctic
1585 temperature amplification. *Nature*, 464(7293), 1334–1337. <https://doi.org/10.1038/nature09051>
- 1586 Sedlar, J., Shupe, M. D., & Tjernström, M. (2012). On the Relationship between Thermodynamic
1587 Structure and Cloud Top, and Its Climate Significance in the Arctic. *Journal of Climate*, 25(7),
1588 2374–2393. <https://doi.org/10.1175/JCLI-D-11-00186.1>
- 1589 Sejas, S. A., & Cai, M. (2016). Isolating the Temperature Feedback Loop and Its Effects on Surface
1590 Temperature. *Journal of the Atmospheric Sciences*, 73(8), 3287–3303.
1591 <https://doi.org/10.1175/JAS-D-15-0287.1>
- 1592 Sejas, S. A., Cai, M., Hu, A., Meehl, G. A., Washington, W., & Taylor, P. C. (2014). Individual
1593 Feedback Contributions to the Seasonality of Surface Warming. *Journal of Climate*, 27(14), 5653–
1594 5669. <https://doi.org/10.1175/JCLI-D-13-00658.1>
- 1595 Sellers, W. D. (1969). A Global Climatic Model Based on the Energy Balance of the Earth-
1596 Atmosphere System. *Journal of Applied Meteorology and Climatology*, 8(3), 392–400.
1597 [https://doi.org/10.1175/1520-0450\(1969\)008<0392:AGCMBO>2.0.CO;2](https://doi.org/10.1175/1520-0450(1969)008<0392:AGCMBO>2.0.CO;2)
- 1598 Semenov, V. A., Park, W., & Latif, M. (2009). Barents Sea inflow shutdown: A new mechanism for
1599 rapid climate changes. *Geophysical Research Letters*, 36(14).
1600 <https://doi.org/10.1029/2009GL038911>
- 1601 Semmler, T., Pithan, F., & Jung, T. (2020). Quantifying two-way influences between the Arctic and
1602 mid-latitudes through regionally increased CO₂ concentrations in coupled climate simulations.
1603 *Climate Dynamics*, 54(7), 3307–3321. <https://doi.org/10.1007/s00382-020-05171-z>
- 1604 Serreze, M. C., Barrett, A. P., Stroeve, J. C., Kindig, D. N., & Holland, M. M. (2009). The emergence
1605 of surface-based Arctic amplification. *The Cryosphere*, 3(1), 11–19. <https://doi.org/10.5194/tc-3-11-2009>
- 1607 Serreze, Mark C., & Barry, R. G. (2011). Processes and impacts of Arctic amplification: A research
1608 synthesis. *Global and Planetary Change*, 77(1), 85–96.
1609 <https://doi.org/10.1016/j.gloplacha.2011.03.004>

- 1610 Serreze, Mark C., Schnell, R. C., & Kahl, J. D. (1992). Low-Level Temperature Inversions of the
1611 Eurasian Arctic and Comparisons with Soviet Drifting Station Data. *Journal of Climate*, 5(6), 615–
1612 629. [https://doi.org/10.1175/1520-0442\(1992\)005<0615:LLTIOT>2.0.CO;2](https://doi.org/10.1175/1520-0442(1992)005<0615:LLTIOT>2.0.CO;2)
- 1613 Sévellec, F., Fedorov, A. V., & Liu, W. (2017). Arctic sea-ice decline weakens the Atlantic
1614 Meridional Overturning Circulation. *Nature Climate Change*, 7(8), 604–610.
1615 <https://doi.org/10.1038/nclimate3353>
- 1616 Shaw, T. A., & Tan, Z. (2018). Testing Latitudinally Dependent Explanations of the Circulation
1617 Response to Increased CO₂ Using Aquaplanet Models. *Geophysical Research Letters*, 45(18),
1618 9861–9869. <https://doi.org/10.1029/2018GL078974>
- 1619 Shell, K. M., Kiehl, J. T., & Shields, C. A. (2008). Using the Radiative Kernel Technique to Calculate
1620 Climate Feedbacks in NCAR’s Community Atmospheric Model. *Journal of Climate*, 21(10),
1621 2269–2282. <https://doi.org/10.1175/2007JCLI2044.1>
- 1622 Shupe, M. D., Persson, P. O. G., Brooks, I. M., Tjernström, M., Sedlar, J., Mauritsen, T., Sjogren,
1623 S., & Leck, C. (2013). Cloud and boundary layer interactions over the Arctic sea ice in late
1624 summer. *Atmospheric Chemistry and Physics*, 13(18), 9379–9399. [https://doi.org/10.5194/acp-13-](https://doi.org/10.5194/acp-13-9379-2013)
1625 [9379-2013](https://doi.org/10.5194/acp-13-9379-2013)
- 1626 Shupe, M. D. and coauthors (2020). The MOSAiC Expedition: A year drifting with the Arctic Sea
1627 Ice. *NOAA Arctic Report Card*. <https://doi.org/10.25923/9g3v-xh92>.
- 1628 Singh, H. A., Rasch, P. J., & Rose, B. E. J. (2017). Increased Ocean Heat Convergence Into the High
1629 Latitudes With CO₂ Doubling Enhances Polar-Amplified Warming. *Geophysical Research*
1630 *Letters*, 44(20), 10,583-10,591. <https://doi.org/10.1002/2017GL074561>
- 1631 Skagseth, Ø., Furevik, T., Ingvaldsen, R., Loeng, H., Mork, K. A., Orvik, K. A., & Ozhigin, V.
1632 (2008). Volume and Heat Transports to the Arctic Ocean Via the Norwegian and Barents Seas. In
1633 R. R. Dickson, J. Meincke, & P. Rhines (Eds.), *Arctic–Subarctic Ocean Fluxes: Defining the Role*
1634 *of the Northern Seas in Climate* (pp. 45–64). Springer Netherlands. [https://doi.org/10.1007/978-1-](https://doi.org/10.1007/978-1-4020-6774-7_3)
1635 [4020-6774-7_3](https://doi.org/10.1007/978-1-4020-6774-7_3)
- 1636 Sledd, A., & L’Ecuyer, T. (2019). How Much Do Clouds Mask the Impacts of Arctic Sea Ice and
1637 Snow Cover Variations? Different Perspectives from Observations and Reanalyses. *Atmosphere*,
1638 10(1), 12. <https://doi.org/10.3390/atmos10010012>
- 1639 Smith W. L. *et al.*, (2021). Hyperspectral Satellite Radiance Atmospheric Profile Information
1640 Content and Its Dependence on Spectrometer Technology. *IEEE Journal of Selected Topics in*
1641 *Applied Earth Observations and Remote Sensing*, vol. 14, pp. 4720-4736, doi:
1642 10.1109/JSTARS.2021.3073482.
- 1643 Smith, D. M., Dunstone, N. J., Scaife, A. A., Fiedler, E. K., Copsey, D., & Hardiman, S. C. (2017).
1644 Atmospheric Response to Arctic and Antarctic Sea Ice: The Importance of Ocean–Atmosphere
1645 Coupling and the Background State. *Journal of Climate*, 30(12), 4547–4565.
1646 <https://doi.org/10.1175/JCLI-D-16-0564.1>
- 1647 Smith, D. M., Screen, J. A., Deser, C., Cohen, J., Fyfe, J. C., García-Serrano, J., Jung, T., Kattsov,
1648 V., Matei, D., Msadek, R., Peings, Y., Sigmund, M., Ukita, J., Yoon, J.-H., & Zhang, X. (2019).

- 1649 The Polar Amplification Model Intercomparison Project (PAMIP) contribution to CMIP6:
1650 investigating the causes and consequences of polar amplification. *Geoscientific Model*
1651 *Development*, 12(3), 1139–1164. <https://doi.org/10.5194/gmd-12-1139-2019>
- 1652 Soden, B. J., & Held, I. M. (2006). An Assessment of Climate Feedbacks in Coupled Ocean–
1653 Atmosphere Models. *Journal of Climate*, 19(14), 3354–3360. <https://doi.org/10.1175/JCLI3799.1>
- 1654 Solomon, A., de Boer, G., Creamean, J. M., McComiskey, A., Shupe, M. D., Maahn, M., & Cox, C.
1655 (2018). The relative impact of cloud condensation nuclei and ice nucleating particle concentrations
1656 on phase partitioning in Arctic mixed-phase stratocumulus clouds. *Atmospheric Chemistry and*
1657 *Physics*, 18(23), 17047–17059. <https://doi.org/10.5194/acp-18-17047-2018>
- 1658 Solomon, A., Shupe, M. D., Persson, O., Morrison, H., Yamaguchi, T., Caldwell, P. M., & Boer, G.
1659 de. (2014). The Sensitivity of Springtime Arctic Mixed-Phase Stratocumulus Clouds to Surface-
1660 Layer and Cloud-Top Inversion-Layer Moisture Sources. *Journal of the Atmospheric Sciences*,
1661 71(2), 574–595. <https://doi.org/10.1175/JAS-D-13-0179.1>
- 1662 Song, X., Zhang, G. J., & Cai, M. (2014). Quantifying contributions of climate feedbacks to
1663 tropospheric warming in the NCAR CCSM3.0. *Climate Dynamics*, 42(3), 901–917.
1664 <https://doi.org/10.1007/s00382-013-1805-x>
- 1665 Sotiropoulou, G., Sullivan, S., Savre, J., Lloyd, G., Lachlan-Cope, T., Ekman, A. M. L., & Nenes,
1666 A. (2020). The impact of secondary ice production on Arctic stratocumulus. *Atmospheric*
1667 *Chemistry and Physics*, 20(3), 1301–1316. <https://doi.org/10.5194/acp-20-1301-2020>
- 1668 Spelman, M. J., & Manabe, S. (1984). Influence of oceanic heat transport upon the sensitivity of a
1669 model climate. *Journal of Geophysical Research: Oceans*, 89(C1), 571–586.
1670 <https://doi.org/10.1029/JC089iC01p00571>
- 1671 Spielhagen, R. F., Werner, K., Sorensen, S. A., Zamelczyk, K., Kandiano, E., Budeus, G., Husum,
1672 K., Marchitto, T. M., & Hald, M. (2011). Enhanced Modern Heat Transfer to the Arctic by Warm
1673 Atlantic Water. *Science*, 331(6016), 450–453. <https://doi.org/10.1126/science.1197397>
- 1674 Stapf, J., Ehrlich, A., Jäkel, E., Lüpkes, C., & Wendisch, M. (2020). Reassessment of shortwave
1675 surface cloud radiative forcing in the Arctic: consideration of surface-albedo–cloud interactions.
1676 *Atmospheric Chemistry and Physics*, 20(16), 9895–9914. [https://doi.org/10.5194/acp-20-9895-](https://doi.org/10.5194/acp-20-9895-2020)
1677 2020
- 1678 Stramler, K., Genio, A. D. D., & Rossow, W. B. (2011). Synoptically Driven Arctic Winter States.
1679 *Journal of Climate*, 24(6), 1747–1762. <https://doi.org/10.1175/2010JCLI3817.1>
- 1680 Stroeve, J., Barrett, A., Serreze, M., & Schweiger, A. (2014). Using records from submarine, aircraft
1681 and satellites to evaluate climate model simulations of Arctic sea ice thickness. *The Cryosphere*,
1682 8(5), 1839–1854. <https://doi.org/10.5194/tc-8-1839-2014>
- 1683 Stuecker, M. F., Bitz, C. M., Armour, K. C., Proistosescu, C., Kang, S. M., Xie, S.-P., Kim, D.,
1684 McGregor, S., Zhang, W., Zhao, S., Cai, W., Dong, Y., & Jin, F.-F. (2018). Polar amplification
1685 dominated by local forcing and feedbacks. *Nature Climate Change*, 8(12), 1076–1081.
1686 <https://doi.org/10.1038/s41558-018-0339-y>

- 1687 Susskind, J., J. M. Blaisdell, and L. Iredell (2014). Improved methodology for surface and
1688 atmospheric soundings, error estimates, and quality control procedures: The atmospheric infrared
1689 sounder science team version-6 retrieval algorithm. *J. Appl. Remote Sens.*, 8(1),
1690 doi:[10.1117/1.JRS.8.084994](https://doi.org/10.1117/1.JRS.8.084994).
- 1691 Swart, N. (2017). Natural causes of Arctic sea-ice loss. *Nature Climate Change*, 7(4), 239–241.
1692 <https://doi.org/10.1038/nclimate3254>
- 1693 Swart, N. C., Fyfe, J. C., Hawkins, E., Kay, J. E., & Jahn, A. (2015). Influence of internal variability
1694 on Arctic sea-ice trends. *Nature Climate Change*, 5(2), 86–89.
1695 <https://doi.org/10.1038/nclimate2483>
- 1696 Tan, I., & Storelvmo, T. (2016). Sensitivity Study on the Influence of Cloud Microphysical
1697 Parameters on Mixed-Phase Cloud Thermodynamic Phase Partitioning in CAM5. *Journal of the*
1698 *Atmospheric Sciences*, 73(2), 709–728. <https://doi.org/10.1175/JAS-D-15-0152.1>
- 1699 Tan, I., & Storelvmo, T. (2019). Evidence of Strong Contributions From Mixed-Phase Clouds to
1700 Arctic Climate Change. *Geophysical Research Letters*, 46(5), 2894–2902.
1701 <https://doi.org/10.1029/2018GL081871>
- 1702 Tan, I., Storelvmo, T., & Zelinka, M. D. (2016). Observational constraints on mixed-phase clouds
1703 imply higher climate sensitivity. *Science*, 352(6282), 224–227.
1704 <https://doi.org/10.1126/science.aad5300>
- 1705 Taylor, P. C., Cai, M., Hu, A., Meehl, J., Washington, W., & Zhang, G. J. (2013). A Decomposition
1706 of Feedback Contributions to Polar Warming Amplification. *Journal of Climate*, 26(18), 7023–
1707 7043. <https://doi.org/10.1175/JCLI-D-12-00696.1>
- 1708 Taylor, P. C., Ellingson, R. G., & Cai, M. (2011a). Geographical Distribution of Climate Feedbacks
1709 in the NCAR CCSM3.0. *Journal of Climate*, 24(11), 2737–2753.
1710 <https://doi.org/10.1175/2010JCLI3788.1>
- 1711 Taylor, P. C., Ellingson, R. G., & Cai, M. (2011b). Seasonal Variations of Climate Feedbacks in the
1712 NCAR CCSM3. *Journal of Climate*, 24(13), 3433–3444. <https://doi.org/10.1175/2011JCLI3862>.
- 1713 Taylor, P. C., W. Maslowski J. Perlwitz, and D. J. Wuebbles, 2017: Arctic Changes and their Effects
1714 on Alaska and the Rest of the United States. In: Climate Science Special Report: Fourth National
1715 Climate Assessment, Volume I [Wuebbles, D. J., S. W. Fahey, K. A. Hibbard, D. J. Dokken, B.
1716 C. Steward, and T. K. Maycock (eds.)]. U.S. Global Climate Change Research Program,
1717 Washington, DC, USA, pp. 303-332, doi: 10.7930/J00863GK.
- 1718 Taylor, P. C., Hegyi, B. M., Boeke, R. C., & Boisvert, L. N. (2018). On the Increasing Importance
1719 of Air-Sea Exchanges in a Thawing Arctic: A Review. *Atmosphere*, 9(2), 41.
1720 <https://doi.org/10.3390/atmos9020041>
- 1721 Taylor, P. C., Kato, S., Xu, K.-M., & Cai, M. (2015). Covariance between Arctic sea ice and clouds
1722 within atmospheric state regimes at the satellite footprint level. *Journal of Geophysical Research:*
1723 *Atmospheres*, 120(24), 12656–12678. <https://doi.org/10.1002/2015JD023520>

- 1724 Taylor, P., Maslowski, W., Perlwitz, J., & Wuebbles, D. (2017). Arctic changes and their effects on
1725 Alaska and the rest of the United States. *Publications, Agencies and Staff of the U.S. Department*
1726 *of Commerce*. <https://digitalcommons.unl.edu/usdeptcommercepub/582>
- 1727 Topál, D., Ding, Q., Mitchell, J., Baxter, I., Herein, M., Haszpra, T., Luo, R., & Li, Q. (2020). An
1728 Internal Atmospheric Process Determining Summertime Arctic Sea Ice Melting in the Next Three
1729 Decades: Lessons Learned from Five Large Ensembles and Multiple CMIP5 Climate Simulations.
1730 *Journal of Climate*, 33(17), 7431–7454. <https://doi.org/10.1175/JCLI-D-19-0803.1>
- 1731 Tsushima, Y., Emori, S., Ogura, T., Kimoto, M., Webb, M. J., Williams, K. D., Ringer, M. A., Soden,
1732 B. J., Li, B., & Andronova, N. (2006). Importance of the mixed-phase cloud distribution in the
1733 control climate for assessing the response of clouds to carbon dioxide increase: a multi-model
1734 study. *Climate Dynamics*, 27(2), 113–126. <https://doi.org/10.1007/s00382-006-0127-7>
- 1735 Uttal, T. and coauthors (2002). Surface heat budget of the Arctic Ocean. *Bulletin of the American*
1736 *Meteorological Society*, 83.2, 255-276.
- 1737
- 1738 van der Linden, E. C., Le Bars, D., Bintanja, R., & Hazeleger, W. (2019). Oceanic heat transport into
1739 the Arctic under high and low CO_2 forcing. *Climate Dynamics*, 53(7), 4763–4780.
1740 <https://doi.org/10.1007/s00382-019-04824-y>
- 1741 Vavrus, S. (2004). The Impact of Cloud Feedbacks on Arctic Climate under Greenhouse Forcing.
1742 *Journal of Climate*, 17(3), 603–615. [https://doi.org/10.1175/1520-](https://doi.org/10.1175/1520-0442(2004)017<0603:TIOCFO>2.0.CO;2)
1743 [0442\(2004\)017<0603:TIOCFO>2.0.CO;2](https://doi.org/10.1175/1520-0442(2004)017<0603:TIOCFO>2.0.CO;2)
- 1744 Vavrus, S., Holland, M. M., & Bailey, D. A. (2011). Changes in Arctic clouds during intervals of
1745 rapid sea ice loss. *Climate Dynamics*, 36(7), 1475–1489. [https://doi.org/10.1007/s00382-010-](https://doi.org/10.1007/s00382-010-0816-0)
1746 [0816-0](https://doi.org/10.1007/s00382-010-0816-0)
- 1747 Vavrus, S., Waliser, D., Schweiger, A., & Francis, J. (2008). Simulations of 20th and 21st century
1748 Arctic cloud amount in the global climate models assessed in the IPCC AR4. *Climate Dynamics*,
1749 33(7), 1099. <https://doi.org/10.1007/s00382-008-0475-6>
- 1750 Vignesh, P. P., Jiang, J. H., Kishore, P., Su, H., Smay, T., Brighton, N., & Velicogna, I. (2020).
1751 Assessment of CMIP6 Cloud Fraction and Comparison with Satellite Observations. *Earth and*
1752 *Space Science*, 7(2), e2019EA000975. <https://doi.org/10.1029/2019EA000975>
- 1753 Wang, Y., Zhang, D., Liu, X., & Wang, Z. (2018). Distinct Contributions of Ice Nucleation, Large-
1754 Scale Environment, and Shallow Cumulus Detrainment to Cloud Phase Partitioning With NCAR
1755 CAM5. *Journal of Geophysical Research: Atmospheres*, 123(2), 1132–1154.
1756 <https://doi.org/10.1002/2017JD027213>
- 1757 Warren, S. G., Rigor, I. G., Untersteiner, N., Radionov, V. F., Bryazgin, N. N., Aleksandrov, Y. I.,
1758 & Colony, R. (1999). Snow Depth on Arctic Sea Ice. *Journal of Climate*, 12(6), 1814–1829.
1759 [https://doi.org/10.1175/1520-0442\(1999\)012<1814:SDOASI>2.0.CO;2](https://doi.org/10.1175/1520-0442(1999)012<1814:SDOASI>2.0.CO;2)
- 1760 Washington, W. M., & Meehl, G. A. (1984). Seasonal cycle experiment on the climate sensitivity
1761 due to a doubling of CO₂ with an atmospheric general circulation model coupled to a simple

- 1762 mixed-layer ocean model. *Journal of Geophysical Research: Atmospheres*, 89(D6), 9475–9503.
1763 <https://doi.org/10.1029/JD089iD06p09475>
- 1764 Washington, W. M., & Meehl, G. A. (1986). General circulation model CO2 sensitivity experiments:
1765 Snow-sea ice albedo parameterizations and globally averaged surface air temperature. *Climatic*
1766 *Change*, 8(3), 231–241. <https://doi.org/10.1007/BF00161596>
- 1767 Washington, W. M., & Meehl, G. A. (1989). Climate sensitivity due to increased CO2: experiments
1768 with a coupled atmosphere and ocean general circulation model. *Climate Dynamics*, 4(1), 1–38.
1769 <https://doi.org/10.1007/BF00207397>
- 1770 Washington, W. M., & Meehl, G. A. (1996). High-latitude climate change in a global coupled ocean-
1771 atmosphere-sea ice model with increased atmospheric CO2. *Journal of Geophysical Research:*
1772 *Atmospheres*, 101(D8), 12795–12801. <https://doi.org/10.1029/96JD00505>
- 1773 Webster, M. A., Rigor, I. G., Nghiem, S. V., Kurtz, N. T., Farrell, S. L., Perovich, D. K., & Sturm,
1774 M. (2014). Interdecadal changes in snow depth on Arctic sea ice. *Journal of Geophysical*
1775 *Research: Oceans*, 119(8), 5395–5406. <https://doi.org/10.1002/2014JC009985>
- 1776 Wetherald, R. T., & Manabe, S. (1988). Cloud Feedback Processes in a General Circulation Model.
1777 *Journal of the Atmospheric Sciences*, 45(8), 1397–1416. <https://doi.org/10.1175/1520->
1778 [0469\(1988\)045<1397:CFPIAG>2.0.CO;2](https://doi.org/10.1175/1520-0469(1988)045<1397:CFPIAG>2.0.CO;2)
- 1779 Wetherald, Richard T., & Manabe, S. (1975). The Effects of Changing the Solar Constant on the
1780 Climate of a General Circulation Model. *Journal of the Atmospheric Sciences*, 32(11), 2044–2059.
1781 [https://doi.org/10.1175/1520-0469\(1975\)032<2044:TEOCTS>2.0.CO;2](https://doi.org/10.1175/1520-0469(1975)032<2044:TEOCTS>2.0.CO;2)
- 1782 Wielicki, B. A., Young, D. F., Mlynczak, M. G., Thome, K. J., Leroy, S., Corliss, J., Anderson, J.
1783 G., Ao, C. O., Bantges, R., Best, F., Bowman, K., Brindley, H., Butler, J. J., Collins, W., Dykema,
1784 J. A., Doelling, D. R., Feldman, D. R., Fox, N., Huang, X., ... Xiong, X. (2013). Achieving Climate
1785 Change Absolute Accuracy in Orbit. *Bulletin of the American Meteorological Society*, 94(10),
1786 1519–1539. <https://doi.org/10.1175/BAMS-D-12-00149.1>
- 1787 Wilson, C. A., & Mitchell, J. F. B. (1987). A doubled CO2 climate sensitivity experiment with a
1788 global climate model including a simple ocean. *Journal of Geophysical Research: Atmospheres*,
1789 92(D11), 13315–13343. <https://doi.org/10.1029/JD092iD11p13315>
- 1790 Wilson, T. W., Ladino, L. A., Alpert, P. A., Breckels, M. N., Brooks, I. M., Browse, J., Burrows, S.
1791 M., Carslaw, K. S., Huffman, J. A., Judd, C., Kilthau, W. P., Mason, R. H., McFiggans, G., Miller,
1792 L. A., Nájera, J. J., Polishchuk, E., Rae, S., Schiller, C. L., Si, M., ... Murray, B. J. (2015). A
1793 marine biogenic source of atmospheric ice-nucleating particles. *Nature*, 525(7568), 234–238.
1794 <https://doi.org/10.1038/nature14986>
- 1795 Winker, D. M., Pelon, J., Coakley, J. A., Jr., Ackerman, S. A., Charlson, R. J., Colarco, P. R.,
1796 Flamant, P., Fu, Q., Hoff, R. M., Kittaka, C., Kubar, T. L., Le Treut, H., McCormick, M. P., Mégie,
1797 G., Poole, L., Powell, K., Trepte, C., Vaughan, M. A., & Wielicki, B. A. (2010). The CALIPSO
1798 Mission, *Bulletin of the American Meteorological Society*, 91(9), 1211-1230. Retrieved Jul 30,
1799 2021, from https://journals.ametsoc.org/view/journals/bams/91/9/2010bams3009_1.x

- 1800 Winton, M., Griffies, S. M., Samuels, B. L., Sarmiento, J. L., & Frölicher, T. L. (2013). Connecting
1801 Changing Ocean Circulation with Changing Climate. *Journal of Climate*, 26(7), 2268–2278.
1802 <https://doi.org/10.1175/JCLI-D-12-00296.1>
- 1803 Woods, C., & Caballero, R. (2016a). The Role of Moist Intrusions in Winter Arctic Warming and
1804 Sea Ice Decline. *Journal of Climate*, 29(12), 4473–4485. <https://doi.org/10.1175/JCLI-D-15-0773.1>
- 1806 Woods, C., & Caballero, R. (2016b). The Role of Moist Intrusions in Winter Arctic Warming and
1807 Sea Ice Decline. *Journal of Climate*, 29(12), 4473–4485. <https://doi.org/10.1175/JCLI-D-15-0773.1>
- 1809 Wuebbles, D. J., Fahey, D. W., Hibbard, K. A., DeAngelo, B., Doherty, S., Hayhoe, K., Horton, R.,
1810 Kossin, J. P., Taylor, P. C., Waple, A. M., & Yohe, C. P. (2017). *Executive summary. Climate*
1811 *Science Special Report: Fourth National Climate Assessment, Volume I*. U.S. Global Change
1812 Research Program. <https://doi.org/10.7930/J0DJ5CTG>
- 1813 Xie, S., Liu, X., Zhao, C., & Zhang, Y. (2013). Sensitivity of CAM5-Simulated Arctic Clouds and
1814 Radiation to Ice Nucleation Parameterization. *Journal of Climate*, 26(16), 5981–5999.
1815 <https://doi.org/10.1175/JCLI-D-12-00517.1>
- 1816 Yang, F., Ovchinnikov, M., & Shaw, R. A. (2015). Long-lifetime ice particles in mixed-phase
1817 stratiform clouds: Quasi-steady and recycled growth. *Journal of Geophysical Research:*
1818 *Atmospheres*, 120(22), 11,617–11,635. <https://doi.org/10.1002/2015JD023679>
- 1819 Yoshimori, M., Abe-Ouchi, A., & Laîné, A. (2017). The role of atmospheric heat transport and
1820 regional feedbacks in the Arctic warming at equilibrium. *Climate Dynamics*, 49(9), 3457–3472.
1821 <https://doi.org/10.1007/s00382-017-3523-2>
- 1822 Yoshimori, M., Watanabe, M., Abe-Ouchi, A., Shiogama, H., & Ogura, T. (2014). Relative
1823 contribution of feedback processes to Arctic amplification of temperature change in MIROC
1824 GCM. *Climate Dynamics*, 42(5), 1613–1630. <https://doi.org/10.1007/s00382-013-1875-9>
- 1825 Yu, Y., Taylor, P. C., & Cai, M. (2019). Seasonal Variations of Arctic Low-Level Clouds and Its
1826 Linkage to Sea Ice Seasonal Variations. *Journal of Geophysical Research: Atmospheres*, 124(22),
1827 12206–12226. <https://doi.org/10.1029/2019JD031014>
- 1828 Zelinka, M. D., Klein, S. A., & Hartmann, D. L. (2012). Computing and Partitioning Cloud
1829 Feedbacks Using Cloud Property Histograms. Part II: Attribution to Changes in Cloud Amount,
1830 Altitude, and Optical Depth. *Journal of Climate*, 25(11), 3736–3754.
1831 <https://doi.org/10.1175/JCLI-D-11-00249.1>
- 1832 Zeppetello, L. R. V., Donohoe, A., & Battisti, D. S. (2019). Does Surface Temperature Respond to
1833 or Determine Downwelling Longwave Radiation? *Geophysical Research Letters*, 46(5), 2781–
1834 2789. <https://doi.org/10.1029/2019GL082220>
- 1835 Zhang, J., Rothrock, D., & Steele, M. (2000). Recent Changes in Arctic Sea Ice: The Interplay
1836 between Ice Dynamics and Thermodynamics. *Journal of Climate*, 13(17), 3099–3114.
1837 [https://doi.org/10.1175/1520-0442\(2000\)013<3099:RCIASI>2.0.CO;2](https://doi.org/10.1175/1520-0442(2000)013<3099:RCIASI>2.0.CO;2)

- 1838 Zhao, X., Liu, X., Phillips, V. T. J., & Patade, S. (2021). Impacts of secondary ice production on
1839 Arctic mixed-phase clouds based on ARM observations and CAM6 single-column model
1840 simulations. *Atmospheric Chemistry and Physics*, 21(7), 5685–5703. [https://doi.org/10.5194/acp-](https://doi.org/10.5194/acp-21-5685-2021)
1841 21-5685-2021
- 1842 Zhu, T., Huang, Y., & Wei, H. (2019). Estimating Climate Feedbacks Using a Neural Network.
1843 *Journal of Geophysical Research: Atmospheres*, 124(6), 3246–3258.
1844 <https://doi.org/10.1029/2018JD029223>